NAVAL
POSTGRADUATE
SCHOOL

MONTEREY, CALIFORNIA

THESIS

**A LINEAR PHYSIOLOGICAL VISUAL-VESTIBULAR
INTERACTION MODEL FOR THE PREDICTION OF
MOTION SICKNESS INCIDENCE**

by

Panagiotis Matsangas

September 2004

Thesis Advisors:	Michael McCauley
	Nita Miller
Second Reader:	Alan Washburn

Approved for public release, distribution unlimited.

THIS PAGE INTENTIONALLY LEFT BLANK

REPORT DOCUMENTATION PAGE		*Form Approved OMB No. 0704-0188*

Public reporting burden for this collection of information is estimated to average 1 hour per response, including the time for reviewing instruction, searching existing data sources, gathering and maintaining the data needed, and completing and reviewing the collection of information. Send comments regarding this burden estimate or any other aspect of this collection of information, including suggestions for reducing this burden, to Washington headquarters Services, Directorate for Information Operations and Reports, 1215 Jefferson Davis Highway, Suite 1204, Arlington, VA 22202-4302, and to the Office of Management and Budget, Paperwork Reduction Project (0704-0188) Washington DC 20503.

1. AGENCY USE ONLY *(Leave blank)*	2. REPORT DATE September 2004	3. REPORT TYPE AND DATES COVERED Master's Thesis
4. TITLE AND SUBTITLE: A Linear Physiological Visual-Vestibular Interaction Model for the Prediction of Motion Sickness Incidence		5. FUNDING NUMBERS
6. AUTHOR(S) Matsangas, Panagiotis		
7. PERFORMING ORGANIZATION NAME(S) AND ADDRESS(ES) Naval Postgraduate School Monterey, CA 93943-5000		8. PERFORMING ORGANIZATION REPORT NUMBER
9. SPONSORING /MONITORING AGENCY NAME(S) AND ADDRESS(ES) N/A		10. SPONSORING/MONITORING AGENCY REPORT NUMBER

11. SUPPLEMENTARY NOTES The views expressed in this thesis are those of the author and do not reflect the official policy or position of the Department of Defense or the U.S. Government.

12a. DISTRIBUTION / AVAILABILITY STATEMENT Approved for public release; distribution is unlimited	12b. DISTRIBUTION CODE

13. ABSTRACT (maximum 200 words)

    This thesis proposes a linear model based on human physiology for the explanation of the Motion Sickness Incidence (MSI) data found in previously reported experiments. The major human sensory systems taken into account are vestibular, visual, and the interaction between these two. The model is validated against the previous descriptive model and the corresponding experimental data.

    The proposed model predicts MSI with adequate precision (less than ±5%) in the frequency range between 0.07 Hz and 0.25 Hz. The difference between the proposed model and the previous descriptive model is increased at the outer frequency regions of the data.

14. SUBJECT TERMS Human physiology, human performance, motion sickness, motion sickness incidence, human modeling.			15. NUMBER OF PAGES 186
			16. PRICE CODE

17. SECURITY CLASSIFICATION OF REPORT Unclassified	18. SECURITY CLASSIFICATION OF THIS PAGE Unclassified	19. SECURITY CLASSIFICATION OF ABSTRACT Unclassified	20. LIMITATION OF ABSTRACT UL

NSN 7540-01-280-5500

Standard Form 298 (Rev. 2-89)
Prescribed by ANSI Std. 239-18

i

THIS PAGE INTENTIONALLY LEFT BLANK

**A LINEAR PHYSIOLOGICAL VISUAL-VESTIBULAR INTERACTION MODEL
FOR THE PREDICTION OF MOTION SICKNESS INCIDENCE**

Panagiotis G. Matsangas
Lieutenant, Hellenic Navy
B.S., Hellenic Naval Academy, 1992

Submitted in partial fulfillment of the
requirements for the degrees of

MASTER OF SCIENCE IN OPERATIONS RESEARCH
and
**MASTER OF SCIENCE IN MODELING, VIRTUAL ENVIRONMENTS AND
SIMULATION**

from the

NAVAL POSTGRADUATE SCHOOL
September 2004

Author: Panagiotis G. Matsangas

Approved by: Dr. Michael E. McCauley
                 Thesis Advisor

                 Dr. Nita Lewis Miller
                 Thesis Co-Advisor

                 Dr. Alan Washburn
                 Second Reader

                 Dr. Rudolph Darken, Chairman
                 MOVES Academic Committee

                 Dr. James Eagle, Chairman
                 Operations Research Department

THIS PAGE INTENTIONALLY LEFT BLANK

ABSTRACT

This thesis proposes a linear model based on human physiology for the explanation of the Motion Sickness Incidence (MSI) data found in previously reported experiments. The major human sensory systems taken into account are vestibular, visual, and the interaction between these two. The model is validated against the previous descriptive model and the corresponding experimental data.

The proposed model predicts MSI with adequate precision (less than ±5% difference) in the frequency range between 0.07 Hz and 0.25 Hz. The difference between the proposed model and the previous descriptive model is increased at the outer frequency regions of the data.

THIS PAGE INTENTIONALLY LEFT BLANK

TABLE OF CONTENTS

THIS PAGE INTENTIONALLY LEFT BLANK

LIST OF FIGURES

THIS PAGE INTENTIONALLY LEFT BLANK

LIST OF TABLES

THIS PAGE INTENTIONALLY LEFT BLANK

ACKNOWLEDGMENTS

This work is dedicated to my parents, Panagiota Pavlopoulou and George Matsangas.

THIS PAGE INTENTIONALLY LEFT BLANK

EXECUTIVE SUMMARY

This thesis proposes a linear model based on human physiology for the explanation of the Motion Sickness Incidence (MSI) found in experiments reported by McCauley, Royal, Wylie, O'Hanlon, and Mackie (1976). The major human sensory systems taken into account are vestibular, visual, and the interaction between these two sensory systems.

The proposed model combines the error produced in the aforementioned two major sensory systems to estimate the MSI:

- The error produced in the estimation of gravity vector in the vestibular system, and

- The error produced from the retinal slip in the visual system (residual optical flow).

The model is validated against the Human Factors Research, Inc. (HFR) descriptive model and the corresponding experimental data (McCauley et al., 1976). The predicted MSI approximates the experimental data with adequate precision (less than ±5% error) in the frequency range between 0.07 Hz and 0.25 Hz. The difference between the proposed model and the HFR model is increased at the outer regions of the McCauley et al. (1976) experiments. The existing differences can be attributed to the constrained nature of this thesis (not all human systems known to be contributing to motion sickness are taken into account).

The model is designed to predict seasickness in populations and may not accurately predict seasickness in a specific individual. Connection between a specific parameter

and susceptibility to motion sickness has yet to be found
(Bles, de Jong, & Oosterveld, 1984; Lentz, 1984).

I.   INTRODUCTION

A. OVERVIEW

The demand for 24-hour continuous, extensive and high operational tempo missions in naval operations combined with the use of complex systems, the need for reduced reaction times, and minimal errors, results in very high stress levels on ships' crews. In conjunction with rapid transitions from daytime to nighttime duty hours, extended duty hours, rotating work schedules, extreme weather conditions, sea states and limited crew experience, these requirements reduce performance and motivation to work, increasing risk and compromising safety.

The human element is susceptible to degraded performance in a number of ways. Driskell and colleagues (Driskell, Hughes, Willis, Cannon-Bowers, & Salas, 1991; Driskell, Mullen, Johnson, Hughes, & Batchelor, 1992) have conducted two reviews of the stress literature. These reports were supplemented by material from another collection of reviews (Driskell & Salas, 1996). Figure 1 is a diagram of a general model of the effects of stressors on performance. The listing of stressor conditions is divided into two general categories: the physical environment and the conditions of the task itself. Physical stressors include noise, extremes of temperature, vibration, physical isolation, threat of failure or injury, and the use of chemical or biological agents. Stressful conditions of the task include time pressure, multiple task demands, and sustained performance that lead to sleep deprivation and fatigue. In the center of the diagram are modulating conditions of the individual and social setting that can

1

moderate the effects of these stressors on performance. They include individual factors such as training, experience, personality factors, and motivation, as well as social factors such as unit cohesion, leadership, group pressure, and social supports. The effects of these stressors can manifest in a variety of performance and physiological effects: speed of responding, decreased accuracy, physiological responses and psychological effects such as altered mood, motivation and psychiatric illness (Hursh & Bell, 2001).

GENERAL MODEL OF STRESS EFFECTS ON PERFORMANCE

STRESSORS

Physical Environ.
Noise
Extreme Temp.
Vibration
Isolation
Threat of Failure/
Injury (eg. NBC)

Task Variables
Time Pressure
Sustained OPS
& Fatigue
Multiple Tasks
Ambiguity
Controllability

CONFIDENCE

Goals Achieved
Positive
 Exchange Ratios
Mission Competed
Increased Support

MODULATORS

Individual Factors
Training
Experience
Personality
Intelligence
Motivation

Social Factors
Cohesion
Leadership
Communication
 Skills
Group Pressure
Social Supports

STRESS EFFECTS

Performance/Psych.
Speed of Response
Decision Accuracy
Commo Quality
Mood
Combat Stress
 Disorders

Physiological
Heart Rate
Blood Pressure
Hormone
Neurochemical
Autonomic Effects

Figure 1: General model of stress effects on performance (Hursh & Bell, 2001).

The consequences of the aforementioned factors can be serious and have resulted in numerous accidents examples (Lauber & Kayten, 1988). Research on the effects of stress

2

on human performance is of vital concern because, in the military, we are interested in intervening to improve personnel performance before it can deteriorates into disaster.

B. BACKGROUND

In the military there are many stations and duties that are directly affected by an operator's performance. Especially aboard a ship a large proportion of the crew is dealing with duties sensitive to performance deterioration. Therefore, it is of primary concern to analyze how overall effectiveness may be vulnerable to human performance degradation.

Part of the aforementioned deterioration is a direct result of the influence of motion sickness through its symptomatology. Unfortunately, the models existing in the literature fall into two categories:

- They are descriptive and not etiologic (McCauley et al., 1976; O'Hanlon & McCauley, 1974)[1], or

- They are based on human physiology, but qualitative (Griffin, 1990b; Oman, 1982).

C. OBJECTIVES

The purpose of this thesis is to develop an etiologic model based on human physiology, describing the severity of motion sickness through MSI accumulation. The model will be based on known physiological processes. The sub-factors that

---

[1] Because the McCauley et al. (1976) Technical Report is not readily accessible, we have made a PDF copy available at a web page of the Naval Postgraduate   School: http:// http://www.nps.navy.mil/orfacpag/resumePages/publications/mccauleypu.htm

will be examined are the vestibular system function and afferent signals, the visual system through its contribution to motion sickness, and adaptation issues. The output MSI from the final model will be verified and validated against the McCauley et al (1976) experimental data.

D. PROBLEM STATEMENT

The primary research questions being investigated by this research are:

1) How do the main contributing factors of motion sickness (the intra-vestibular error and the error between vestibular and visual systems) interact?

2) Are the intra-vestibular error and the error between vestibular and visual system the major contributors to the Motion Sickness Incidence?

E. SCOPE, LIMITATIONS, AND ASSUMPTIONS

The proposed model is limited to vertical motions and thus the underlying main assumption will be that the major contributor to motion sickness aboard ships is vertical motion, as already stated by several authors (Guignard & McCauley, 1990; McCauley et al., 1976; Morales, 1949). It is outside the scope of this thesis to develop a model that will account for every possible aspect and symptom of motion sickness.

The assumption about vertical motion will enable us verify the output data of the Motion Sickness Incidence (MSI) model with the experimental data obtained by McCauley et al. (1976).

F. THESIS ORGANIZATION

Chapter II reviews literature covering the major concepts, issues and systems underlying motion sickness: the vestibular system, the visual system, vestibulo-ocular and optokinetic reflex, motion sickness theories and models. The methods used are presented in Chapter III. Chapter IV covers the analytical strategy and presents the statistical results. Finally, conclusions and recommendations for future research are offered in Chapter V.

THIS PAGE INTENTIONALLY LEFT BLANK

II. LITERATURE REVIEW

A. OVERVIEW

This chapter reviews the literature on the vestibular system and the existing models, the visual system and its corresponding existing models, the vestibulo-ocular reflexes and their importance, the interaction between vestibular nystagmus and visual pursuit, the effects of motion and the induced motion sickness, and the models of motion sickness incidence.

Where possible, the review focuses on existing research concerning motion sickness and motion sickness models, the independent factors that influence motion sickness and the contribution of the correlation between these factors to MSI.

B. TERMINOLOGY FOR HEAD AND BODY ORIENTATION

In the following paragraphs certain terminology will be used to indicate head and body orientation. The convention used is the transecting of the human body, horizontally and vertically, by three main planes. These planes (coronal, sagittal, and transverse) intersect at the body's center of gravity (Boff & Lincoln, 1988):

The intersection of the mid-sagittal plane and the mid-coronal plane forms the z-axis (also called the spinal axis). This mid-body, vertical axis passes through the center of gravity of a standing body. Rotation about the z-axis is called yaw.

The intersection of the mid-frontal plane and the mid-transverse plane forms the y-axis. Rotation about the y-axis is called pitch.

The intersection of the mid-sagittal plane and the mid-transverse plane forms the x-axis. Rotation about the x-axis is called roll.
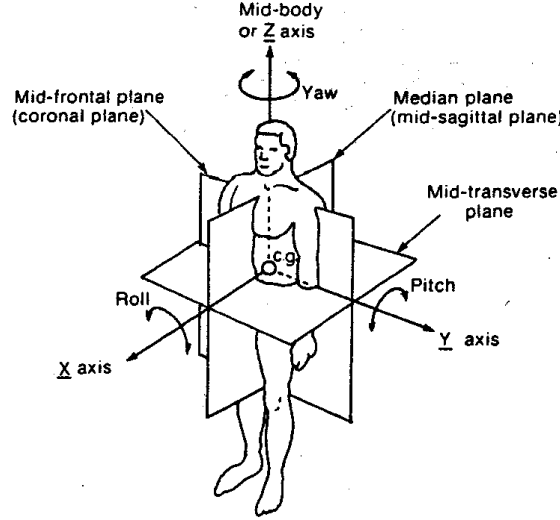
Figure 2: The principal planes and axis of reference of the human body (Howard, 1986a)

C. INTRODUCTION TO LAPLACE TRANSFORM AND SYSTEMS

1. Laplace Transform

Frequently, a system is represented by differential equations and integrals. Therefore, a system combined by several subsystems may be difficult to model. With the Laplace transform we can represent the input, the output, and the system as separate entities interconnected algebraically (Nise, 2004).

The Laplace transform is defined as:

$$f(s) = L\big[f(t)\big] = \int_{0-}^{\infty} f(t)e^{-st}dt \qquad (1.1)$$

Where: $s = \sigma + j\omega$, a complex variable

8

2. Convention

Assume that f is a function of time. Whenever we refer to this function in time domain, representation $f(t)$ will be used.

Whenever we refer to the Laplace transform of function f (s-domain), representation $f(s)$ will be used.

3. Transfer Function

Let's assume that we have a simple linear system where $r(t)$ is the input and $c(t)$ is the output. The corresponding signals in s-domain are $r(s)$ and $c(s)$. Then, the ratio of the output signal divided by the input signal is called the *transfer function* $g(s)$:

$$g(s) = \frac{c(s)}{r(s)} \tag{1.2}$$

4. Linear and Nonlinear Systems

A system is called *linear* if it possesses the following properties (Nise, 2004):

Superposition: The output response of the system to the sum of inputs, is the sum of the responses to the individual inputs.

Homogeneity: The multiplication of an input by a scalar yields a response which is multiplied by the same scalar.

A system is called *nonlinear* if it does not possess the aforementioned properties.

A system is called linear time-invariant (LTI) when its components are linear and their characteristics remain constant over time.

All the systems considered in this work are linear, except the adaptation mechanism, which includes non-linear elements.

5. Bode Plots

Let us assume the following linear system:

$$M_i(\omega)\angle\phi_i(\omega) \qquad\qquad M_o(\omega)\angle\phi_o(\omega)$$

$$\boxed{M(\omega)\angle\phi(\omega)}$$
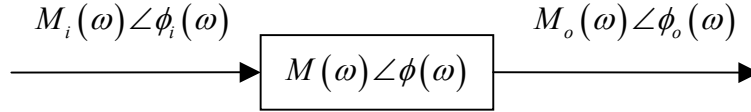
Figure 3: Linear system, after (Nise, 2004)

The input signal, represented with complex numbers, is the sinusoid $M_i(\omega)\angle\phi_i(\omega)$, and the output signal is the sinusoid $M_o(\omega)\angle\phi_o(\omega)$. M_i and M_o are the amplitudes of the signals. ϕ_i and ϕ_o are the phase angles of the sinusoids.

The steady state output signal is:

$$M_o(\omega)\angle\phi_o(\omega) = M_i(\omega)M(\omega)\angle\left[\phi_i(\omega) + \phi(\omega)\right]$$

Thus, the system function is:

$$M(\omega) = \frac{M_o(\omega)}{M_i(\omega)}$$

and:

$$\phi(\omega) = \phi_o(\omega) - \phi_i(\omega)$$

$M(\omega)$ is called the magnitude frequency response and $\phi(\omega)$ is called the phase frequency response (Nise, 2004).

The Bode plot is a convention for representing the change in amplitude frequency response and the phase frequency response produced by a linear system (Jagacinski & Flach, 2003).

It includes two curves. The gain or magnitude curve is depicting the amplitude $M(\omega)$ in decibels ($20\log(M)$) versus logarithm of frequency. The phase curve is depicting phase angle in degrees versus the logarithm of frequency.

The following example from Nise (2004) will clarify how a Bode plot is derived from a transfer function. Let us assume we have the transfer function $g(s) = \dfrac{1}{s+2}$. By substituting $s = j\omega$, we obtain $g(j\omega) = \dfrac{1}{j\omega+2} = \dfrac{2-j\omega}{\omega^2+4}$. The magnitude of $g(j\omega)$ is $\left|g(j\omega)\right| = M(\omega) = \dfrac{1}{\sqrt{\omega^2+4}}$. The phase angle of $g(j\omega)$ is:

$$\phi(\omega) = \tan^{-1}\left(\dfrac{-\dfrac{\omega}{\omega^2+4}}{\dfrac{2}{\omega^2+4}}\right) = -\tan^{-1}\left(\dfrac{\omega}{2}\right)$$

The Bode plot of $g(s)$ is the following.
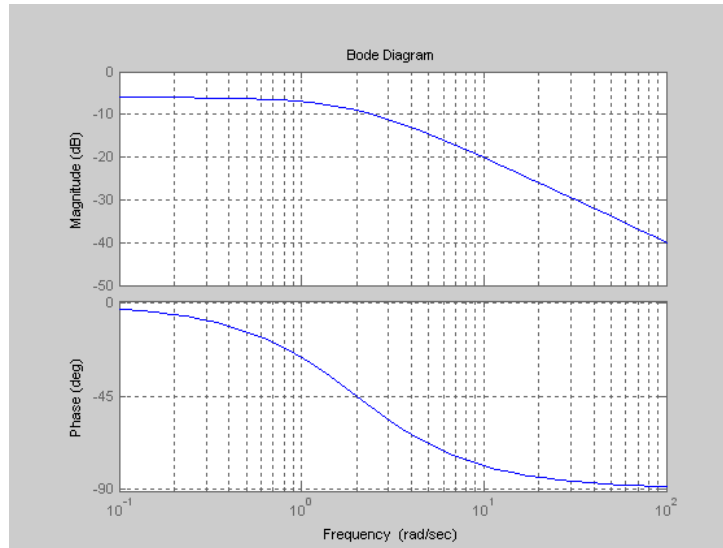
Figure 4: Bode plot of $g(s) = 1/(s+2)$

D. VESTIBULAR SYSTEM

The vestibular apparatus is located in the labyrinth at each inner ear and consists of two principal sets of structures or organs: the semicircular canals (SCC) and the otolith organs that work together to provide head motion and orientation information (Howard, 1986b).
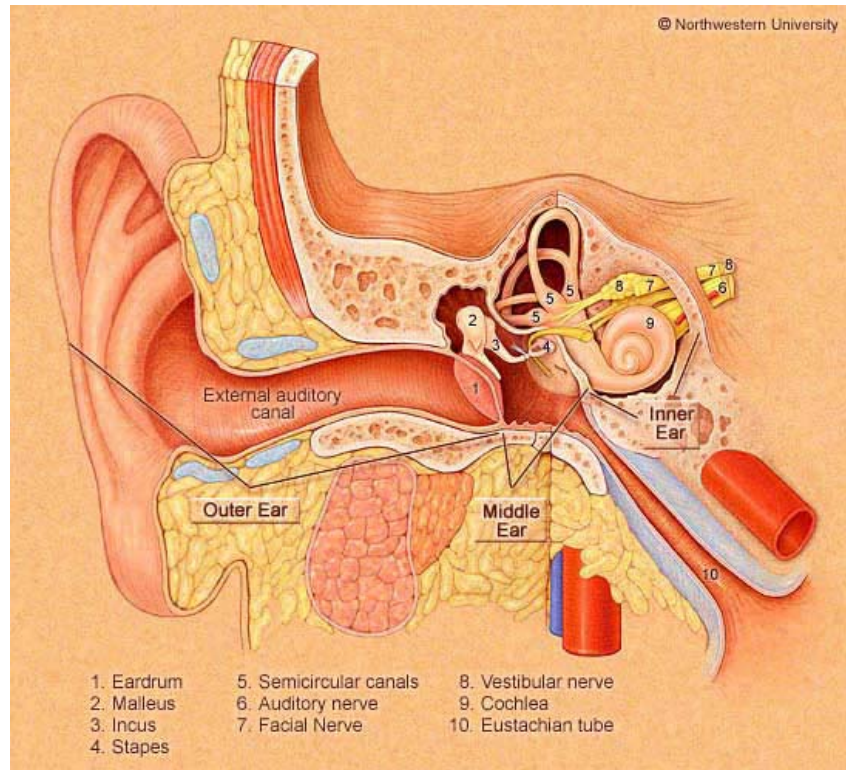
Figure 5: Overview of the vestibular system (downloaded
from **www.dizziness-and-balance.com**, 01-26-03)
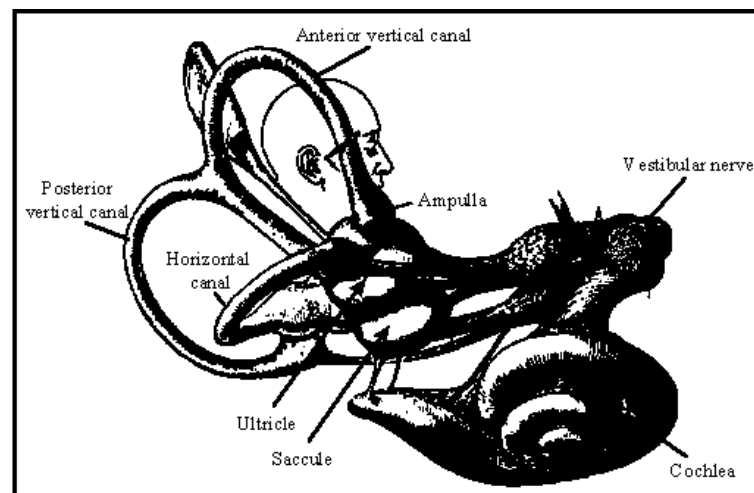
Figure 6: The vestibular system (from Hardy, 1934)

The main functions of the vestibular system are:

13

- To minimize the retinal image motion (slip) during head/body movements by rotating the eyes and keeping gaze stable in space, thus, maintaining visual acuity,

- To enhance the perception of spatial orientation and self-motion (locomotion), and

- To enable the control of posture and equilibrium.

From a technical point of view, the vestibular system is an inertial sensor system detecting and measuring 6 degrees of freedom. There are three semicircular canals (called anterior, posterior, and horizontal) in each vestibular organ. The SCCs are endolymph-filled semicircular ducts almost perpendicular (orthogonal) to each other. Individuals with partial or complete loss of vestibular functioning have found it difficult to perform even the most basic of tasks (Howard, 1986a).
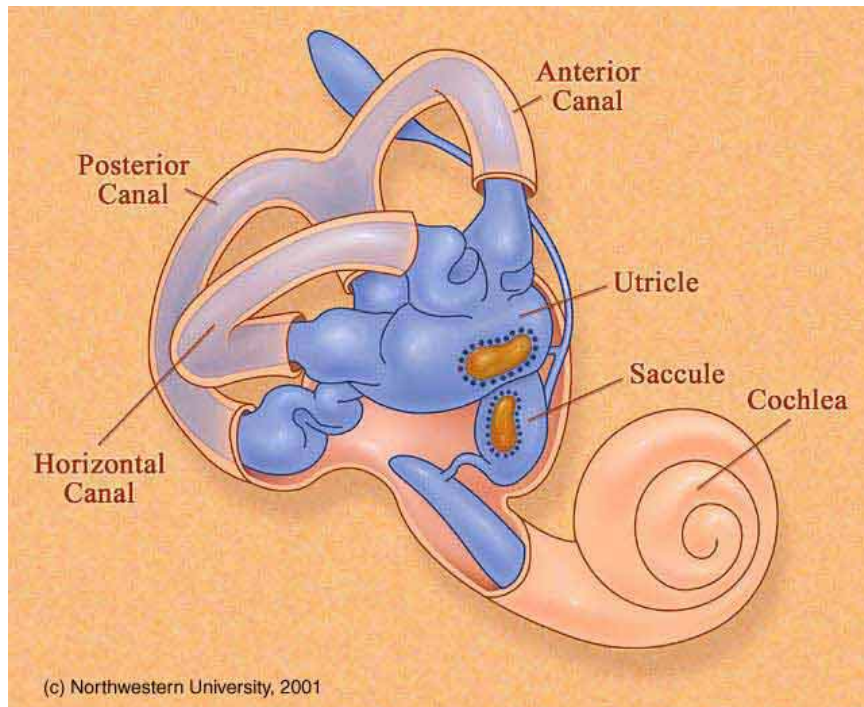
Figure 7: The semicircular canals (downloaded from www.dizziness-and-balance.com, 01-26-03)

One is approximately horizontal, whereas the anterior and posterior are vertical and approximately 45° from the sagittal plane.
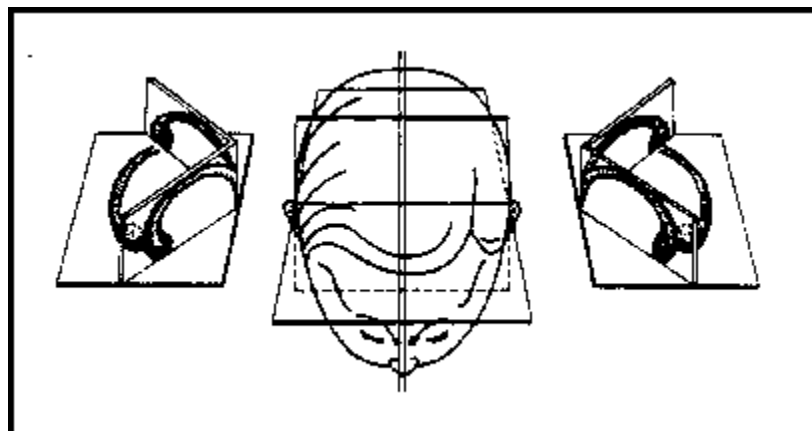
Figure 8: Orientation of semicircular canals

The SCCs work in pairs, thus each canal has a partner in the other labyrinth. Their organization is push-pull (when one is maximally excited the other is maximally inhibited).

The semicircular canals detect rotational motion (angular acceleration). When there is a change in head rotation speed, the endolymph fluid lags behind because of inertia, pushing on and distorting the cupula. Though sensitive to rotational acceleration, the SCC efferent signal is proportional to head rotational velocity for most normal head movements (Howard, 1986a). The SCCs response threshold is as low as 0.1 deg/sec^2.

Each vestibular apparatus contains two otolith organs (two membranous sacs) called the utricle and the saccule (Howard, 1986b). The utricle and the saccule consist of a two-layer structure (the otolithic membrane), which is attached to a base containing sensory cells. The upper layer of the membrane is the otoconial layer and the lower part is the gelatinous layer. A portion of the membrane is thickened and is called the macula, which is rigidly attached to the skull and therefore moves with the head. The macula contains hair cells innervated by neurons of the 8th cranial nerve. The hair cells project into the gelatinous substance (the otolith membrane). Calcium carbonate crystals, which are called otoconia or "ear stones", are embedded in this gel and add mass to the membrane.
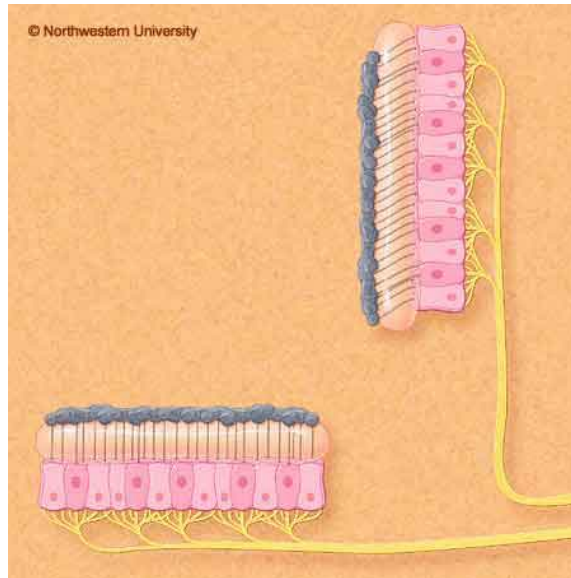
Figure 9: Otolith organs (utricle and saccule)
(downloaded from **www.dizziness-and-balance.com**, 01-26-03)

The otoliths provide linear motion sensation, through the activation of the hair cells, to the central nervous system (CNS). The utricle's macula is located approximately in the horizontal plane and thus is sensitive to horizontal linear accelerations. The saccule's macula is located vertically and thus is sensitive to vertical linear acceleration, including gravity (Robinson, 1981).

These organs are responsive to specific force, the gravitoinertial reaction force per unit mass, which is defined as $\vec{f} = \vec{g} + \vec{a}$ where $\vec{a}$ is the head acceleration with respect to a body-fixed reference system and $\vec{g}$ is the local gravitoinertial force vector.

The otoliths respond to both linear acceleration of the head and tilting of the head with respect to the gravity vector. The utricle primarily senses motion in the longitudinal and lateral planes, while the saccule primarily senses motion in the vertical plane. The otolith reference

frame is fixed to the head and, thus, motion in this frame is relative to the head.

According to Einstein's equivalence principle, linear accelerations experienced during translational motion are physically indistinguishable from changes in orientation relative to gravity experienced during tilting movements. Therefore, otolith afferents can not distinguish between linear acceleration and gravity. This problem is referred to as gravito-inertial force (GIF) resolution. Despite these ambiguous sensory cues provided by the primary otolith afferents, the brain resolves the ambiguity problem by integrating/ combining multi-sensory information so as to resolve the ambiguity (perceptual and motor responses discriminate between gravity and translational acceleration) (Angelaki, Wei, & Merfeld, 2001).

1. Mathematical Models of the Otolith Organs

Meiry (1965) investigated subjective responses to linear motion by measuring the subjective indication of direction. His transfer function of perceived velocity to actual velocity is:

$$\frac{\hat{v}(s)}{v(s)} = \frac{K\tau_1 s}{(\tau_1 s + 1)(\tau_2 s + 1)} \tag{1.3}$$

Where:

- $\hat{v}(s)$ is the perceived velocity

- $v(s)$ is the actual velocity

- Long time constant $\tau_1 = 10$ sec

- Short time constant $\tau_2 = 10$ sec

18

- Gain K is undetermined

The revised model, which modelled both perceived tilt and acceleration in response to acceleration input (Young & Meiry, 1968), is the following:

$$\frac{\hat{f}(s)}{f(s)} = \frac{0.4(13.2s + 1)}{(5.33s + 1)(0.66s + 1)} \tag{1.4}$$

Where:

- $\hat{f}(s)$ is the perceived acceleration by the otoliths

- $f(s)$ is the acceleration input signal

This model acts as velocity transducer over the frequency of 0.19 to 1.5 rad/sec.

Ormsby developed a model of otolith motion based on a mass-spring model (Ormsby, 1974). This model was later refined (Grant & Best, 1986, 1987; Grant, Best, & LoNigro, 1984). The general form is the following:

$$\frac{x(s)}{f(s)} = \left(1 - \frac{\rho_e}{\rho_o}\right) \frac{\tau_1 \tau_2}{\left(1 + \tau_1 s\right)\left(1 + \tau_2 s\right)} \tag{1.5}$$

Where:

- The term $\left(1 - \dfrac{\rho_e}{\rho_o}\right)$ refers to the system sensitivity or gain to the stimulus. The time constants τ_1, τ_2 are related to the lumped parameters.

Grant and Best (1987) calculated the time constants of the model through theoretical continuum mechanics analysis.

Fernandez and Goldberg (1976b) studied the discharge of peripheral otolith neurons in response to sinusoidal force variations in the squirrel monkey and proposed a model that takes into account both regular and irregular units. Their transfer function has the form:

$$\frac{AFR(s)}{f(s)} = G_s \left(\frac{1+k_A\tau_A s}{1+\tau_A s} \right) \left(\frac{1+k_V(\tau_V s)^{k_V}}{1+\tau_M s} \right) \Rightarrow$$

$$\Rightarrow \frac{AFR(s)}{f(s)} = G_s H_A(s) \frac{H_V(s)}{H_M(s)}$$

(1.6)

Where:

- $AFR(s)$ is the afferent signal of the peripheral otolith neurons

- $f(s)$ is the sinusoidal motion

- G_s is the static sensitivity in terms of afferent firing rate per unit of acceleration

- $H_A(s)$ is the adaptation operator

- $H_V(s)$ is a velocity-sensitive operator with a fractional exponent ($k_v < 1$)

- $H_M(s)$ is a first order lag operator

Finally, Telban, Cardullo and Guo (2000), by selecting time constants and the gain from prior models, proposed the following transfer function for otoliths:

$$\frac{AFR(s)}{f(s)} = 33.3 \frac{(10s + 1)}{(5s + 1)(0.016s + 1)} \qquad (1.7)$$

Where:

- $AFR(s)$ is the afferent signal of the otolith dynamics

- $f(s)$ is the input motion

E. VISUAL SYSTEM

The sensory detectors of the eye are sensitive to wavelengths in the spectrum of approximately 370 nm to 730 nm. Light passes through the cornea, which provides the majority of focusing. The rest of focusing is accomplished by the lens, whose power depends on the object's distance from the observer. The lens is active (its curvature changes) at distances from 20 cm (near point) to 3 m (far point).
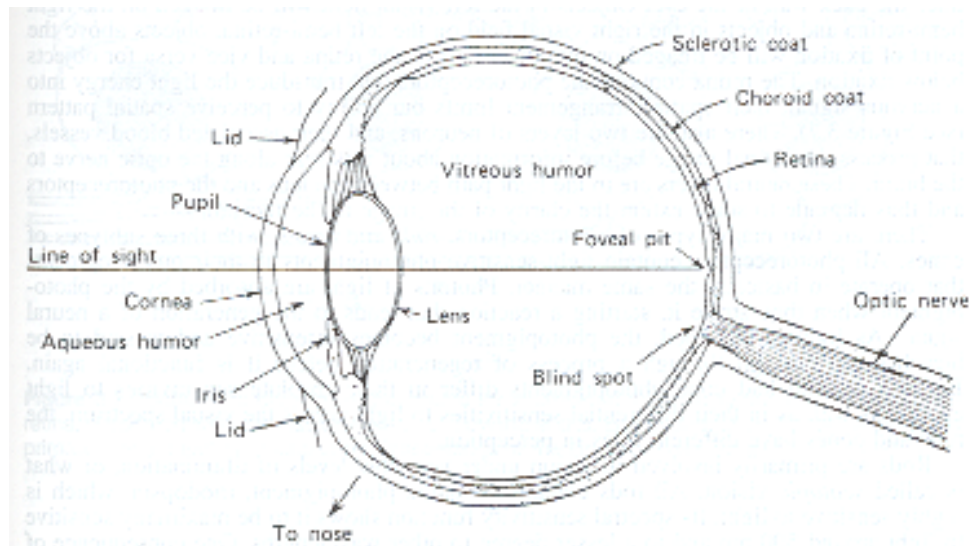
Figure 10: Structure of the human eye (Proctor & Proctor, 1997)

This process at the lens, called accommodation, is needed to localize the focal point at the retina.

When the eyes fixate on an object at a distance of approximately 6 m or further, the lines of sight are parallel. As the object is moved closer the lines converge (a process called vergence) (Proctor & Proctor, 1997).

The visual system is insensitive to images that are stabilized at the retina.

```
Abrupt ——— Conjugate ———— SACCADES
                           FAST PHASES OF NYSTAGMUS


                                   SMOOTH PURSUIT
Smooth ——— Conjugate <——— OPTOKINETIC SLOW PHASE
                                   VESTIBULAR SLOW PHASE

        Disjunctive        VERGENCE
```
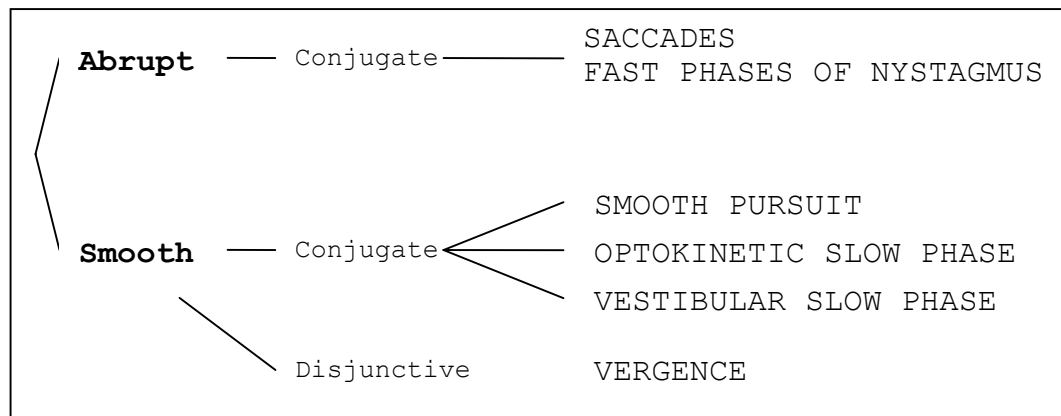
Figure 11: Classification of eye movements (Hallett, 1986).

There are two categories of eye movements, which are of concern:

- Saccadic eye movements involve a rapid shift in fixation from one point to another. Typically, four to five saccadic movements will be made each second (Proctor & Proctor, 1997). Most saccades are around 50-msec duration (20-150 msec), usually less than 15° in amplitude (3 min arc to 70°) of simultaneous onset (e.g., ±5 msec or better), and similarly directed (i.e. conjugate) in the two eyes. Fast phases of nystagmus

are believed to be very similar in al respects (Hallett, 1986).

• Smooth pursuit movements are those made when a moving stimulus is tracked by the eye. Pursuit is relatively accurate for relatively slow moving targets with increasingly greater error occurring as movement speed increases (Proctor & Proctor, 1997). Smooth movements are easily separated into those similarly directed (conjugate) and those oppositely directed (disjunctive). Otherwise all smooth movements are similar and relative contributions can only be estimated by changing the viewing conditions and instructions (Hallett, 1986).

1. Retinal Slip

For the purposes of this paper, the main issue concerning the visual system is the error signal produced when the oculomotor plant is involved in smooth pursuit movements.

In this kind of movement, the eye is continuously tracking the target to stabilize gaze on it.

If the image on the retina stays fixed, it means that the stabilization mechanisms involved have sensed correctly the externally induced motion (we assume only passive subjects' movements), estimated accurately the output motor command and, finally, the oculomotor plant which received the command has acted accordingly without lags.

Unfortunately, in reality multiple errors are combined, thus creating inaccurate gaze stabilization. The outcome is a shifted target image on the retina.

The rate of image shifting is called retinal slip.

F. VESTIBULO-OCULAR REFLEXES (VOR)

1. Background

When moving, it is of great importance to avoid degradation of visual functions. For effective vision, the eyes must be held steady with respect to the object under focus. This is achieved with two required eye-stabilization reflexes, one to compensate for movements of the head and one to compensate for movements of the object. The vestibulo-ocular reflexes (VOR) are driven by vestibular stimuli (otolith organs, semicircular canals). The cervico-ocular reflexes are driven by receptors in the neck, and may be seen as part of arthro-ocular reflexes.

When the subject is rotated about a vertical axis, the eyes are rotated in the opposite direction of rotation to stabilize the retinal image. This eyes' motion is the slow phase (pursuit) of the response. The eyes after pursuing the target for a certain time, return rapidly in order to begin the same motion sequence again. This saccadic movement is the quick phase of the response and is extremely rapid (almost 800 °/sec).

Origin of Signals	Response of Eyes	Characteristics
Vestibular Canals		
Rotary Acceleration	Nystagmic slow phase	A short-latency, high gain, compensatory pursuit movement of the eyes in phase with head position
Rotary Acceleration	Nystagmic deviation	A deviation of the eyes in phase with head velocity
Unknown	Nystagmic quick phase	A saccadic return of gaze, following slow phase of nystagmus
Deceleration	Postrotary nystagmus	Phase-reversed nystagmus persisting for about 20 sec after rotation ceases
Recovery from vestibular adaptation	Secondary nystagmus	A second phase-reversed nystagmus following postrotary nystagmus
Vision		
Visual motion	Optokinetic pursuit of stationary scene	A long-latency pursuit of the visual scene supplementing vestibular nystagmus at low or constant velocities of body rotation
Visual integrator	Optokinetic afternystagmus	A continuation of optokinetic nystagmus after cessation of simulation
Otolith Organs		
Linear acceleration	Deviation	Steady eye deviation opposite to linear body acceleration
Head tilt	Countertorsion	Tendency of eyes to remain upright when head is tilted (up to 10°)
Head inclination	Doll's eye reflex	Tendency of eyes to remain level
Proprioceptors		
Neck rotation	Cervico-ocular nystagmus	A low-gain nystagmus induced by neck proprioceptors
Neck rotation	Cervico-ocular deviation	A deviation of eyes induced by neck proprioceptors
Twisting of trunk or walking around	Arthro-ocular nystagmus	Eye movements induced by walking etc.

Table 1: Types of eye movements induced by movements of the
head and body (Howard, 1986a)

The vestibular reflexes, depending on the responses generated, are subdivided into (Paige, 1991a; Schwarz, Busettini, & Miles, 1989):

- Angular VOR (AVOR) – generating oculo-motor responses to angular head rotation

- Translational VOR (TVOR) – generating oculo-motor responses to linear head motion. TVOR depends on target distance and target orientation (Paige, 1989, 1991b; Paige & Tomko, 1991b; Schwarz et al., 1989; Schwarz & Miles, 1991; Tomko & Paige, 1992).

The total VOR is the sum of the angular and translational VOR (Paige & Sargent, 1991).

2. Vestibulo-ocular Nystagmus

Any rhythmic involuntary motion of the eyes (compensatory movements) used to maintain the image on the retina stable irrespectively of the observer's movements is known as nystagmus. When induced by vestibular stimulation, it is called vestibular nystagmus.

In the following figure we see how the VOR compensates for the head movements to achieve gaze stability.
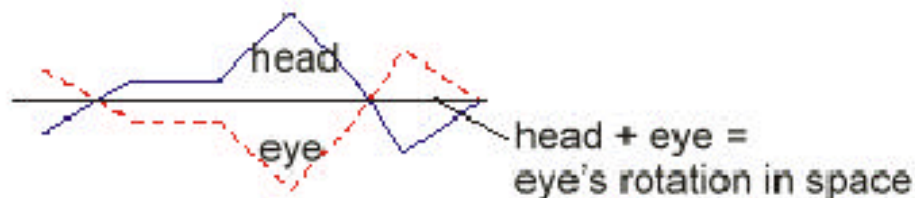
Figure 12: VOR compensation

The general case of vestibular nystagmus is the following:
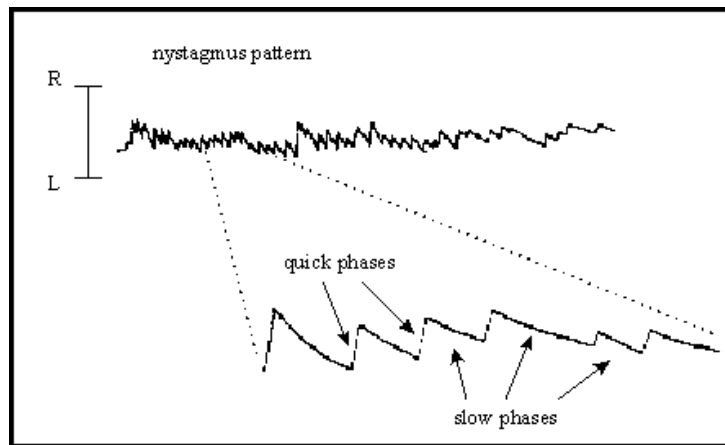
Figure 13: Nystagmus pattern and phases

During head motion the vestibular nystagmus (which is exponential) is generating the slow phases that keep our eyes on target. When the eye approaches the limits of the oculomotor range, a saccade (quick phase) is generated in the opposite direction.

According to Angelaki and colleagues (2000), the otolith-ocular responses in primates are classified into three functional categories (Angelaki, 1998; Angelaki & Hess, 1996a, 1996b; Hess & Angelaki, 1997a, 1997b):

1) Translational vestibulo-ocular reflexes (TVOR), which generate short-latency, high-frequency horizontal and vertical eye movements that are compensatory to linear translation (Angelaki, 1998; Angelaki, McHenry, & Hess, 2000; Angelaki, McHenry, Newlands, & Dickman, 1999; Paige & Tomko, 1991a, 1991b; Schwarz & Miles, 1991; Telford, Seidman, & Paige, 1997);

27

2) A neural system that encodes the angular velocity of the head in space, referred to as the "inertial vestibular system" (Angelaki & Hess, 1994, 1995; Merfeld & Young, 1995; Merfeld, Young, Oman, & Shelhamer, 1993; Merfeld, Young, Paige, & Tomko, 1993). A manifestation of the inertial vestibular system is the sustained steady-state nystagmus during constant velocity off-vertical axis rotations (OVAR) and the low-frequency enhancement of the VOR dynamics during sinusoidal oscillations (Angelaki & Hess, 1996b; Cohen, Suzuki, & Raphan, 1983; Correia & Guedry, 1966; Correia & Money, 1970; Harris, 1987; Rude & Baker, 1988; Tomko, Wall, & Robinson, 1988);

3) Linear acceleration-dependent modulation of mean torsional and vertical eye position (counter-rolling and counter-pitching, respectively) (Citek & Ebenholtz, 1996; Collewijn, Van der Steen, Ferman, & Jansen, 1985; Diamond, Markham, & Simpson, 1979; Ebenholtz & Shebilske, 1975; Hannen, Kabrisky, Replogle, Hartzler, & Roccaforte, 1966; Kellogg, 1965; Lichtenberg, Young, & Arrott, 1982; Merfeld, Teiwes, Clarke, Scherer, & Young, 1996; Woellner & Graybiel, 1959; Young et al., 1981).

The angular vestibulo-ocular reflex (AVOR) adapts its behavior in response to image motion across the retina associated with head movements. The combination of signals required for such adaptation occurs naturally in instances such as changes in the peripheral vestibular system associated with aging or illness, as well as with optically induced changes in vision.

28

The VOR response depends, among other factors, on the duration of head motion. Constant velocity or prolonged motions lead to VOR stop.

In general, the vestibular reflexes operate in open-loop, are very rapid and work best for higher frequency velocity movements of the head (Benson, Guedry, & Jones, 1970; Keller, 1978; Wilson & Jones, 1979). The VOR is less accurate for frequencies lower than 0.1 Hz.

3. Interaction between Vestibular Nystagmus and Visual Pursuit

The VOR is decreased or eliminated during large saccades. It increases gradually as gaze error becomes small and becomes fully operational during the final part of the head movement, when the gaze is on target but the head is still completing its motion (Guitton & Volle, 1987; Laurutis & Robinson, 1986; Tomlinson & Bahra, 1986; Tweed, Glenn, & Vilis, 1995).

Optimally, the brain should shut off the VOR in the direction of the saccade but leave it on in other directions, because only head movements in the direction of the saccade should affect the motion of the eye in space. This design specification is at least roughly implemented in the actual VOR, which switches off in the direction of the saccade (Guitton & Volle, 1987; Laurutis & Robinson, 1986; Tomlinson & Bahra, 1986) , but remains on in the opposite (Pelisson & Prablanc, 1986; Pelisson, Prablanc, & Urquizar, 1988) and orthogonal directions (Tomlinson & Bahra, 1986) .

It has been shown that saccadic movements of the eye plant and visual pursuit are inherently modulated by the gravity vector (Hess & Angelaki, 2003).

G. OPTOKINETIC REFLEX (OKR) AND OPTOKINETIC NYSTAGMUS (OKN)

The optokinetic reflex is the mechanism that generates compensatory eye movements, and thus stabilized gaze, through visual input alone. The generated eye movements are called optokinetic nystagmus (OKN).

In general, the optokinetic reflexes operate in closed-loop, are slower than vestibular reflexes, and have a better response at lower frequencies (Baarsma & Collewijn, 1974; Michael & Jones, 1966). The OKN has the opposite performance characteristics compared to VOR. Its latency is much longer due to the time needed to process visual input. At frequencies lower than 0.1 Hz, OKN is more accurate than VOR. At frequencies between 0.1 and 1 Hz its gain is decreased and a phase lag is developed (Peterka, Black, & Schoenhoff, 1987).

H. MODELS OF VISUAL – VESTIBULAR INTERACTIONS

The proposed model deals with smooth pursuit eye movement, which is the eye-tracking response. As shown by Robinson (1977), this pursuit movement does not function to keep the entire retinal image from slipping, but only the image on the fovea.

Research has shown that eye velocity signals (eye movement commands) are referenced to a space frame rather than to a head frame (Hess, 2001; Tweed, 1997).

1. The Visual-vestibular Gaze Stabilization Model of Robinson

In 1977 Robinson proposed a model that accounts for how visual and vestibular signals cooperate to produce eye

movements, which stabilize retinal images. The hypothesis supported was that the optokinetic and semicircular-canal (vestibular) signals are combined simply by linear addition in the cells of the vestibular nucleus (Robinson, 1977).
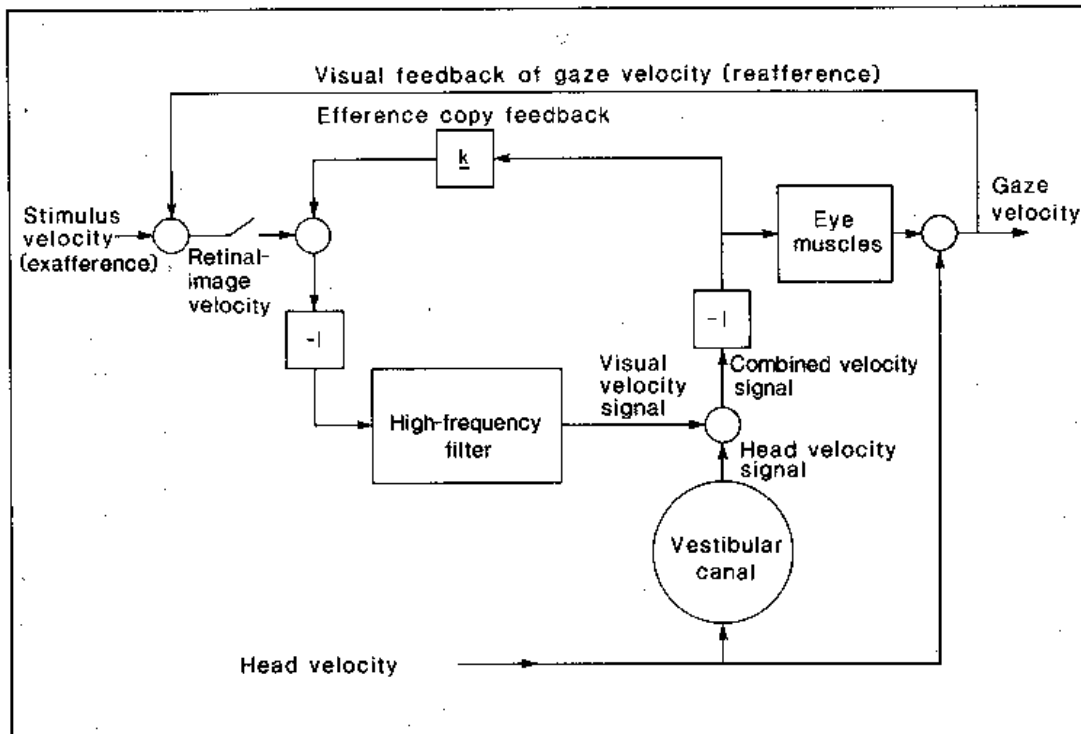
Figure 14: Simplified version of the visual-vestibular gaze stabilization model proposed by Robinson in 1977 (Howard, 1986a)

In Robinson's model, the retinal image is moving on the retina at a velocity that depends on the velocity of the stimulus, the head movement and the pursuit eye movements.

Starting at the left of the diagram in Figure 14, the stimulus velocity is combined with the visual feedback to generate the retinal image-slip velocity signal. This signal is modulated by the prediction information of the current eye movement. The error has the form of the resulting

31

retinal slip velocity due to the feedback of the efferent signals to the eye muscles.

The high-frequency filter rejects high frequency visual signals, and the resulting visual velocity signal is added to the velocity signal from the vestibular system. The final signal to the oculomotor system muscles is phase shifted and fed to the eye muscles to achieve stabilization of the retinal image.

2. The Gaze Stabilization Model of Panerai, Metta, and Sandini

A limitation of Robinson's initial model is that it deals only with rotational VOR.

Panerai, Metta, and Sandini (2000b) proposed a model concerning visual-vestibular stabilization of gaze, which was later successfully used in the stabilization of a robot gaze (Panerai et al., 2000b; Sandini, Panerai, & Miles, 2001). This model accounts for rotational and translational VOR.

In the following paragraph we shall only describe the model dealing with TVOR.

In general, stabilization performance is related to target-head distance and TVOR is inversely proportional to the viewing distance (Paige, 1989; Schwarz et al., 1989; Schwarz & Miles, 1991; Telford et al., 1997). Especially, TVOR depends on the direction of gaze with respect to the direction of heading (Howard, 1993; Paige & Tomko, 1991a, 1991b).

The vestibular stabilization information is added linearly with the visual information. The major part of the

TVOR depends on target distance d; only a small fraction of
TVOR is not related to visual target distance.

The aforementioned characteristics are depicted in the
following model diagram.
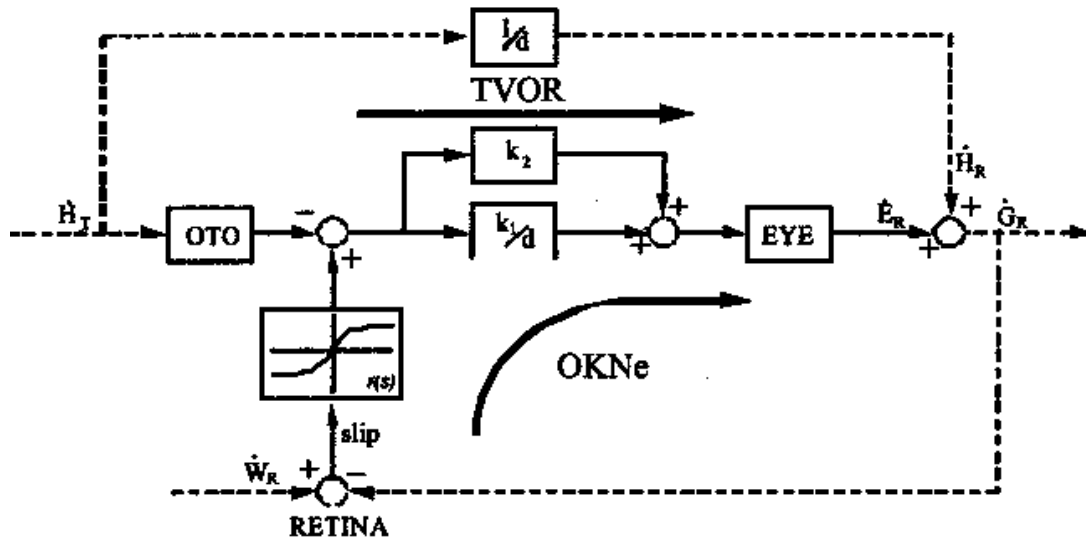
Figure 15: Linkage between visual and vestibular
reflexes stabilizing gaze (Sandini et al., 2001)

Where:

- $\dot{H}_T$ is the translational movement of the head in
linear coordinates

- $\dot{H}_R$ is the translational movement of the head in
angular coordinates

- $\dot{E}_R$ is the translational movement of the eyes
relative to head, in angular coordinates

- $\dot{G}_R$ is the translational movement of gaze relative
to space, in angular coordinates

33

- $\dot{W}_R$ is the translational movement of the visual surroundings in angular coordinates

- d is distance between the subject's head and the visual target

- $\dfrac{k_1}{d}$ is the variable gain element, which depends on visual target distance

- k_2 is the fixed gain element

The researchers, by evolving the proposed model, created an adaptive neural network enabling robots to "learn stabilization reflexes" (Panerai, Metta, & Sandini, 2000a).

The basic structure of the model is depicted in the following diagram.
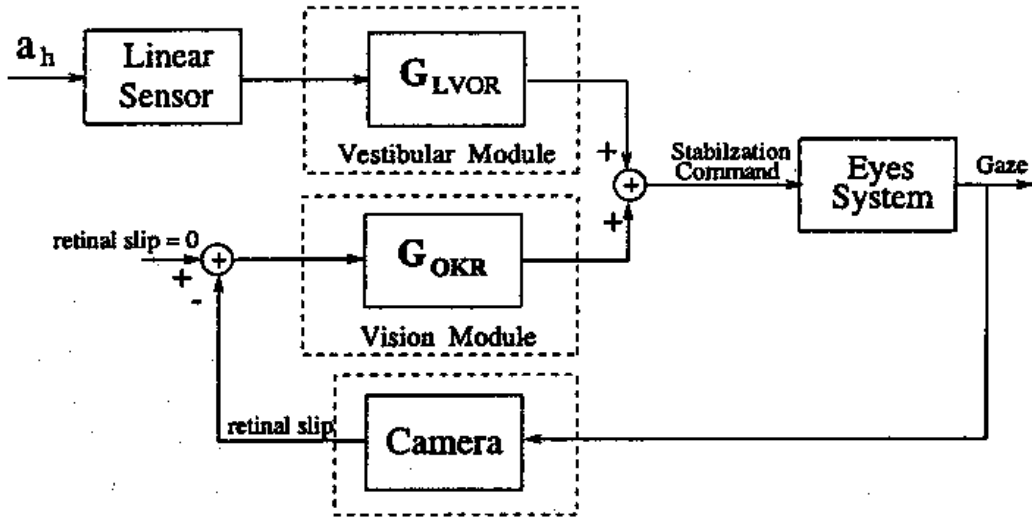
Figure 16: Block diagram of visuo-inertial mechanism to stabilize robot's gaze. The linear accelerometer senses translational movements of the head (Panerai et al., 2000b)

34

The Panerai et al. model will be the basis of the visual subsystem in the model proposed in the present paper. The main characteristics (addition of VOR and OKN, combined gain element) will be the same. The vestibular input signal will be derived from the proposed vestibular error estimation subsystem.

I. MOTION SICKNESS

Motion sickness is a general term that describes the discomfort and associated emesis induced by numerous kinds of motions. Unfortunately, the term is a misnomer according to Benson (1999):

- Motion sickness may be induced in the absence of motion as during a virtual reality simulation.

- "Sickness" implies that it is a type of disease, when in fact it is a perfectly normal response of a healthy individual without any functional disorders.

1. Causal Factors of Motion Sickness

The most widely accepted theory is called by several names, the conflict mismatch theory, sensory rearrangement theory (Reason & Brand, 1975) or neural mismatch theory (Benson, 1999). According to the above theories, the cause of motion sickness is that the vestibular apparatus provides the brain with information about self motion that does not match the sensations of motion generated by visual or kinaesthetic (proprioceptive) systems, or what is expected from previous experience (Wertheim, 1998). As Reason noted, incongruity among the normally synergistic channels of information (principally the eyes, the vestibular system and

the proprioceptive receptors in the joints, tendons and muscles) is the causal factor (Reason, 1978b).

The neural mismatch hypothesis is comprised of two basic components (Reason & Graybiel, 1973):

- A neural storage unit that retains the informational characteristics of the previous sensory input.

- A comparator unit that matches the contents of the store with the informational characteristics of the prevailing sensory influx from the motion and position senses.
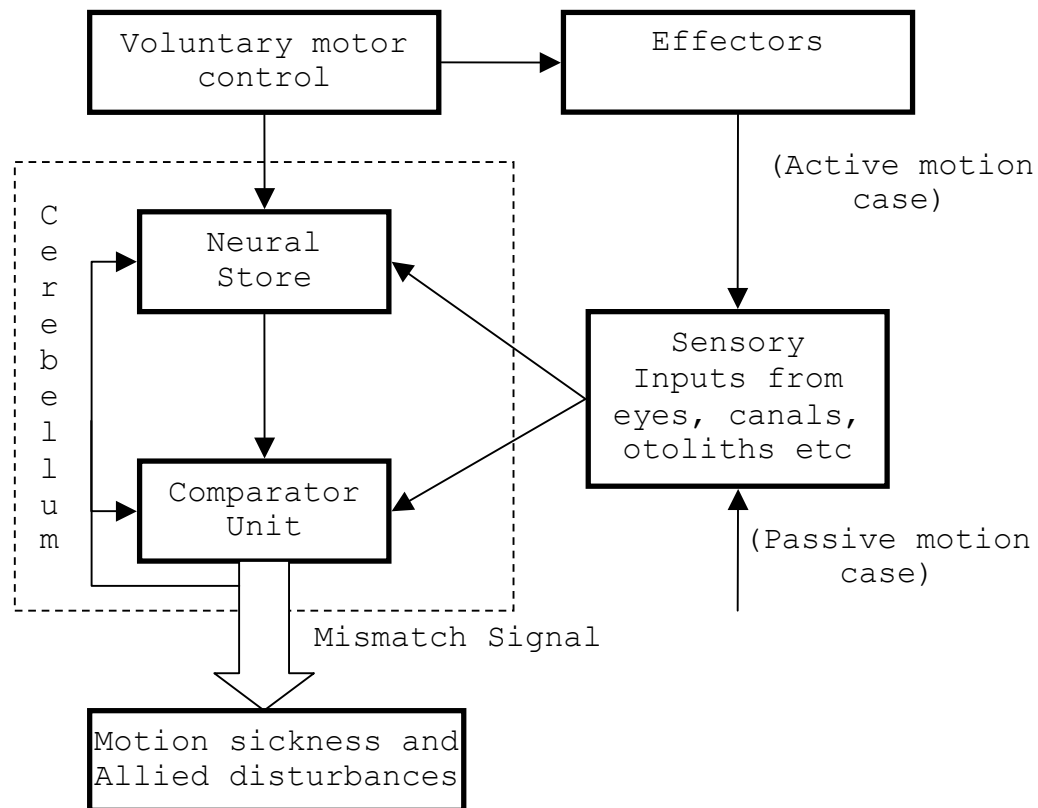
Figure 17: Structural components of Reason's (1978) revised neural mismatch model.

Motion sickness is the outcome of the mismatch between the total pattern of information from the spatial senses and that held in store. Thus motion sickness is triggered by the conflict between the prevailing sensory inputs and those expected on the basis of past experience (Reason & Graybiel, 1973). The theoretical concept was based on earlier work by Holst (1954) and Held (1961).

The hypothesis that the central nervous system (CNS) includes an internal model of previous sensory input (sensory dynamics, body dynamics, and physical relationships) has been the basis of multiple proposed observer models (Bos & Bles, 1998; Bos, Bles, & Dallinga, 2000; Bos, Bles, & Hosman, 2001a, 2001b; Glasauer, 1992, 1993; Glasauer & Merfeld, 1997; Merfeld, 1995a, 1995b; Merfeld, Young, Oman et al., 1993; Oman, 1982)

Benson (1988) defined motion sickness as a condition that occurs when people (as well as fish and other animals) are exposed to real or apparent motion stimuli to which they are unfamiliar and hence unadapted.

The sensory conflict may be induced by two main categories of motion cue mismatches depending on the sensory systems involved, intersensory conflict or an intrasensory conflict. The intersensory conflict deals with the visual-vestibular mismatch and the intrasensory conflict deals with the canal-otolith mismatch. Furthermore, these mismatches are classified into two types of conflicts: type I, when both systems fire simultaneously contradictory motion information, and type II, when one system fires motion in the absence of a corresponding signal from the other system.

Guedry (1991) extended the two initial categories with a third one dealing with vestibular-proprioceptor mismatch and Griffin (1991) included one more type of motion sickness. Table 2 depicts the categories of conflicts and Table 3 depicts the kind of motions that lead to the aforementioned conflicts.

Type of Conflict	Category of Conflict	
	Intersensory (Visual – Vestibular)	Intrasensory (Canal – Otolith)
Type I	Visual and vestibular systems simultaneously signal different (i.e. contradictory or uncorrelated) information	Canals and otoliths simultaneously signal different (i.e. contradictory or uncorrelated) information
Type II	Visual system signals in the absence of an expected vestibular signal	Canals signal in the absence of an expected otolith signal
Type III	Vestibular system signals in the absence of an expected visual signal	Otoliths signal in the absence of an expected canal signal

Table 2: Types and categories of sensory conflict (Griffin, 1991)

Type of Conflict	Category of Motion Cue Mismatch	
	Intersensory (Visual [A] – Vestibular [B])	Intrasensory (Canal [A] – Otolith [B])
Type I A and B simultaneously signal different (i.e. contradictory or uncorrelated) information	Watching waves from a ship Use of binoculars in a moving vehicle Making head movements when vision is distorted by optical device "Pseudo Coriolis" stimulation	Making head movements whilst rotating (Coriolis or cross-coupled stimulation) Making head movements in an abnormal acceleration environment which may be constant (hyper – or hypo-gravity) or fluctuating (linear oscillation) Space sickness Vestibular disorderd
Type II A signals in the absence of an expected B signal	Cinerama sickness Simulator sickness Circular vection	Positional alcohol nystagmus Caloric stimulation of semi-circular canals Vestibular disorders
Type III B signals in the absence of an expected A signals	Looking inside moving vehicle without external reference; below deck in a boat Reading in a moving vehicle	Low-frequency (<0.5 Hz) translational oscillation Rotating linear acceleration vector ("barbeque spit" rotation, rotation about an off-vertical axis)

Table 3: Type of motion cue mismatch produced by various stimuli (Griffin, 1991)

Motion sickness is induced by whole-body vibration at the frequency range between slightly below 0.1 Hz to slightly above 0.5 Hz (Griffin, 1990b). Golding et al. (2001) found that the motion sickness maximum for horizontal translational oscillation was around 0.2 Hz.

In general, vertical oscillation is the principal provocative stimulus at sea (Griffin, 1990b; McCauley et al., 1976; Morales, 1949; O'Hanlon & McCauley, 1974). The effects are greatest between approximately 0.125 Hz and 0.25 Hz. Increase in acceleration magnitude of this frequency of vertical oscillation and in the duration of exposure over many hours leads to increased sickness. Aboard a ship, the two main sources of vertical motion are heave and pitch (the effect of pitch depends on the individual's position relative to the axis of rotation). The principal effect of higher sea states is an increase in magnitude rather than a change in frequency. The main vertical acceleration of most ships is close to 0.2 Hz, just where motion sickness sensitivity is believed to be at a maximum (Griffin, 1990b; McCauley et al., 1976).

Money (1970) suggested that the extent of motion sickness incidence related to various modes of transportation is determined in part by the frequency and acceleration response of the vehicle to its environment, the susceptibility of the individual, and the amount of recent exposure of the passenger or crew to a similar motion environment. Howarth and Griffin (2003) concluded that motion sickness associated with pure roll oscillation will usually be less than the sickness associated with pure translational oscillation or the sickness associated with combined translation and rotation.

In general, precise estimate of motion sickness incidence is difficult to derive and individual differences in susceptibility are large (Dobie, 2000; Kennedy, Dunlap, & Fowlkes, 1990). There are numerous factors involved; for example (Dobie, 2000):

- The characteristics of the stimulus in terms of frequency, intensity, direction, and duration of the motion.

- The susceptibility of the individual, based upon physiological characteristics, past experiences, psychological and personality factors.

- Individual activity at the time of exposure to the stimulus.

- Other factors, such as food, ambient air temperature, and maybe certain odors.

Numerous studies have dealt with the incidence of motion sickness at sea, but the results are extremely variable (for example, over 90% (Hill, 1936), 25%-30% (Chinn, 1951), 10%-30% (Pethybridge, 1982)). There exists a major difference between MSI observed in laboratory experiments versus real life data. This difference is attributed to the fact that laboratory research, generally, focuses on simple sinusoidal motion whereas in real-life moving platforms subjects face complex periodic waveforms and aperiodic motions (Guignard & McCauley, 1982).

Studies on small marine craft have found an incidence of emesis ranging 11 to 70% of the crew depending on the sea state (Holling et al., 1944; Tyler & Bard, 1949; Llano, 1955). Emesis was experienced by 15 to 60% of the passengers aboard ships making winter crossings of the Atlantic Ocean during the first few days of the crossing (Chinn, 1956; Chinn, 1963).

a. Drawbacks of Neural Mismatch Theory

According to Oman (1982) there are three major issues that can be seen as drawbacks to the conflict hypothesis underlying Reason's neural mismatch model:

- Guedry has observed that there appear to be "several forms of vestibular stimulation that produce motion sickness without obvious intralabyrinthine conflict or intermodality conflict" (Guedry, 1968).

- Additional hypotheses seem to be needed to account for the transfer of generalized adaptation from one nauseogenic situation to another.

- The limited practical value of the conflict model in its present form, because it is impossible to predict exactly who will become sick in a given situation, and how fast the afflicted will adapt (Parker & Money, 1978; Watt, 1983).

2. Symptomatology

The signs and symptoms of motion sickness include breathing irregularities, yawning, the sensation of warmth, disorientation, pallor, nausea and vomiting (Benson, 1988; Reason & Brand, 1975). The sequence of the symptoms is idiosyncratic and depends on individual susceptibility and the intensity of the motion stimuli.

Numerous researchers have associated the onset of motion sickness with the development of facial pallor, cold sweating, nausea and emesis (Clark & Graybiel, 1961; Crampton, 1955). It has been reported that postural instability precedes motion sickness (Smart, Stoffregen, &

Bardy, 2002). Schwab (1954) noted that motion sickness includes a wide range of minor symptoms that escalate before actual nausea and vomiting occurs.

One interesting issue about the motion sickness symptoms is that emesis does not seem to have a logically established relation to motion sickness causality. It was proposed that the relations between the spatial frameworks defined by the visual, vestibular, or proprioceptive inputs are repeatedly and unpredictably perturbed. Such perturbations may be produced by certain types of motion, or by disturbances in sensory input or motor control produced by ingested toxins. Thus, the latter being the important cause, the main function of emesis is to get rid of the neurotoxins. Therefore, the occurrence of emesis as a response to motion would be an accidental byproduct (Treisman, 1977). As Oman noted, though, "…it has not yet been shown that emetic poisons actually act on the inner ear, or that they cause vomiting if applied there in physiologic doses" (Oman, 1998)

One manifestation of motion sickness is called "sopite syndrome" (A. Graybiel & Knepton, 1976) and is characterized by drowsiness and mental depression, fatigue, difficulty in concentrating and disruption of sleep. Individuals will demonstrate symptoms soon after initial exposure to a provocative stimulus, in some very rare cases after a matter of seconds (Ashton Graybiel, Deane, & Colehour, 1969). Highly susceptible people, or those with low rate of adaptation, may continue vomiting for several days.

3. Susceptibility

The range in susceptibility to motion sickness is wide, both between people (inter-subject variability) and within an individual on different occasions (intra-subject variability) (Griffin, 1990b).

Sex (Benson, 1999; Jokerst et al., 1999; Lawther & Griffin, 1988), age (Benson, 1999; Lawther & Griffin, 1988; Wertheim, 1998), sleep deprivation (Dowd, 1974), and a person's personality and past experiences (Guedry, 1991; Kottenhoff & Lindahl, 1960; Reason, 1972) affect susceptibility to motion sickness.

Cowings and colleagues have reported success in using biofeedback techniques to reduce Space Adaptation Syndrome in astronauts (Kornilova et al., 2003).

Dobie and colleagues found little relation between an individual's level of physical activity and susceptibility of motion sickness (Dobie, McBride, Dobie, & May, 2001).

Reason and Brand (1975) explain susceptibility by noting that the body continuously expects to receive signals from its sensory organs in a recognizable pattern. Thus, motion sickness is the normal response during the period where the body is gradually learning a new signal combination, which is different from the known pattern (mismatch). In this case, susceptibility to motion sickness can be seen as the rate at which the internal model (of expected motion stimuli) can be changed. This rate is affected by three factors: receptivity, adaptability, and retentiveness. Receptivity is the subject's internal amplification of the motion stimulus. Adaptability is the

rate at which the internal model is changed. Retentiveness is the subject's ability to retain the internal model and continuously adapt it to a motion environment in successive exposures (Reason, 1972).

4. Adaptation

According to Money (1970), adaptation describes three different phenomena:

- The "change in response to stimuli", especially a diminution of response ("response decline"),

- "The change in bodily mechanisms that is responsible for the response decline",

- "The acquisition or process of acquiring the change in bodily mechanisms".

The severity of motion sickness symptoms declines over time as the subject adapts to the motion environment. This adaptation and habituation is believed to be a response to changes in acceleration stimuli associated with the growth and aging processes (Collins, 1974; Reason & Graybiel, 1970). Unfortunately, in almost five per cent of the population adaptation does not occur (Hemingway, 1945; Tyler & Bard, 1949)

The following diagram depicts the general timeline of adaptation through the discrepancy between sensory input and the neural store. According to neural mismatch hypothesis, the magnitude and duration of the mismatch signal is directly related to the onset of motion sickness (Reason & Graybiel, 1973).

45
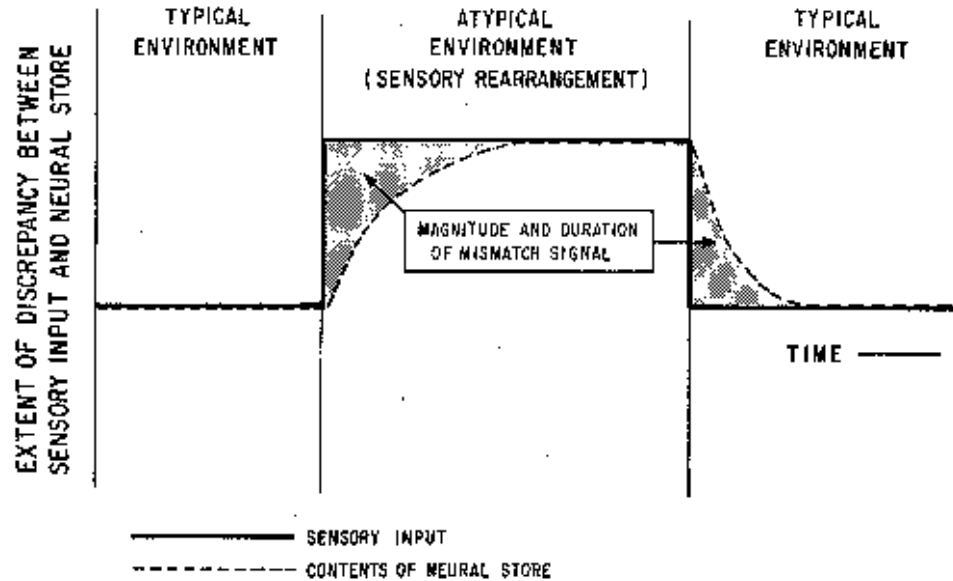
Figure 18: Diagram illustrating the adaptation effects
and after-effects of sensory rearrangement as predicted by
the neural mismatch model (Reason & Graybiel, 1973)

5. Effects of Motion Sickness on Performance

Reseach has shown that motion sickness adversely
affects performance, for example (Colwell, 1989; Hettinger,
Kennedy, & McCauley, 1990). On the other hand, Birren
pointed out that most people who experience transient motion
sickness can exert themselves sufficiently to perform
adequately when necessary (Birren, 1949).

6. Effects of Sopite Syndrome on Performance

One way in which motion sickness affects human
performance is the sopite syndrome. The qualitative effects
of sopite syndrome have been found to be: inefficiency,
accident proneness, and, most interesting, the fact that
this decrement in performance is not readily identifiable by
the sufferer or a supervisor. This latter finding about
sopite syndrome is important because, in many cases, it is
among the cardinal symptoms of motion sickness (A. Graybiel

& Knepton, 1976). In 1954, Schwab noted that in some cases "no visible signs [of motion sickness] are shown by the subject at this point and a great many travelers bothered by motion sickness may pass through this phase alone and never develop further symptoms or complaints because of the termination of their trip" (Schwab, 1954).

Furthermore, it is suggested that sopite syndrome could have profound effects in different transport environments where, for other reasons, sleep disturbances exist (Lawson & Mead, 1998).

Another issue concerning sopite syndrome is that it commonly appears but before nausea and persists well after nausea has disappeared (Dobie, 2003; Lawson & Mead, 1998).

J. MOTION SICKNESS MODELS

There exist multiple attempts by researchers to develop motion sickness models. The two major categories involve models that are not etiologic but merely descriptive, and models that attempt to simulate the main mechanisms involved in the development of motion sickness.

1. Human Factors Research, Inc (HFR) Model

McCauley and O'Hanlon (1974) and McCauley et al (1976), described Motion Sickness Incidence (MSI) as a function of vertical sinusoidal motion with data obtained in a ship motion simulator. The experiments were conducted on more than 500 subjects. Twenty-five combinations of ten frequencies (ranged from 0.083 to 0.700 Hz) and various magnitudes (ranged from 0.27 to 5.5 $m*s^{-2}$ RMS were used. The Motion Sickness Incidence (MSI) was defined as the percentage of subjects who vomited.

The primary contributor to motion sickness was the vertical component of motion, whereas pitch and roll motions had little or no effects. The empirical model predicts MSI (%) from the magnitude, frequency and duration of vertical accelerations (McCauley et al., 1976). The maximum MSI was found to occur at a frequency of 0.167 Hz.

According to McCauley et al. (1976):

$$MSI = 100\Phi(z_a)\Phi(z_t')$$

(1.8)

Where – $\Phi(z)$ is the cumulative distribution function of the standardized normal variable z,

$$\Phi(z) = \frac{1}{2\pi}\int_{-\infty}^{z} e^{-\frac{1}{2}x^2} dx$$

(1.9)

The standardized normal variables z_a and z_t' are defined as:

$$z_a = 2.128\log_{10}(a) - 9.277\log_{10}(f) - 5.809\log_{10}^2(f) - 1.851$$

(1.10)

$$z_t' = 1.13z_a + 1.989\log_{10}(t) - 2.904$$

(1.11)

Where:

- a is the RMS magnitude of the vertical acceleration, in g

- f is the frequency of vertical acceleration, in Hz

- t is the duration of exposure, in min

48

The following figure depicts the MSI predicted by the HFR model.
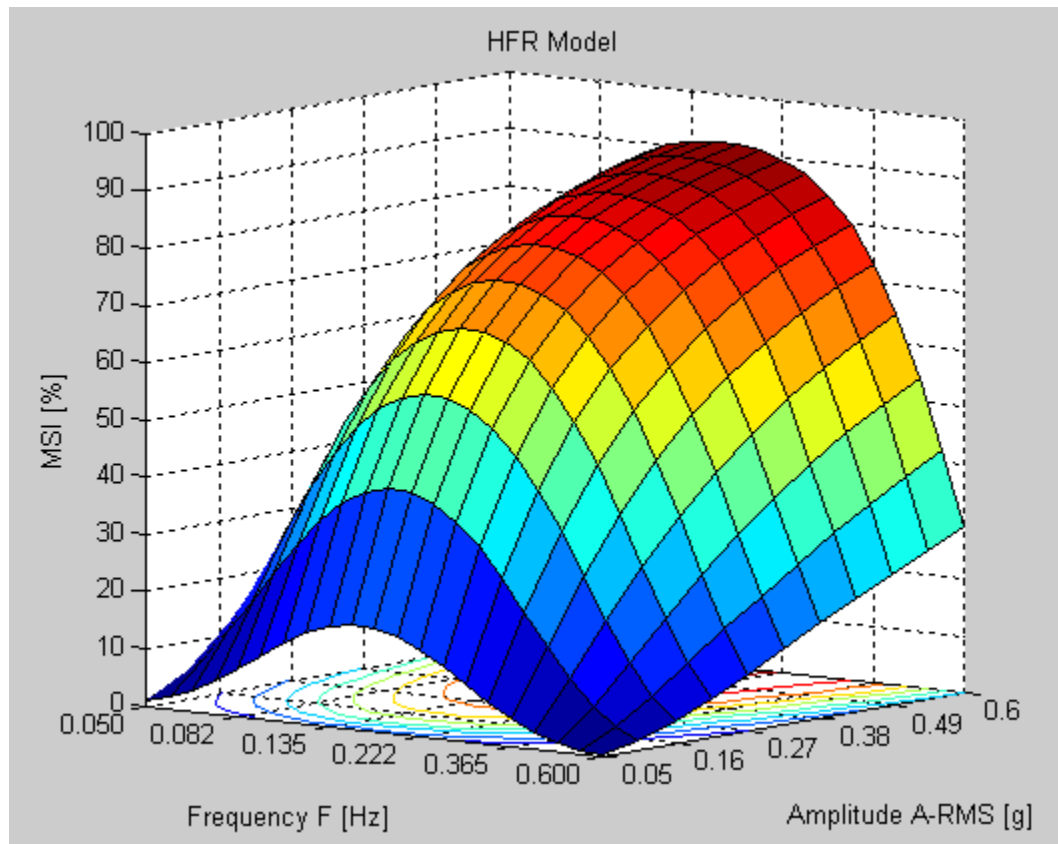
Figure 19: Predicted MSI by the HFR model (McCauley et al., 1976).

2. Oman's Model of Subjective Discomfort

In 1982, Oman proposed a model for the estimation of subjective discomfort. The model postulates a major functional role for sensory conflict signals in movement control and in sensory-motion adaptation. The following diagram depicts the model (Oman, 1982).
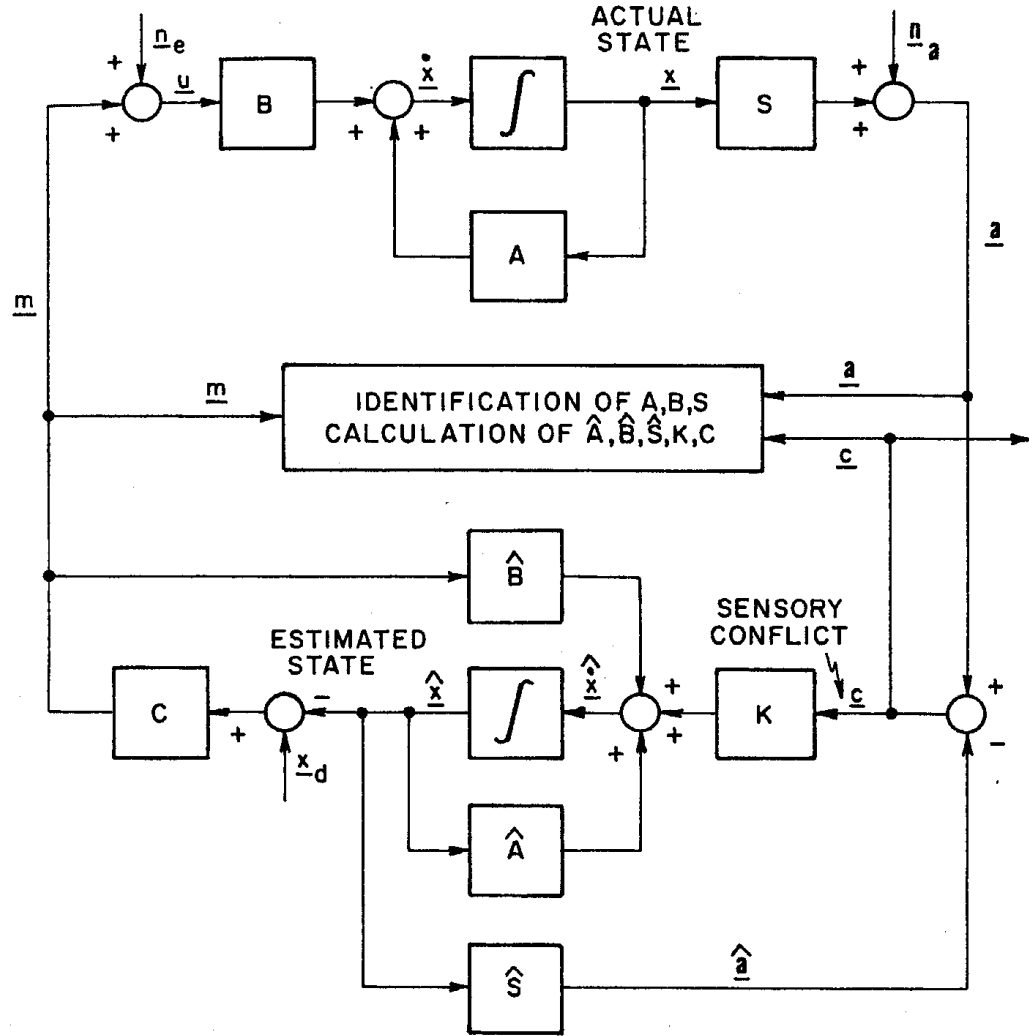
Figure 20: General overview of Oman's model for the
dynamics of sensory conflict and motion sickness (Oman,
1982)

Where:

- x is the body "actual state" vector

- m is the motor outflow vector (from CNS)

- n_e is the external disturbance "noise" vector

- B is the matrix describing the effect of forcing vector u on $\dot{x}$

- A is the matrix describing the effect of x on $\dot{x}$; unforced behavioral characteristics of body and sense organs

- S is the matrix of sensory organ dynamics

- n_a is the sense organ output "noise" vector

- K is a Kalman-type weighting function

- C are the postural control commands

- c is the vector representing the generalized multi-modal sensory conflict

- x_d is the desired state

- $\hat{A}$, $\hat{B}$, and $\hat{S}$ are the internal models of the corresponding entities

The inputs of the model are:

- The external disturbances n_e of an unpredictable nature.

- Vector n_a, which represents noise in each afferent sensory modality.

The output is the generalized multi-modal sensory conflict vector c.

In this model additional symptom production pathways were indicated, such as nausea, pallor, sweating etc.

Oman (1982) noted that conceptual validity can be derived from the proposed model because:

- It incorporates and extends many concepts in the qualitative model proposed by Held (1961), Holst (1954), and Reason (1978a; 1978b).

- It employs a model for orientation estimation and movement control that is mathematically congruent with the approach to modeling orientation and manual control defined by Young (1970).

- It accounts for experimental evidence for preprogrammed movement control.

- It employs a preliminary model for symptom production dynamics, which mimics certain nonlinear dynamic aspects of symptom time course.

Figure 21 below depicts Oman's (1982) preliminary model for motion sickness response pathways for sensory conflict generation mechanisms. The model consists of two linear elements (low n-th order pass filters) with "averaging" characteristics, a threshold element and a "power law" subjective magnitude estimation characteristic.

FAST AVERAGING DYNAMICS

$$\frac{1}{(T_F S+1)^{n_F}}$$

BIAS DUE TO
EXTRINSIC
FACTORS

$F(t)$
$I(t)$
+ +

$h(t)$
WEIGHTED
SENSORY
CONFLICT
(SCALAR)

$S(t)$
+

N

I_0 S

THRESHOLD

$N(t)$

R
R_0

N_0 N

SUBJECTIVE
DISCOMFORT
$R(t)$

SUBJECTIVE MAGNITUDE
ESTIMATION CHARACTERISTIC

$$R(t) = K_R R_0^{(1-m)} N(t)^m$$

$$\frac{K_S}{(T_S S+1)^{n_S}}$$

SLOW AVERAGING DYNAMICS

DESCRIBING FUNCTION
FOR SYMPTOM GENERATION
DYNAMICS

TIME INVARIANT RESPONSE NONLINEARITIES
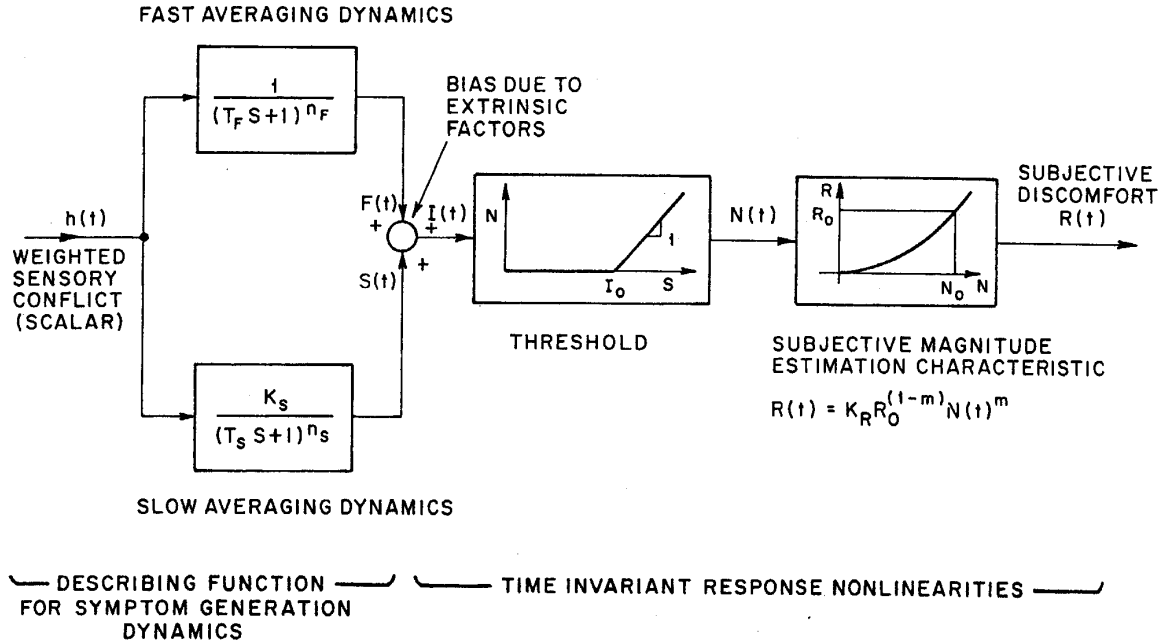
Figure 21: Preliminary dynamic model for motion
sickness response pathways (Oman, 1982)

Without describing the model in detail, it accounts for
two major symptoms production, the onset time of subjective
discomfort and the non-linear effect of the externally
induced motion amplitude.

3. Bos and Bles Model Description

The Bos and Bles model (Bles, Bos, de Graaf, Groen, &
Wertheim, 1998; Bos & Bles, 1998, 2002; Bos et al., 2001b)
is an extension of the Oman model. The main assumption
underlying the theoretical construction is a redefinition of
the sensory rearrangement theory (Merfeld, 1990): "All
situations which provoke motion sickness are characterized
by a condition in which the *sensed vertical* as determined on
the basis of integrated information from the eyes, the
vestibular system and the nonvestibular proprioceptors is at

53

variance with the *subjective vertical* as predicted on the basis of previous experience". In this manner, the determination of the internal representation of the vertical (i.e. the subjective vertical) is the simplification of the classic sensory rearrangement theory.

The proposed mechanism of sensory integration, before the main model, is the following (Bos et al., 2001a):
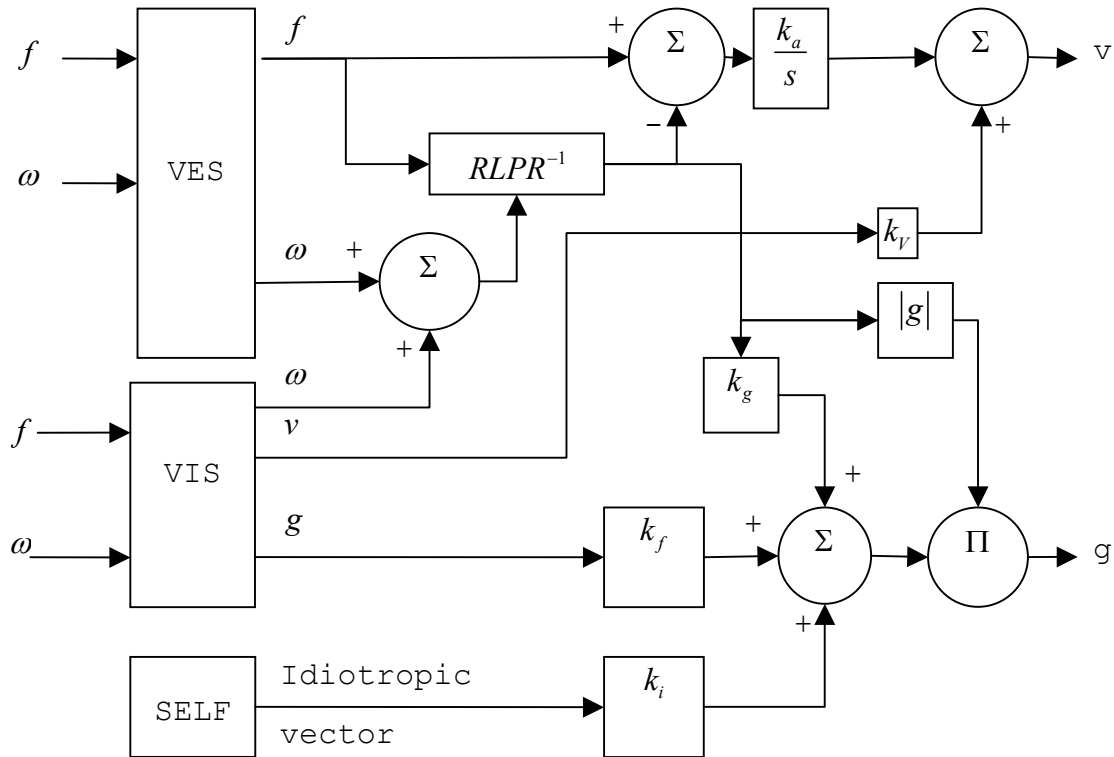
Figure 22: Resolving the sensed vertical, linear acceleration and velocity by means of integrated vestibular (VES) and visual (VIS) input, together with the idiotropic vector (subjective head referenced vertical). After (Bos et al., 2001a)

It is assumed that (Bos & Bles, 2002; Bos, Bles, Hosman, & Groen, 2002):

- The vestibular system senses linear acceleration and angular acceleration ($\vec{f}$ and $\vec{\omega}$)

54

- The visual system senses linear velocity, angular velocity, and attitude ($\vec{f}$, $\vec{\omega}$, and $\vec{g}$)

- Vestibular and linear velocity are added linearly with a dominance of visual information

- Vestibular and visual attitude are weighted linearly, and combined with the idiotropic vector (Bos et al., 2002)

The sensory afferents, as already described, become input to the following vestibular mechanism for spatial orientation. The process estimates both the gravitational component and the inertial acceleration.
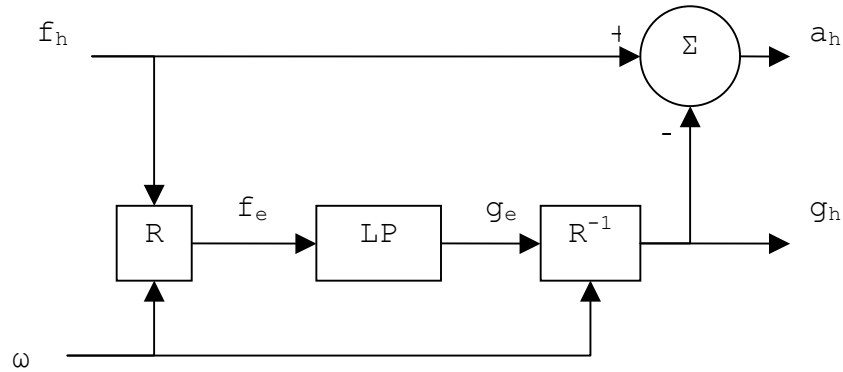
Figure 23: Vestibular based orientation model, after (Bles & Graaf, 1993).

The center of the mechanism in Figure 23 is the low pass filter, which operates in an earth fixed reference frame. Canal information (ω) is used to rotate (R) the head referenced vector (f_h). The estimation of gravity (g_h) is inversely rotated to earth reference frame.

The mathematical equivalent of this model is (Bos & Bles, 2002):

$$\frac{d\vec{g}}{dt} = \frac{\vec{f} - \vec{g}}{\tau} - \vec{\omega} \times \vec{g} \tag{1.12}$$

Where: – τ is the time constant of the low pass filter

As noted by (Bos et al., 2002) this description is the three dimensional equivalent of the two-dimensional model proposed by (Mayne, 1974).

The final model for the derivation of spatial orientation and motion sickness is the following:
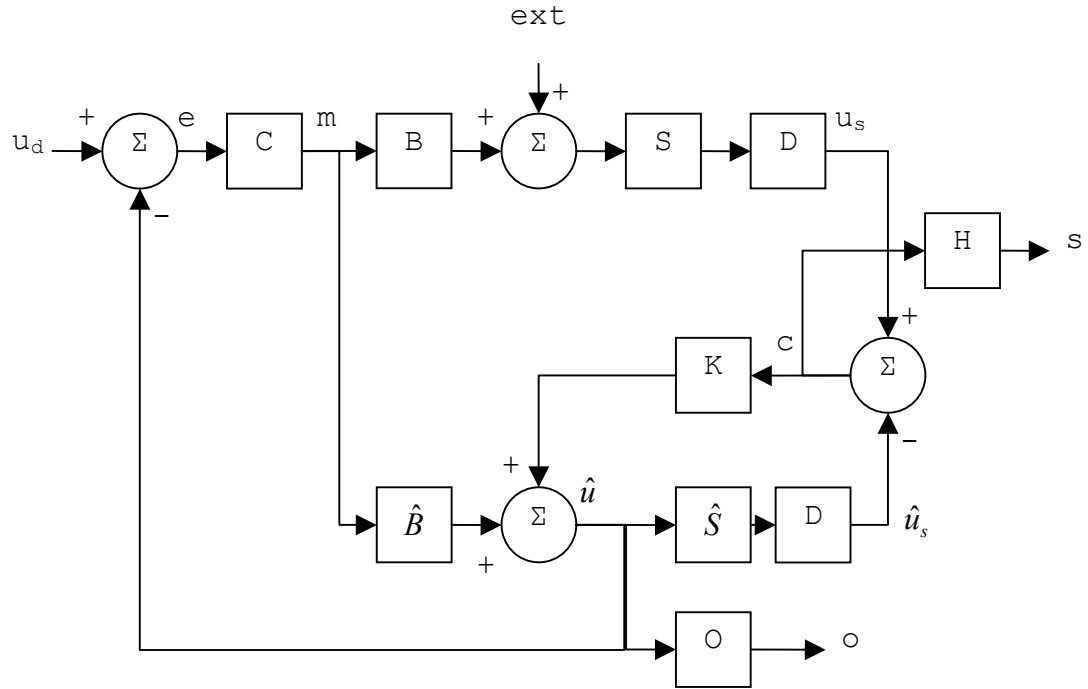
Figure 24: Spatial orientation and motion sickness model, after (Bos et al., 2000; Bos et al., 2001a)

The model uses the observer's theory approach. There is the desired body state (u_d), which directs a controller (C) generating motor commands (m) that subsequently drive the muscles. Together with external perturbations (ext, by a car, ship or airplane e.g.), this results in the actual body

56

state (u), which has several components (angular velocity $\vec{\omega}$, linear acceleration $\vec{a}$, and gravity $\vec{g}$). This state is sensed by somatosensory, visual, and vestibular sensors (S) which, after some central nervous system processing and delay (D), results in signals representing the state of the body (u_s) (Bos et al., 2001a). The neural store is the copy of B and S. The conflict derives from the body state and the output of the internal model.

$$c = u_s - \hat{u}_s \tag{1.13}$$

This conflict signal is passed through a non-linear normalization function and a second order leaky integrator so as to give MSI (Bos et al., 2001b).

4. Merfeld's Model

This model is fully presented in multiple papers (Merfeld, 1990, 1995a, 1995b; Merfeld, Young, Oman et al., 1993; Merfeld & Zupan, 2002). Initially it was developed to help understand complex three-dimensional eye movement responses and was later extended to include perceived orientation relative to gravity (Glasauer & Merfeld, 1997). The model correctly estimates human responses to roll and tilt, post-rotational tilt and centrifugation.

The model is conceptualised around the principle of an internal model. The purpose of the internal model is the estimation of external variables (such as gravity, acceleration, velocity etc.) by mimicking the physical relationships between those variables and the sensory systems and thereby predicting their time-course from incomplete, noisy, and/ or inaccurate sensory information (Glasauer & Merfeld, 1997). Such an approach has been used

extensively in the modelling literature (Merfeld, Young, Oman et al., 1993; Reason & Graybiel, 1973; Zupan, Merfeld, & Darlot, 2002).
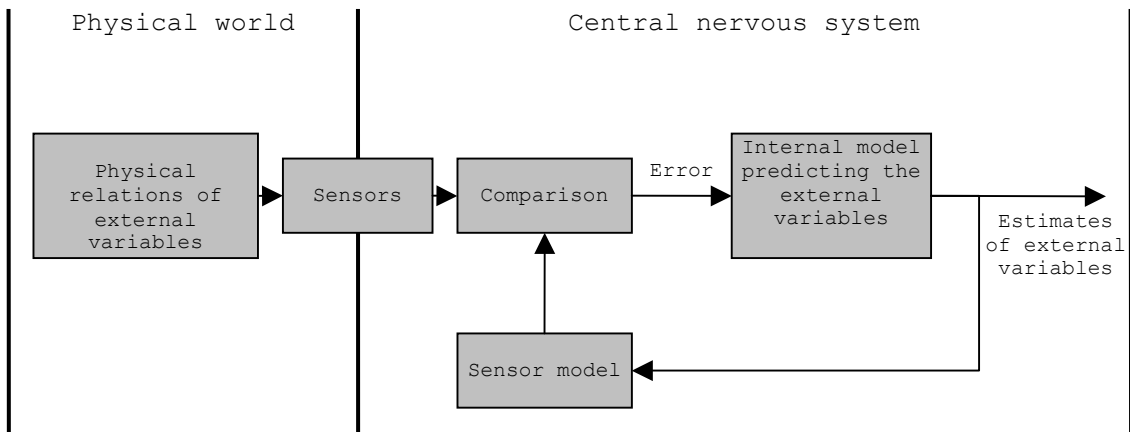
Figure 25: Principle outline of the internal model concept for the estimation of external physical variables (Glasauer & Merfeld, 1997).
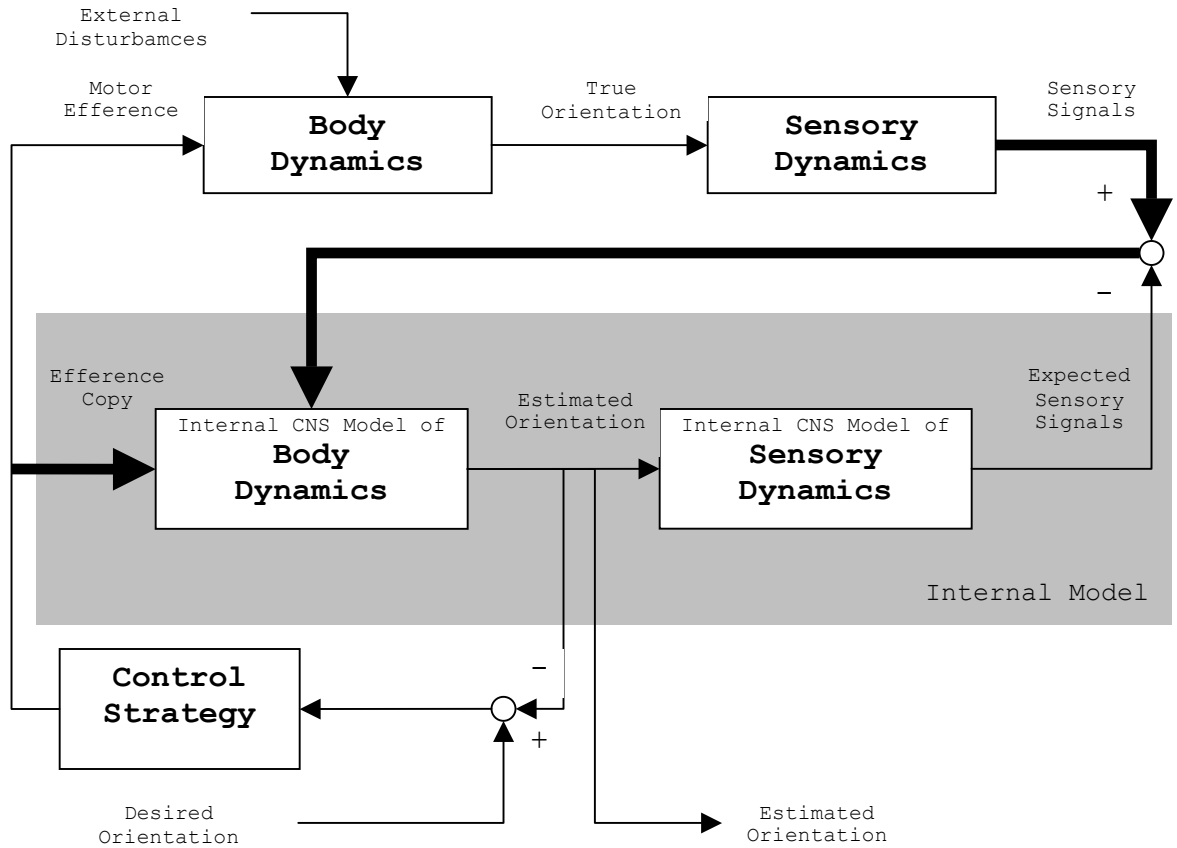
Figure 26: Block diagram of the internal representation
model (Merfeld, 2001)

In this model, the body dynamics correspond to muscle
dynamics, limb inertia, etc.

The main input is the desired orientation, which is
compared to the estimated orientation, yielding the motor
reference via a control strategy. The true orientation is
derived from the latter signal and the external
disturbances, filtered by the body dynamics. The latter
signal is measured by the sensory system through the sensory
dynamics so as to derive the sensory signals. In parallel to

the real world body dynamics and sensory dynamics, there exists a second neural pathway that includes an internal representation of the body dynamics and an internal representation of the sensory dynamics. Copies of the efferent commands (efference copy) are processed by these internal representations to yield the expected sensory signals, which when compared to the sensory signals yield an error (mismatch). This error is fed back to the internal representation of body dynamics to help minimize the difference between the estimated and the true orientation (Merfeld, 2001).
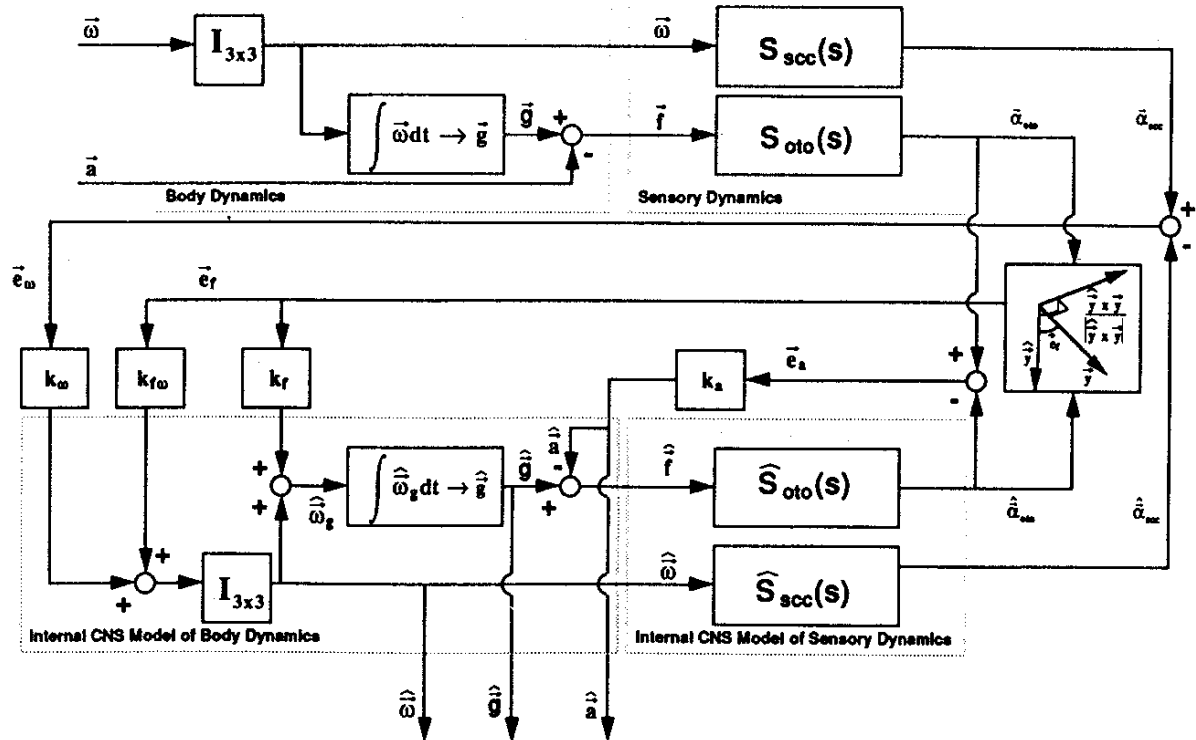
Figure 27: Outline of the three-dimensional sensory conflict model (Glasauer & Merfeld, 1997; Merfeld, Young, Oman et al., 1993).

60

Briefly describing the Merfeld model, the semicircular canals sense the angular velocity $\vec{\omega}$ of the head, while otolith organs sense both linear acceleration $\vec{a}$ of the head and gravity $\vec{g}$. The above signals are the three-dimensional model inputs. The output of the model is the above three variables' estimators $\hat{\vec{\omega}}$, $\hat{\vec{a}}$, and $\hat{\vec{g}}$. All vectors are in head-fixed coordinates. The internal model (neural representation) is comprised of the gravity estimator, the model of otolith dynamics, and the model of semicircular canals dynamics.

K. SUMMARY

In this chapter we gave a brief description of the existing literature on vestibular system, a system view of visual system, the way that vestibular and visual systems interact, and, finally, the major models regarding motion sickness.

The HFR model (McCauley et al., 1976) will be used as the basis for the validation of the proposed model.

From the models by Oman, Bos and Bles, and Merfeld et al. we will extract useful concepts and sub-systems which will be implemented in the proposed model. In the next chapter a detailed description of the proposed model will be given, including its characteristics, analysis in time domain and the outcome of the model.

THIS PAGE INTENTIONALLY LEFT BLANK

III. METHODOLOGY

A. OVERVIEW

The model we propose is based on the main ideas of (Bles et al., 1998; Merfeld, Young, Oman et al., 1993; Oman, 1982) and, furthermore, combines the errors produced in the vestibular and the visual system to estimate the motion sickness incidence:

- The intra-vestibular error derives from the estimation of gravity.

- The vestibulo-ocular error derives from the residual optical flow.

1. Model Assumptions

The main assumptions of the proposed model are the following:

(a) The subject is passive to the motions induced. There is no motion generated by the subject.

(b) The major proportion of motion sickness incidence derives from the following error signals:

(1) Within the vestibular system. Especially from the error signal developed in the main loop of gravity estimation.

(2) Between the vestibular and the visual system, through the vestibulo-ocular and optokinetic reflexes. The error is the ROF (residual optical flow).

(c) All calculations performed and all vectors concerned are in head-fixed reference frame. The

positive directions are forward (x), towards the subject's left (y), and toward the top of the head (z). This reference frame is right-handed orthogonal coordinate system, where the x-axis is aligned with the naso-occipital axis, the y-axis is aligned with the interaural axis, and the z-axis is orthogonal to both x- and y-axis. Such a frame was used by Merfeld in his model of tilt and translational responses (Merfeld & Zupan, 2002). Furthermore, research has shown that spatial organization of translational and angular visual motion cues is performed in a head-fixed, vestibular, coordinate system (Graf, Simpson, & Leonard, 1988; Wylie, Bischof, & Frost, 1998; Wylie & Frost, 1993).

(d) The internal model (neural representation) is composed of the gravity estimator and the model of otolith dynamics. (In a three-dimensional model it would include the canal dynamics, because, then, canal afferents have an effect on the estimation of linear acceleration).

(e) The combined error, which is used to derive the estimation of the MSI, is the linear combination of the absolute values of the "gravity estimation" normalized error and the "residual optical flow" normalized error.

Gravity is important in multiple aspects of human physiology, both as a sensory input and as an internal estimate. It influences spatial orientation, spatial stabilization, locomotion, and vestibulo-ocular reflex.

2. Model Characteristics

a. Motion

The model deals only with simple sinusoidal motion in the Z axis (vertical). Constraining the input to such motion gives us the ability to better understand the characteristics of the problem and minimize the effect of numerous complicating factors.

Furthermore:

- The model's output can be easily compared to the MSI data from McCauley et al. (1976);

- Minimal assumptions are necessary about the way the central nervous system is adapted to motion.

b. Environmental Factors

It is assumed that the subject is seated inside a closed, lighted simulator, without being able to receive visual, or other, information from the outside environment.

c. Adaptation

One main question underlying adaptation is, "what motion is the subject adapted to during his every day life?" We assume that a human is adapted to self motion. This assumption is difficult to quantify because:

1. The range of self motion characteristics is wide (walking to running).

2. Motion characteristics in the neural store are changing over time because adaptation is a dynamic process.

The problem to solve, therefore, is to derive an average motion for the part of the day a subject is normally awake. Simplifying the problem, let's assume that there are two situations faced by CNS, walking condition and no motion condition.

Human kinematics and gait are complicated activities. Numerous models have been proposed and they are being extensively studied; (Inman, Ralston, & Todd, 1981; McMahon, 1984; Miura & Shimoyama, 1984; Miyakoshi, Cheng, & Kuniyoshi, 2001). We are interested in defining the average characteristics of human walking.

Miyakoshi et al. (2001) used a fixed length leg version of a biped. Then they implemented a stretch and contract ability to the legs. The corresponding motion of the legs was found to be sinusoidal.

Figure 28: Compass-like biped model, after (Miyakoshi et al., 2001)

Menz and colleagues (2003), in an experiment with subjects walking on a corridor at various speeds, found that the speed of subjective comfortable walking ensures that movements of the head are smooth and that the lower limbs

and trunk act as shock absorbers. Thus, the walking accelerations are largely attenuated at the head. Their latter finding about attenuation confirms findings of previous research (Light & McLellan, 1977). The mean cadence was 109.31 steps/ minute (1.822 Hz) and the mean RMS vertical acceleration at the head was 0.21 g. The average RMS vertical acceleration at the head for the subjective comfortable condition was approximately 0.15 g. Frequency analysis of raw data reveled that the vertical motion was dominated by the frequency derived from cadence, thus 1.822 Hz. This will be the average motion characterizing subjective comfortable walking, for the analysis that follows.

It is interesting to observe that the cadence found by Menz and colleagues (2003), was much larger than what was expected. Yamanaka (1999) came to the same conclusion in an experiment about human's walking when holding a child. It was found that the preferred pace of walking was 92.28 steps per minute (1.538 Hz), a value larger than expected.

With the adaptation mechanism, described in detail on page 73, at any given time the motion input in the neural store is the linear combination of the sensed motion and the one already in the neural store.

Thus, in a simplified analysis of the problem, the motion in the neural store will be a weighted average of a walking motion, as already described, and no motion. We will assume that a subject is adapted to this average motion.

The simulation model created for the evaluation of the average motion, has the following characteristics:

67

- The 24-hour day is divided into three 8-hour periods:

    o 00:00-08:00 The normal 8-hour sleep period.

    o 08:01-16:00 "Motion" period.

    o 16:01-23:59 "Less motion" period.

- Circadian rhythms are not simulated.

- The adaptation process is continuous, day and night.

- During sleep time the subject senses no motion

- During the rest of the day the subject senses periods of walking-characteristics motion or no motion. The decision "motion/ no-motion" is based is random (Bernoulli trials). The duration of motion/ no-motion periods is determined by an exponential random variable with mean:

    o 08:01-16:00

-      Motion: 10 minutes

-      No motion: 5 minutes

    o 16:01-23:59

-      Motion: 5 minutes

-      No motion: 10 minutes

The first step is to find the motion that a subject is adapted to before going to bed. We assume that, at the beginning of the first day, the subject is fully adapted to motion with characteristics $A_{RMS} = 0.15$ g and f=1.822 Hz (derived from Menz et al., 2003). At the end of

the third day, motion characteristics are statistically stabilized to $A_{RMS} = 0.0567$ g, a value which is much lower than the initial one (A. Program 1). In the second phase of the simulation (B. Program 2) we calculate the average motion characteristics in the "awaken" 16-hour period of the 24-hour day (between 08:00 and 23:59). The motion used as the one that a subject is adapted to, before the beginning of a day, is $A_{RMS} = 0.0567$ g and f=1.822 Hz.

After statistical analysis of the simulation data, it was found that the average amplitude was 0.0253 g (RMS value).

Therefore, we assume that the efference copy (or internal neural store) which corresponds the motion to which the subject is adapted, is a sinusoidal motion with acceleration characteristics $A_{RMS} = 0.0253$ g and f=1.822 Hz.

d. Implications

An internal characteristic of the model is that sensory conflict is always present. The fact that it is not perceived relates to the magnitude of sensory conflict and the cumulative aspect of it. Thus, short sensory conflicts will have no effect on MSI.

As Oman (1982) noted "A sudden increase in sensory conflict vector components may mean only that an external disturbance is being encountered".

Another issue that is always present is the adaptation process. The existence of sensory conflict, which is decreased by time, is the indication that the central nervous system is always rearranging the contents of the

neural store (internal model), used in state estimation and control, to minimize the sensory conflict.

3. Otolith Organs

The otolithic primary afferents are modeled through a simplified transfer function that combines tonic (regular) and phasic (irregular) afferents. This model resembles a low pass filter to represent the gravity vector.

In our model we began with Young and Meiry's (1968) revised model for otolith dynamics:

$$S_{OTO}(s) = \frac{0.4(13.2s+1)}{(5.33s+1)(0.66s+1)} \qquad (1.14)$$

Part of our model's analysis revealed that we could use a simplified version of the otolith transfer function without losing information or changing our model characteristics.

Thus, the following otolith transfer function is used:

$$S_{OTO}(s) = \frac{1}{\tau_{OTO}s+1} \qquad (1.15)$$

where τ_{OTO}=0.66 s

The Bode plot of the two transfer functions is the following:
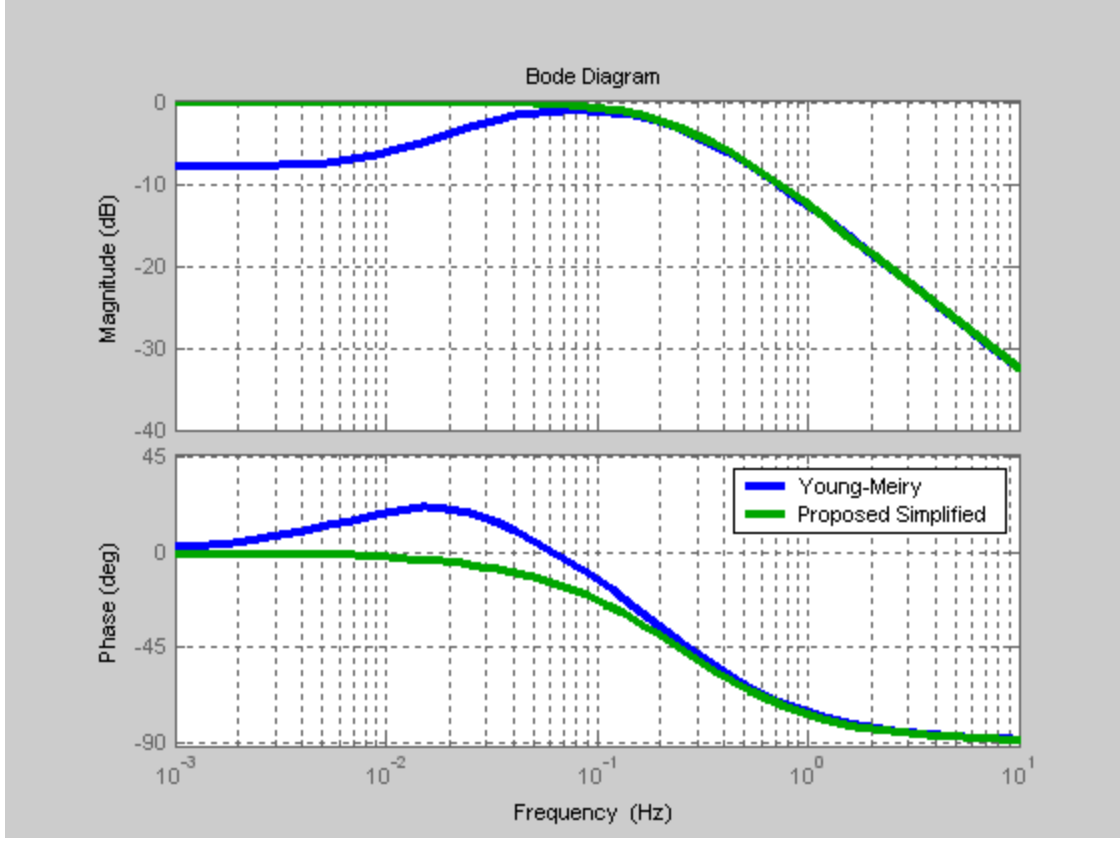
Figure 29: Otolith output

It's obvious that our simplified transfer function has the same frequency characteristic as the Young-Meiry model, but it doesn't show a decrement in magnitude below 0.3 rad/s.

4. Oculomotor Plant

The neural integrator of the oculomotor plant, referring to the mechanics of eye movement, is modeled as (Fuchs, Scudder, & Kaneko, 1988):

$$EYE(s) = \frac{\tau_{E1}s + 1}{(\tau_{E2}s + 1)(\tau_{E3}s + 1)(\tau_{E4}s + 1)} \qquad (1.16)$$

71

Where τ_{E1}=0.14 s, τ_{E2}=0.28 s, τ_{E3}=0.037 s, and τ_{E4}=0.003 s.
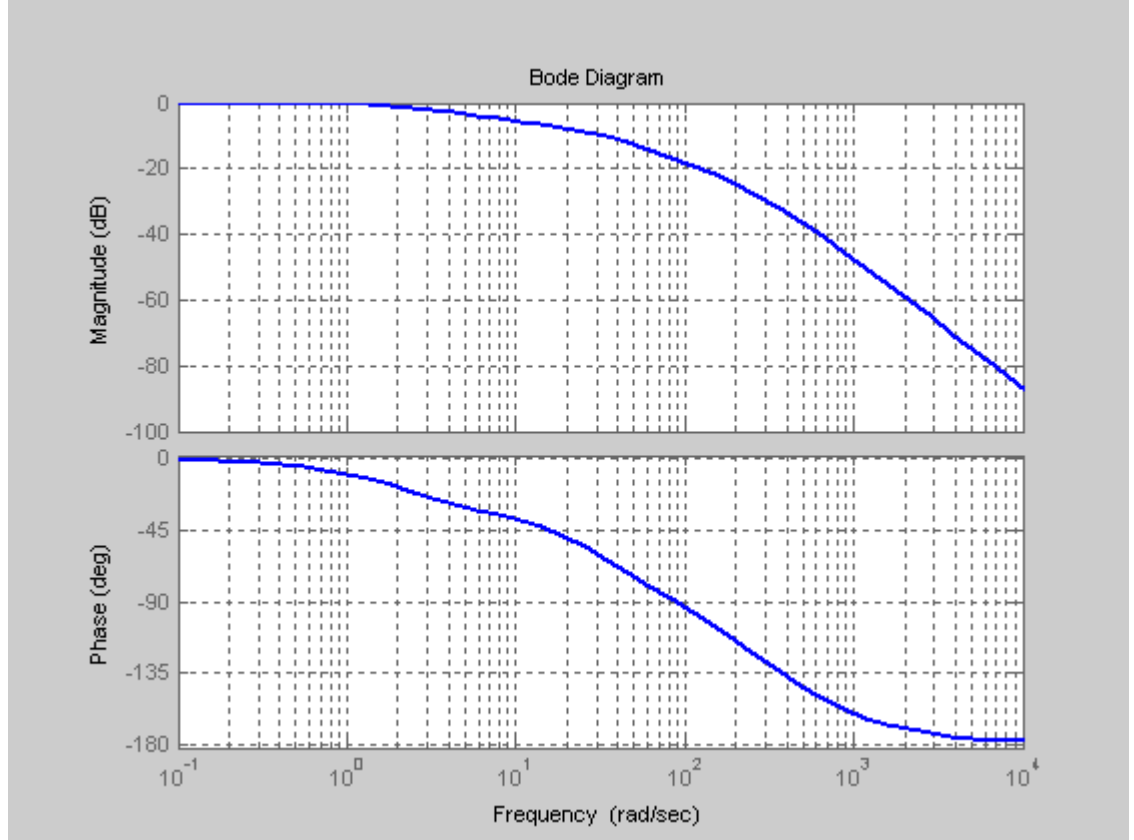
Figure 30: Oculomotor Plant Bode plot

The part of the visual system that extracts linear information from image deformation (detection of motion taking place on the retina) because of the retinal slip, is modeled through a low-pass filter:

$$RETINA(s) = \frac{1}{\tau_V s + 1}$$
(1.17)

Where: time constant of retinal slip τ_V=0.15 s

This time constant is chosen to fit eye movements during translation of the visual surround (Busettini, Miles, Schwarz, & Carl, 1994).

This thesis will not deal with:

- The visual processing that divides the optic flow into self-motion and movement of the visual surround (Droulez & Cornilleau-Peres, 1993). We assume no self motion in the seated subject.

- The part of the visual system that extracts angular information from retinal slip due to visual surround rotation. The kind of motion we are dealing does not lead to rotation.

B. MODEL DESCRIPTION

The proposed model is composed of four main sub-models and one interface:

- Sub-models:

  1) The sensors of the vestibular system.

  2) The visual system.

  3) The error estimation subsystem, which includes the neural store. Actually, the vestibular system and the error estimation subsystem are not separate but we have included such a division for depictive purposes.

  4) The adaptation mechanism.

- Interface:

  1) The vestibulo-ocular reflex interface, which passes information from the vestibular to the visual system.

1. Vestibular System

Due to the constraints dealing with the proposed model (motion in one axis), only part of the vestibular system is modeled. Specifically, the subsystems included are the otolith organs and the mechanism to extract independent linear acceleration and gravity information from the combined induced motion.

The model to extract the gravity estimate from the otolith afferents is a low-pass filter, as suggested by (Mayne, 1974) and later implemented by (Angelaki & Hess, 1996a; Bos & Bles, 1998; Bos et al., 2001b). Pure linear acceleration is of a variable nature, therefore has a frequency easily distinguishable and filtered out by a low-pass filter, whereas gravity remains constant in time. Thus the output of an LP filter would be an estimate of gravity.

In the three-dimensional sensory-weighting model, proposed by Zupan, Merfeld and Darlot (2002), the gravitointerial force separation into estimates of gravity and linear acceleration is based on central interaction of otolith information with canal and visual information.

The implementation of an inverter before the otoliths takes into account the dynamics of the otolith organs. The inverter is needed because the otoliths sense gravitational acceleration in the opposite direction to the gravitational force.
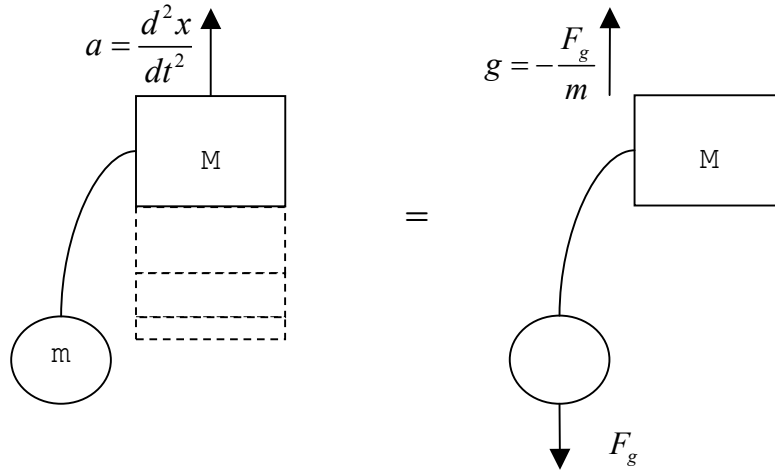
Figure 31: Schematic representation of an otolith crystal with mass m , connected by a hair functioning as a leaf spring to the body with mass M (Bos et al., 2002)

As we can see in the above diagram, mass M (the otolithic macula membrane) is moved by the gravitational acceleration $\vec{a}$. Due to inertia, the otolithic crystal of mass m wants to remain in place, but is dragged upwards via the spring by M. The resulting steady state condition is equal to a condition of rest/ no motion in earth (Bos et al., 2002). The consequence is that the gravitational acceleration should be directed opposite to the gravitational force vector. This conclusion is further extended to linear accelerations other than gravity. The otoliths can not distinguish between gravity and other forms of linear acceleration. Therefore, the inverter implemented in the proposed model is inverting the sum of the external linear accelerations.

The aforementioned analysis is depicted in Figure 32. External motion f_{EXT} is sensed by the otolith organs, thus it is inverted and passed through the orolith organ dynamics

$S_{OTO}(s)$. The central interaction of otolith information with canal and visual information, is modeled with a comparator that subtracts the otolith efferent signals (corresponding to perceived gravity $\hat{g}$) from the external motion. The outcomes correspond to the perceived linear acceleration $\hat{a}$.
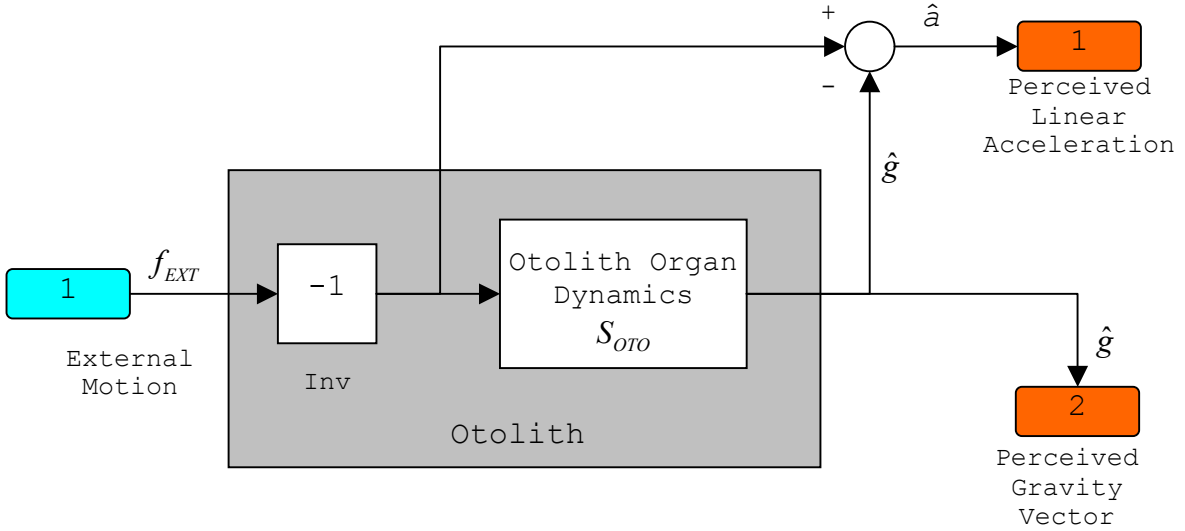
Figure 32: Model of the vestibular system sensors, after (Angelaki & Hess, 1996a; Bos & Bles, 1998; Bos et al., 2001b)

2. Adaptation Mechanism

The adaptation mechanism is derived from a simplification of Reason's neural mismatch model. Because of the kind of motion that our proposed model deals with (vertical oscillation), Reason's model (Reason, 1978a) is simplified to include only passive motions (involuntary). The voluntary motor control block and the effectors block, which correspond to active motion, have been excluded.
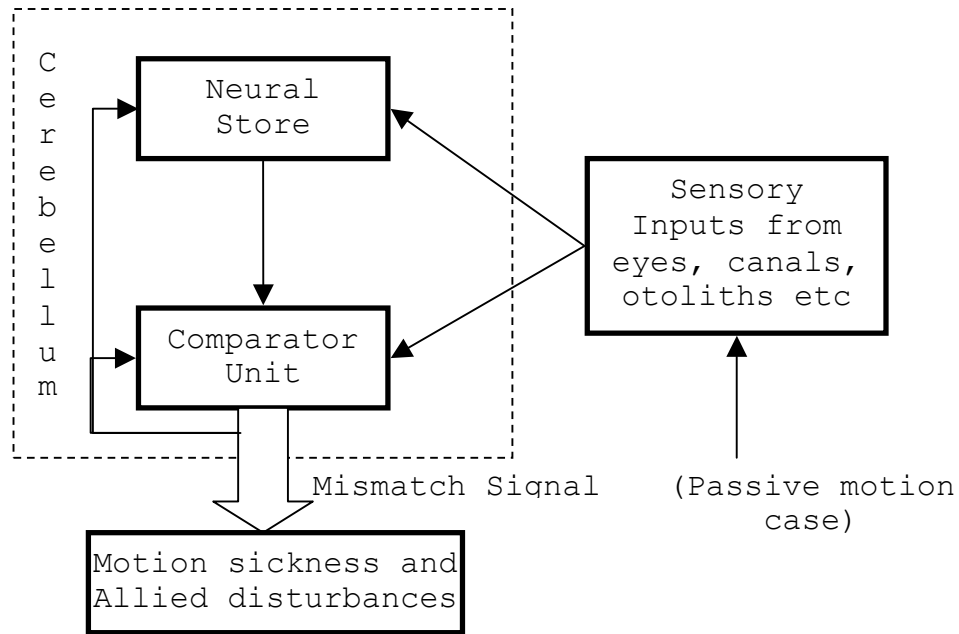
Figure 33: Structural components of simplified Reason's model.

The adaptation mechanism includes the two basic components of the neural mismatch hypothesis, the neural store and the comparator unit.
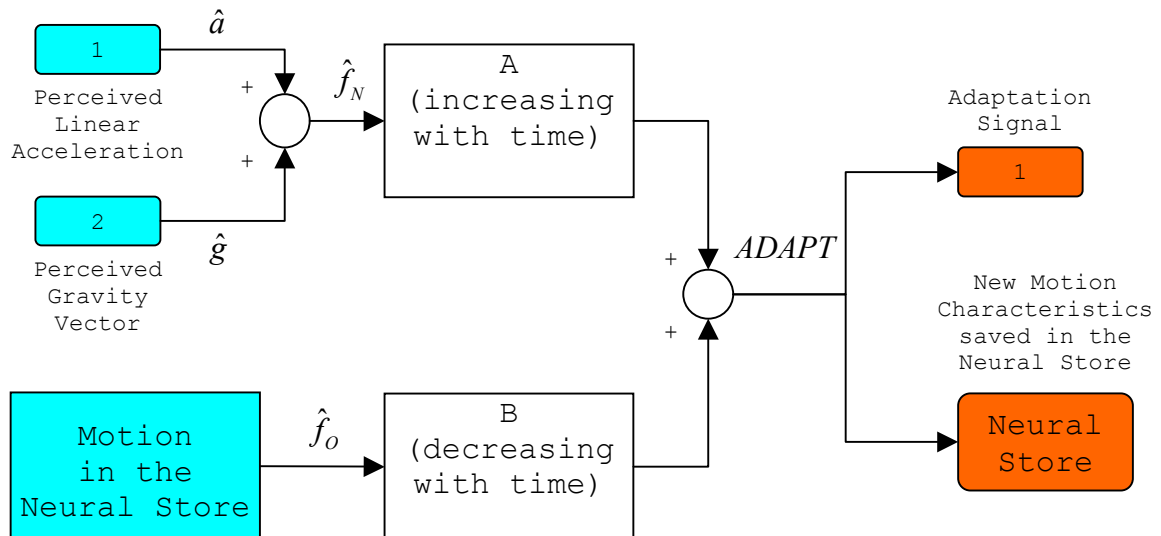
Figure 34: Proposed model of the adaptation mechanism

The inputs are the perceived motion from the vestibular sensors (afferent signals) and the motion already existing in the neural store (motion that the subject is adapted to).

The theoretical idea underlying the change of the existing neural store information to the new sensory input is the neural memory concept. We assume that earlier motion characteristics exist in the Neural Store as memory traces. Obviously, the process of saving new motion characteristics in the Neural Store is dynamic and continuous in time because we always input sensory information. Thus, the neural store may be seen as a queue with limited capacity or a moving window. The more recent input is fed to the back of the queue and pushes the already existing ones to the front where they "overflow". In our case this means that the old motion is "forgotten" over time. The combined motion in the neural store is the linear combination of the sensed and the old motion. The weighting parameters are time dependent.

The new motion is multiplied by parameter A, which increases exponentially (asymptotically) with time from 0 to 1. The old motion is multiplied by parameter B, which decreases exponentially (asymptotically) with time from 1 to 0:

$$ADAPT = A\hat{f}_N + B\hat{f}_O$$
$$A = 1 - e^{-at}$$
$$B = e^{-at}$$

In this simplified case, time starts ($t = 0$) when a new motion is sensed and stored into the Neural Store.

In both functions, the exponential factor has the same time constant, which is related to the time needed to

decrease the amplitude of the old motion and, respectively, increase the amplitude of the new input.

3. Error Estimation Subsystem

The basis used for the error estimation sub-system was the internal representation model proposed by Merfeld (shown previously in Figure 26 and Figure 27), which was further modified because of the motion dynamics included (one-axis motion).
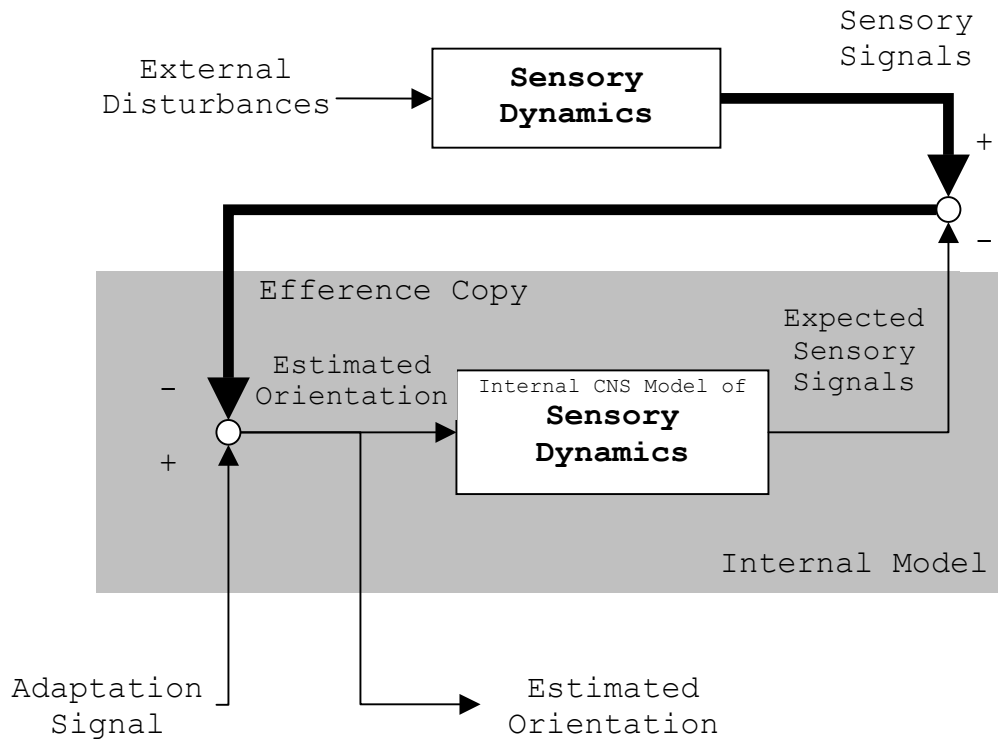
Figure 35: Simplified block diagram of the internal representation model in the vestibular system.

In this simplified internal representation model (derived from Figure 26) certain changes have been made to comply with the basic assumptions and characteristics of our proposed model:

- There is no "Desired Orientation" because we deal only with passive motion, such as the subject seated and belted in a chair. The subject senses the externally induced motion without any attempt to change his posture.

- There is no link between the "Estimated Orientation" and the "True Orientation", therefore the "Control Strategy" and the "Body Dynamics" are excluded.

The main input is the "External Disturbances", which is processed by the sensory system through the sensory dynamics so as to derive the "Sensory Signals". In parallel to the real world sensory dynamics, there exists a second neural pathway that includes an internal representation of the sensory dynamics. A copy of the efferent commands (efference copy) is processed by this internal representation to yield the expected sensory signals, which, when compared to the sensory signals, yields an error (mismatch). This error is fed back to the internal representation of body dynamics to help minimize the difference between the estimated and the true orientation.
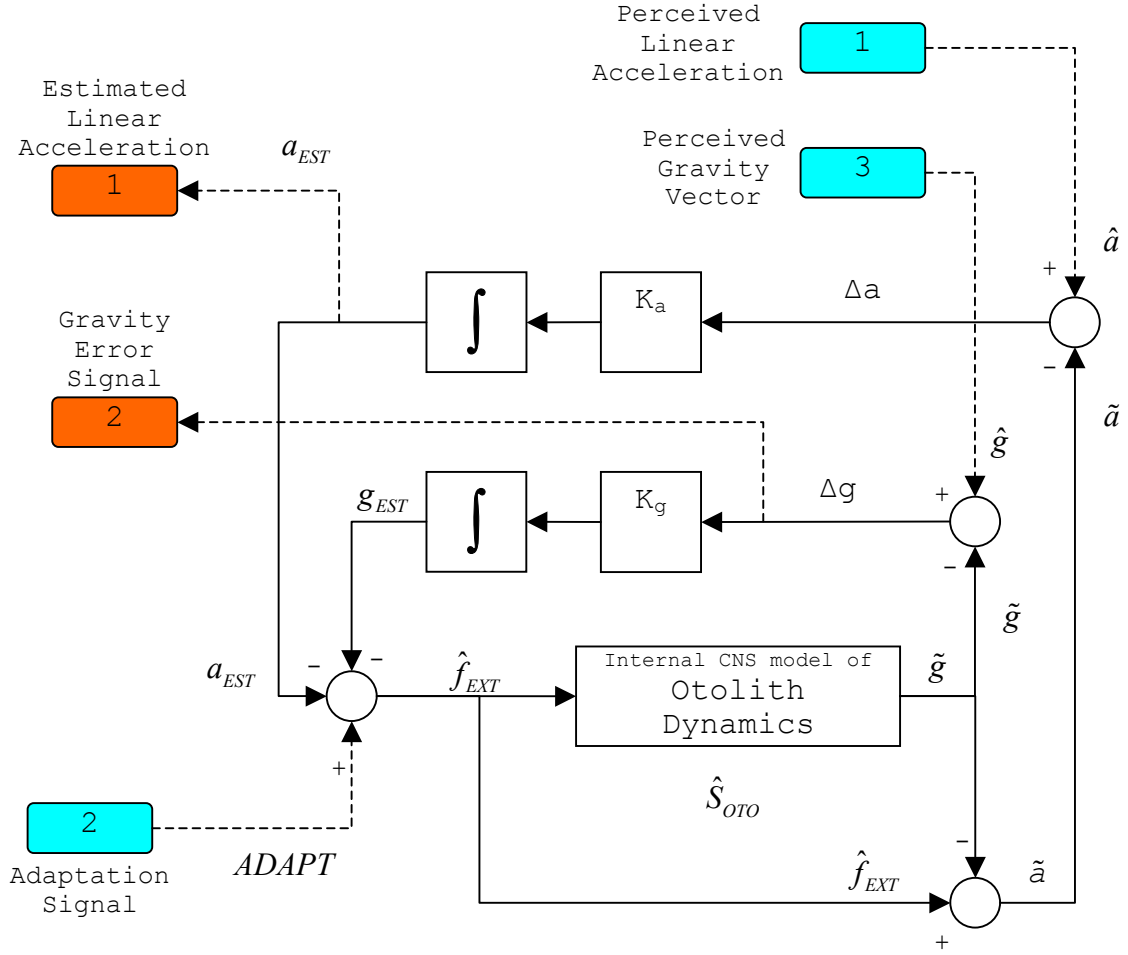
Figure 36: Proposed Error Estimation Subsystem

4. VOR Interface

We have modeled the connection between the error estimation subsystem and the visual system with the interface depicted in Figure 37. This interafce is derived from the model proposed by (Merfeld, Young, Oman et al., 1993).
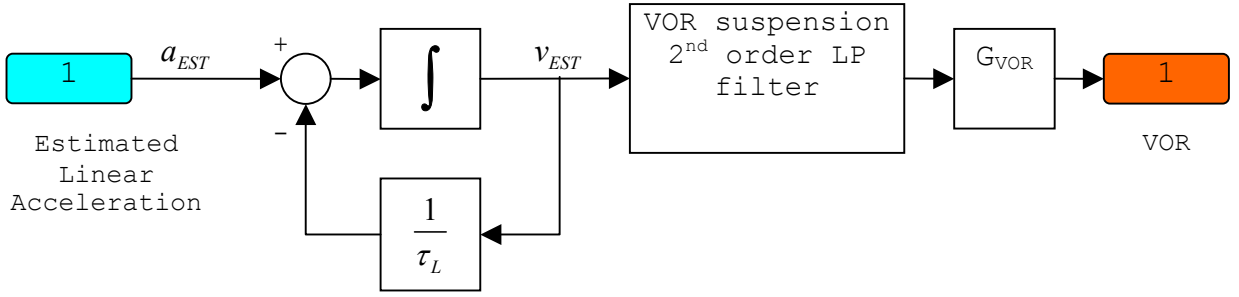
Figure 37: Proposed VOR Interface.

The estimated linear acceleration α_{EST} is integrated (through a leaky integrator with time constant τ_L) and the estimated linear velocity v_{EST} is derived.

It is known that vestibular nystagmus is inhibited when a person's gaze is fixed on an object that rotates with the head. Furthermore, nystagmus is more or less completely inhibited during self-initiated sinusoidal head oscillations up to about 0.5 Hz (Howard, 1986a). Draper noted that such a high pass filter might be included in the Robinson's model of the visual system, to negate the poor low frequency response of the vestibular system at frequencies below 0.05 Hz (Draper, 1998). On the other hand, Benson and Barnes (1978) showed that VOR suppression occurs up to approximately 1 Hz.

Thus, the estimated velocity is passed through a second order low-pass filter with characteristics that comply with the aforementioned findings.

Finally, the interface is integrated with a constant gain element, which will be helpful in the analysis process of the model.

5. Visual System

The model used for the visual system is derived from the one proposed by (Panerai et al., 2000a, 2000b; Sandini et al., 2001) shown previously in Figure 15.

The input signal from the vestibular system is fed into the visual system through the vestibular interface already described in the previous paragraph. The vestibular and visual information are added to compensate for head motions. The main function of the model is that the vestibular compensatory signal drives the eye muscles to stabilize gaze. The visual feedback signal is used to compensate for visual target motion, imperfect vestibular head motion detection and other noise. Thus, the residual optical flow (ROF) corresponds to the residual error in visual stabilization after inertial compensation. The residual error is defined in the literature as the slip of the visual image on the retina.

The feedback loop corresponds to the visual detection of target's motion. In the HFR studies (McCauley et al., 1976) the visual target was a panel of buttons in front of the seated subject. Obviously, this is a simplification because the subject is not constantly watching the buttons. But, the important fact is that the seated subject can view the interior of the cabin, but cannot view the external world. In this case the visual target's motion is equal to the visual world motion $\dot{W}_R$ (visual surroundings), which are static.
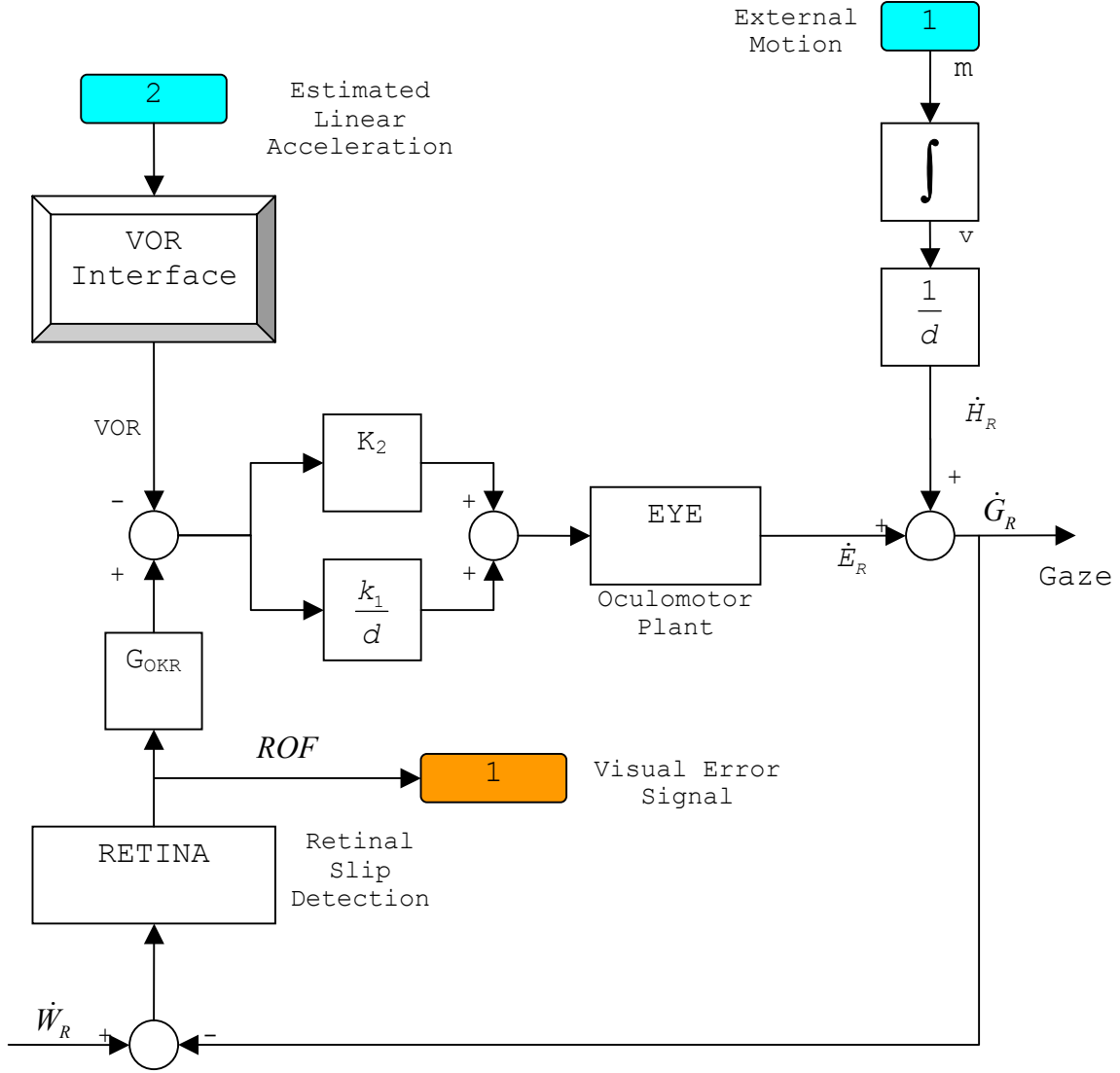
Figure 38: Proposed Visual System Model

Head motion $\dot{H}_R$ is affecting gaze, thus it is added at the output of the oculomotor plant $\dot{E}_R$.

The gain element in the system has two components. From the constant gain component K_2 the small amount of VOR, which is independent of visual target distance, is derived. The second component $\dfrac{k_1}{d}$ is inversely proportional to visual target distance. The relation among otolithic signals,

target distance, and VOR output is suggested by several studies (Crane & Demer, 1999; Crane, Viirre, & Demer, 1997; Paige, Telford, Seidman, & Barnes, 1998; Telford et al., 1997; Viirre & Demer, 1996; Viirre, Tweed, Milner, & Vilis, 1986).

6. Model Overview

The following diagram depicts the combined model.
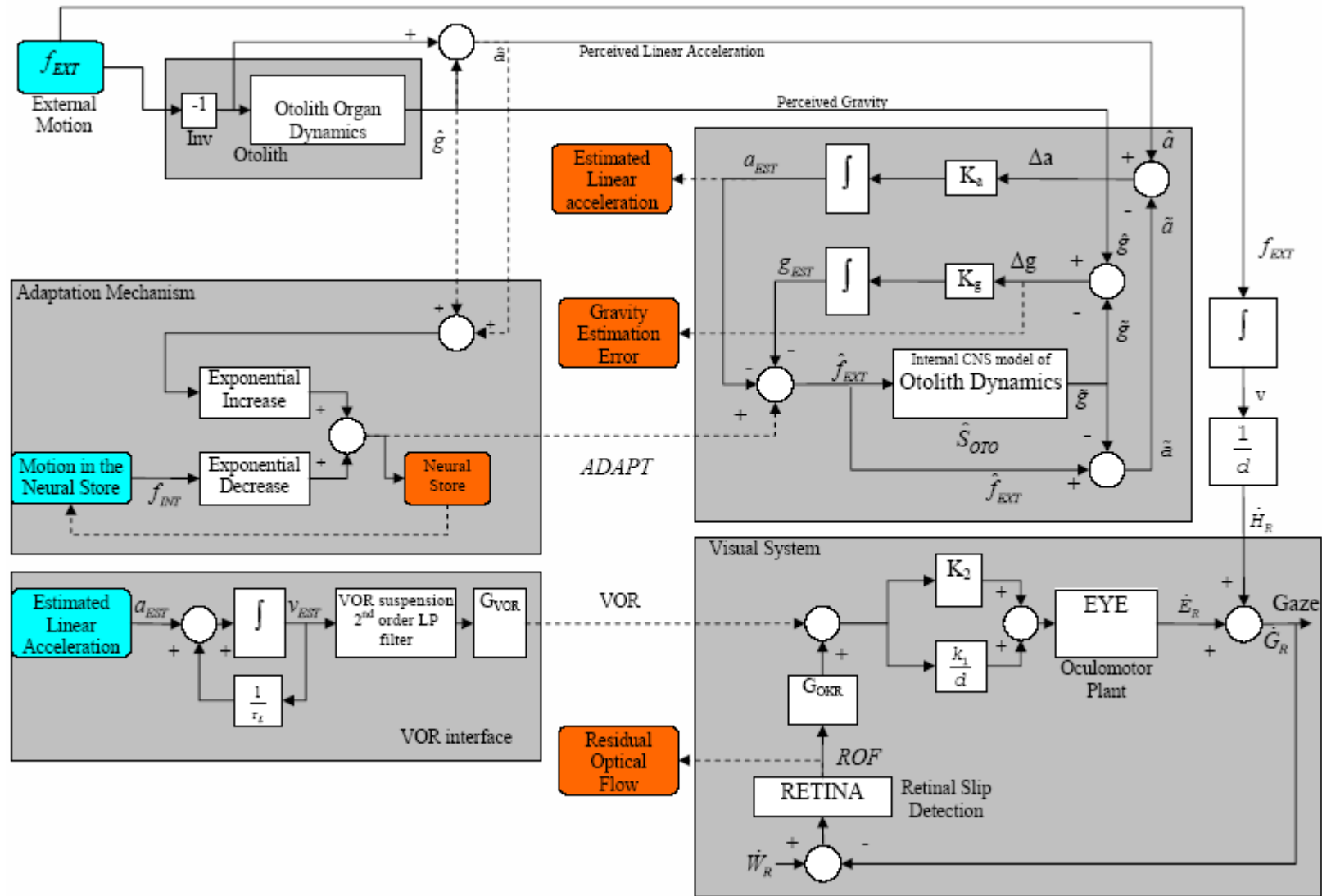
Figure 39: Proposed Model

7. MSI Calculation

The relationship between the multi-sensory conflict and motion sickness was suggested by Oman (1982) as postulated by (Reason & Brand, 1975).

The Motion Sickness Incidence (MSI) calculation is completed in three steps.

(1) The error signal in the estimation of gravity and the error signal derived from the visual system are normalized independently. This process is needed because the two signals have different magnitude levels. Thus, a combination of the two at a later step would lead to the dominating influence of the greater one on the overall (combined) error. This outcome, though, would mean that, if we assume that the gravity estimation error has greater amplitude, situations where there is only intra-vestibular error would lead to increased incidence of emesis. On the other hand, if the residual optical flow error has greater amplitude then situations with dominant visual error would lead to increased incidence of emesis. The results of experiments done so far, by researchers dealing with motion sickness, do not establish such a relation. Furthermore, the independent "normalization" of errors means that CNS is more interested in the sustained existence of error from sensory subsystems than in the absolute value of the error, which seems reasonable.

Another issue concerning the two errors is the manner in which they should be combined. We excluded multiplicative functions because this would mean that, if an error is zero, then the total error, and thus MSI, would be zero. For example, the absence of light in the environment leads to non-existing residual optical flow. Nevertheless, humans

face motion sickness symptoms during nighttime. The approach was to combine the two errors additively.

(2) The independent error signals are combined by calculating the mean of the absolute values. The sign of the existing errors is irrelevant. The existence of sustained error is the crucial issue and not the sign of it relative to some basis. As Oman (1989) noted, "Rectification is required because sensory conflict components are signed quantities. The information carried in the sign is presumably useful in correcting orientation perception and posture control errors. However, stimuli which presumably produce sensory conflicts of opposite signs produce the same type and intensity of nausea" (Oman, 1989).

The non-linear function used for the normalization of the errors accounts for:

- The fact that MSI values must lie between 0 and 1. Therefore no matter how large the error signals are, 1 must be the asymptote for MSI.

- The MSI, as derived from the McCauley et al. (1976) experiments is non-linearly dependent on the magnitude of the induced motion.

(3) The signal is integrated through a second order leaky integrator, which accounts for the cumulative characteristic of motion sickness.

C. ANALYSIS

1. Analytical Solution in S-domain

The following analysis will lead to the derivation of analytical solutions for gravity estimation error Δg and residual optical flow ROF. The only input signal of the model is the externally induced motion f_{EXT}.

Analysis of the vestibular model (Figure 32) and the gravity error estimation subsystem (Figure 31), in s-domain, leads to the following system of equations:

$$\left.\begin{aligned}
\Delta g(s) &= \hat{g}(s) - \tilde{g}(s) \\
\hat{g}(s) &= -S_{OTO}(s) f_{EXT}(s) \\
\tilde{g}(s) &= \hat{S}_{OTO}(s) \hat{f}_{EXT}(s) \\
\hat{f}_{EXT}(s) &= -\frac{k_g}{s} \Delta g(s) - \frac{k_a}{s} \Delta a(s) + ADAPT(s) \\
\Delta a(s) &= \hat{a}(s) - \tilde{a}(s) \\
\hat{a}(s) &= S_{OTO}(s) f_{EXT}(s) - f_{EXT}(s) \\
\tilde{a}(s) &= \hat{f}_{EXT}(s) - \hat{S}_{OTO}(s) \hat{f}_{EXT}(s)
\end{aligned}\right\}$$

Where:

- $\Delta g(s)$ is the error in the estimation of gravity

- $\hat{g}(s)$ is the perceived gravity vector

- $\tilde{g}(s)$ is the output (estimated gravity vector) of the internal otolithic dynamics model

- $S_{OTO}(s)$ is the transfer function of the otolith organs

- $\hat{S}_{OTO}(s)$ is the transfer function of the otolithic dynamics stored in the internal model (neural store)

- $f_{EXT}(s)$ is the externally induced gravitointerial force

- $\hat{f}_{EXT}(s)$ is the motion sensed or estimated

- k_a is a constant gain in the linear acceleration estimation loop

- k_g is a constant gain in the gravity estimation loop

- $ADAPT(s)$ is the adaptation signal

- $\Delta a(s)$ is the error in the estimation of external motion (without gravity)

- $\hat{a}(s)$ is the perceived linear acceleration

- $\tilde{a}(s)$ is the output (estimated linear acceleration) of the internal otolithic dynamics model

Although Oman (1982) noted that "it may be possible that the CNS employs somewhat simplified models for the behaviour of the body", we assumed that the internal model of the otolith organs' dynamics is the same as the true dynamic model. This approach has also been used by Bos and Bles (2001).

The input signal is assumed to be the externally induced motion $f_{EXT}(s)$ with characteristics which will be defined further on. The output signals to be estimated are:

- The gravity error signal $\Delta g(s)$, which will be used at the end for the estimation of MSI

- The linear velocity error signal $\Delta a(s)$, will be used as input signal at the visual system analysis

Assuming $\hat{S}_{OTO}(s) = S_{OTO}(s)$, the solution of the aforementioned system for $\Delta g(s)$ and for $\Delta a(s)$ in terms of $f_{EXT}(s)$ and $ADAPT(s)$, is the following (Δa will be used later for the derivation of ROF):

$$
\left.
\begin{aligned}
&\Delta g(s) = \hat{g}(s) - \tilde{g}(s) \\
&\hat{g}(s) = -S_{OTO}(s) f_{EXT}(s) \\
&\tilde{g}(s) = \hat{S}_{OTO}(s) \hat{f}_{EXT}(s) \\
&\hat{f}_{EXT}(s) = -\frac{k_g}{s}\Delta g(s) - \frac{k_a}{s}\Delta a(s) + ADAPT(s) \\
&\Delta a(s) = \hat{a}(s) - \tilde{a}(s) \\
&\hat{a}(s) = S_{OTO}(s) f_{EXT}(s) - f_{EXT}(s) \\
&\tilde{a}(s) = \hat{f}_{EXT}(s) - \hat{S}_{OTO}(s) \hat{f}_{EXT}(s) \\
&\hat{S}_{OTO}(s) = S_{OTO}(s)
\end{aligned}
\right\} \Rightarrow
$$

$$
\left.
\begin{aligned}
&\Delta g(s) = -S_{OTO}(s) f_{EXT}(s) - S_{OTO}(s) \hat{f}_{EXT}(s) \\
&\Delta a(s) = S_{OTO}(s) f_{EXT}(s) - f_{EXT}(s) - \left(\hat{f}_{EXT}(s) - \hat{S}_{OTO}(s) \hat{f}_{EXT}(s) \right) \\
&\hat{f}_{EXT}(s) = -\frac{k_g}{s}\Delta g(s) - \frac{k_a}{s}\Delta a(s) + ADAPT(s) \\
&\hat{S}_{OTO}(s) = S_{OTO}(s)
\end{aligned}
\right\} \Rightarrow
$$

$$
\left.
\begin{aligned}
&\Delta g(s) = -S_{OTO}(s)\left(f_{EXT}(s) - \frac{k_g}{s}\Delta g(s) - \frac{k_a}{s}\Delta a(s) + ADAPT(s) \right) \\
&\Delta a(s) = \left(S_{OTO}(s) - 1 \right)\left(f_{EXT}(s) - \frac{k_g}{s}\Delta g(s) - \frac{k_a}{s}\Delta a(s) + ADAPT(s) \right)
\end{aligned}
\right\} \Rightarrow
$$

91

$$\Delta g(s) = -\frac{S_{OTO}(s)}{1 - S_{OTO}(s)\frac{k_g}{s}}\left(f_{EXT}(s) - \frac{k_a}{s}\Delta a(s) + ADAPT(s)\right)$$

$$\Delta a(s) = \frac{S_{OTO}(s) - 1}{1 + (S_{OTO}(s) - 1)\frac{k_a}{s}}\left(f_{EXT}(s) - \frac{k_g}{s}\Delta g(s) + ADAPT(s)\right) \Bigg\} \Rightarrow$$

$$\Delta g(s) = -\frac{s S_{OTO}(s)}{s + (k_a - k_g)S_{OTO}(s) - k_a}\left(f_{EXT}(s) + ADAPT(s)\right)$$

$$\Delta a(s) = \frac{s(S_{OTO}(s) - 1)}{s + (k_a - k_g)S_{OTO}(s) - k_a}\left(f_{EXT}(s) + ADAPT(s)\right) \Bigg\} \Rightarrow$$

$$S_{OTO}(s) = \frac{1}{\tau_{OTO}s + 1}$$

$$\boxed{\Delta g(s) = X_{\Delta g}(s)\left(f_{EXT}(s) + ADAPT(s)\right)} \qquad (1.18)$$

$$\Delta a(s) = X_{\Delta a}(s)\left(f_{EXT}(s) + ADAPT(s)\right) \qquad (1.19)$$

Where:

- $\Delta g(s)$ is gravity error signal derived from the comparison of the otolithic afferents and the estimation derived from the neural store, with

$$X_{\Delta g}(s) = -\frac{s S_{OTO}(s)}{s + (k_a - k_g)S_{OTO}(s) - k_a}$$

- $\Delta a(s)$ is linear velocity error signal derived from the comparison of the otolithic afferents and the estimation derived from the neural store, with

$$X_{\Delta a}(s) = X_{\Delta g}(s)\left(\frac{1}{S_{OTO}(s)} - 1\right)$$

Furthermore, from the error estimation subsystem (Figure 36) we derive the linear acceleration estimation $a_{EST}(s)$:

$$a_{EST}(s) = \frac{1}{s} k_a \Delta a(s)$$ (1.20)

From the vestibulo-ocular reflex interface (Figure 37), the visual system (Figure 38), and the equations already found for $a_{EST}(s)$ and $\Delta a(s)$ we derive the following system of equations:

$$\left. \begin{aligned} ROF(s) &= RETINA(s)\left(\dot{W}_R(s) - \dot{G}_R(s)\right) \\ \dot{G}_R(s) &= \dot{E}_R(s) + \dot{H}_R(s) \\ \dot{E}_R(s) &= EYE(s)K\left(-VOR(s) + G_{OKR}ROF(s)\right) \\ K &= k_2 + \frac{k_1}{d} \\ VOR(s) &= X_{VOR}(s)v_{EST}(s) \\ v_{EST}(s) &= X_{v_{EST}}(s)a_{EST}(s) \\ a_{EST}(s) &= \frac{1}{s}k_a\Delta a(s) \\ \Delta a(s) &= X_{\Delta a}(s)\left(f_{EXT}(s) + ADAPT(s)\right) \end{aligned} \right\}$$

Where:

- $ROF(s)$ is the residual optical flow, which refers to the retinal slip due to less-than-perfect compensation of external motion

- $\dot{W}_R(s)$ is the angular velocity of the visual surroundings (in space referenced frame)

- $\dot{G}_R(s)$ is gaze angular velocity used to stabilize the visual target on the retina (in space referenced frame)

- $\dot{E}_R(s)$ is the angular velocity signal fed to the oculomotor plant

- d is the distance between the subjects's eyes and the visual terget

- $EYE(s)$ is the transfer function of the oculomotor plant

$$EYE(s) = \frac{\tau_{E1}s + 1}{(\tau_{E2}s + 1)(\tau_{E3}s + 1)(\tau_{E4}s + 1)}$$

- k_2 is the constant gain component related to the small amount of VOR which in independent of target distance

- $\dfrac{k_1}{d}$ is the gain component inversely dependent to visual target distance

- $VOR(s)$ is the stabilization signal derived from the vestibular system, with transfer function

$$X_{VOR}(s) = G_{VOR}\left(\frac{\tau_{VOR}s}{\tau_{VOR}s + 1}\right)^2$$

- $G_{VOR}(s)$ is a constant gain element in the VOR path

- $v_{EST}(s)$ is the estimated linear velocity derived from the vestibular system, with

$$X_{V_{EST}}(s) = \frac{1}{\tau_L s + 1}$$

- $RETINA(s)$ is the transfer function of the eye retinal slip detection mechanism

$$RETINA(s) = \frac{1}{\tau_V s + 1}$$

The solution of the aforementioned system for residual optical flow $ROF(s)$, on terms of $f_{EXT}(s)$ and $ADAPT(s)$, is the following:

$$ROF(s) = \frac{\left(\dot{W}_R(s) - \dot{H}_R(s) + EYE(s) X_{VOR}(s) X_{V_{EST}}(s) K \frac{k_a}{s} X_{\Delta a}(s) \right)}{\frac{1}{RETINA(s)} \left(1 + RETINA(s) G_{OKR} EYE(s) K \right)} \left(f_{EXT}(s) + ADAPT(s) \right)$$

In the case, which we are interested in, the subject's head is moving with a velocity equal to (space reference frame):

$$\dot{H}_R(s) = \frac{1}{s} \frac{1}{d} f_{EXT}(s)$$

The visual world (the part of the visual world the eye is focused on, thus the visual target) has velocity:

$$\dot{W}_R(s) = \dot{H}_R(s)$$

Thus, the following equation stands:

$$\boxed{ROF(s) = X_{ROF}(s) \left(f_{EXT}(s) + ADAPT(s) \right)} \qquad (1.21)$$

Where : $\quad X_{ROF}(s) = \dfrac{RETINA(s) EYE(s) X_{VOR}(s) X_{V_{EST}}(s) \dfrac{k_a}{s} X_{\Delta a}(s) K}{1 + RETINA(s) G_{OKR} EYE(s) K}$

2. Analytical Solution in Time Domain

The external motion impacted to the subjects will be the combination of gravity (constant component) and a

sinusoidal motion (time variant component), therefore $f_{EXT}(t) = g + A_{EXT} \sin(\omega_{EXT}t)$.

The system is Linear Time Invariant (LTI) and we shall assume that it is asymptotically stable. This latter assumption will be proven true later on. The stability analysis, so as to derive accepted values for the model parameters, will be done in a later paragraph.

The amplitudes of the signals in time domain will be derived from the complex modulus (magnitude) of the corresponding transfer functions in s-domain.

From the adaptation mechanism diagram (Figure 34) we derive the following for $ADAPT(s)$:

$$
\left.
\begin{aligned}
ADAPT(t) &= \left(1 - e^{-at}\right)\hat{f}_N(t) + e^{-at}\hat{f}_O(t) \\
\hat{f}_N(t) &= \hat{g}(t) + \hat{a}(t) \\
\hat{f}_O(t) &= \hat{g}_O(t) + \hat{a}_O(t)
\end{aligned}
\right\} \Rightarrow
$$

$$ADAPT(t) = \left(1 - e^{-at}\right)\left(\hat{g}(t) + \hat{a}(t)\right) + e^{-at}\left(\hat{g}_O(t) + \hat{a}_O(t)\right) \Rightarrow$$

$$ADAPT(s) = L\left[\left(1 - e^{-at}\right)\left(\hat{g}(t) + \hat{a}(t)\right) + e^{-at}\left(\hat{g}_O(t) + \hat{a}_O(t)\right)\right] \Rightarrow$$

$$ADAPT(s) = \hat{g}(s) + \hat{a}(s) - \hat{g}(s+a) - \hat{a}(s+a) + \hat{g}_O(s+a) + \hat{a}_O(s+a) \Rightarrow$$

$$ADAPT(s) = -S_{OTO}(s)f_{EXT}(s) + \left(S_{OTO}(s) - 1\right)f_{EXT}(s) + S_{OTO}(s+a)f_{EXT}(s+a)$$

$$-\left(S_{OTO}(s+a) - 1\right)f_{EXT}(s+a) - S_{OTO}(s+a)f_O(s+a) + \left(S_{OTO}(s+a) - 1\right)f_O(s+a) \Rightarrow$$

$$ADAPT(s) = -f_{EXT}(s) + f_{EXT}(s+a) - f_O(s+a)$$

But :

$$
\left.
\begin{aligned}
f_{EXT}(s) &= L\left[f_{EXT}(t)\right] \\
f_O(s) &= L\left[f_O(t)\right] \\
f_{EXT}(t) &= g + A_{EXT}\sin(\omega_{EXT}t) \\
f_O(t) &= g + A_O\sin(\omega_O t)
\end{aligned}
\right\} \Rightarrow
\left.
\begin{aligned}
f_{EXT}(s) &= \frac{g}{s} + A_{EXT}\frac{\omega_{EXT}}{s^2 + \omega_{EXT}^2} \\
\\
f_O(s) &= \frac{g}{s} + A_O\frac{\omega_O}{s^2 + \omega_O^2}
\end{aligned}
\right\}
$$

Therefore:

$$ADAPT(s) = -\frac{g}{s} - A_{EXT}\frac{\omega_{EXT}}{s^2+\omega_{EXT}^2} + A_{EXT}\frac{\omega_{EXT}}{(s+a)^2+\omega_{EXT}^2} - A_O\frac{\omega_O}{(s+a)^2+\omega_O^2}$$

Where:

- $\hat{g}(s) = -S_{OTO}(s)f_{EXT}(s)$ is the estimated gravity from current motion (Figure 32)

- $\hat{a}(s) = (S_{OTO}(s)-1)f_{EXT}(s)$ is the estimated linear acceleration from current motion (Figure 32)

- $\hat{g}_O(s) = -S_{OTO}(s)f_O(s)$ is the estimated gravity sensed by the otoliths from the old motion, already in the neural store. It is assumed that we are fully adapted to this motion.

- $\hat{a}_O(s) = (S_{OTO}(s)-1)f_O(s)$ is the estimated linear acceleration sensed by the otoliths from the old motion, already in the neural store. It is assumed that we are fully adapted to this motion.

By combining the equations for adaptation signal $ADAPT(s)$ and $\Delta g(s)$ we derive the following for $\Delta g(s)$:

$$\Delta g(s) = X_{\Delta g}(s)\left(A_{EXT}\frac{\omega_{EXT}}{(s+a)^2+\omega_{EXT}^2} - A_O\frac{\omega_O}{(s+a)^2+\omega_O^2}\right)$$

Because the system is linear, the last equation corresponds to the response of $\Delta g(s)$ in the linear combination of two independent input signals, which are damped sinusoidals:

97

$$L^{-1}\left[A_{EXT}\frac{\omega_{EXT}}{\left(s+a\right)^{2}+\omega_{EXT}^{2}}\right]=A_{EXT}e^{-at}\sin\omega_{EXT}t$$

$$L^{-1}\left[A_{O}\frac{\omega_{O}}{\left(s+a\right)^{2}+\omega_{O}^{2}}\right]=A_{O}e^{-at}\sin\omega_{O}t$$

Where:

$L^{-1}[\ ]$ is the inverse Laplace transform of the argument in the brackets

Since $\Delta g(s)$ is known, $\Delta g(t)$ can be obtained in principle by inverting the Laplace transform. However, for our purposes it will suffice to know only $\Delta g_{SS}(t)$, the steady state part of $\Delta g(t)$ with the property that $\lim_{t\to\infty}\left(\Delta g(t)-\Delta g_{SS}(t)\right)=0$. Because the system is LTI and the input signals are sinusoids (Nise, 2004), the steady-state solution is based on the transfer function $X_{\Delta g}(s)$ by substituting $s=j\omega$ and taking the magnitude of it $M_{\Delta g}(\omega)=\left|X_{\Delta g}(s)\right|_{s=j\omega}$. Specifically,

$$M_{\Delta g}(\omega)=\frac{\omega}{\sqrt{\left(k_{g}+\tau_{OTO}\omega^{2}\right)^{2}+\omega^{2}\left(1-k_{a}\tau_{OTO}\right)^{2}}}$$

For the analysis to follow, let us define $f_{EXT,1}(t)$ and $f_{EXT,2}(t)$, where:

$$f_{EXT,1}(t) \equiv L^{-1}\left[A_{EXT}\frac{\omega_{EXT}}{(s+a)^2 + \omega_{EXT}^2}\right] = e^{-at}A_{EXT}\sin(\omega_{EXT}t)$$

$$f_{EXT,2}(t) \equiv L^{-1}\left[A_O\frac{\omega_O}{(s+a)^2 + \omega_O^2}\right] = e^{-at}A_O\sin(\omega_O t)$$

Thus:

$$\Delta g(s) = X_{\Delta g}(s)\left(A_{EXT}\frac{\omega_{EXT}}{(s+a)^2 + \omega_{EXT}^2} - A_O\frac{\omega_O}{(s+a)^2 + \omega_O^2}\right)$$

$$X_{\Delta g}(s) = -\frac{sS_{OTO}(s)}{s + (k_a - k_g)S_{OTO}(s) - k_a}$$

$$S_{OTO}(s) = \frac{1}{\tau_{OTO}s + 1}$$

$\left.\vphantom{\begin{array}{c}a\\a\\a\\a\\a\\a\end{array}}\right\}$ $\xrightarrow{\substack{LTI\\ system}}$

$$\Delta g_{SS}(t) = M_{\Delta g}(\omega_{EXT})f_{EXT,1}(t) - M_{\Delta g}(\omega_O)f_{EXT,2}(t)$$

$$f_{EXT,1}(t) = e^{-at}A_{EXT}\sin(\omega_{EXT}t)$$

$$f_{EXT,2}(t) = e^{-at}A_O\sin(\omega_O t)$$

$\left.\vphantom{\begin{array}{c}a\\a\\a\end{array}}\right\} \Rightarrow$

$$\boxed{\Delta g_{SS}(t) = M_{\Delta g}(\omega_{EXT})A_{EXT}e^{-at}\sin\omega_{EXT}t - M_{\Delta g}(\omega_O)A_O e^{-at}\sin\omega_O t}$$

(1.22)

For ROF error we derive the following:

$$ROF(s) = X_{ROF}(s)\left(f_{EXT}(s) + ADAPT(s)\right)$$

$$f_{EXT}(s) = L\left(f_{EXT}(t)\right)$$

$$f_{EXT}(t) = A_{EXT}\sin(\omega_{EXT}t)$$

$$ADAPT(s) = -\frac{g}{s} - A_{EXT}\frac{\omega_{EXT}}{s^2 + \omega_{EXT}^2} + A_{EXT}\frac{\omega_{EXT}}{(s+a)^2 + \omega_{EXT}^2} - A_O\frac{\omega_O}{(s+a)^2 + \omega_O^2}$$

$\left.\vphantom{\begin{array}{c}a\\a\\a\\a\end{array}}\right\} \Rightarrow$

$$ROF(s) = X_{ROF}(s)\left(A_{EXT}\frac{\omega_{EXT}}{(s+a)^2 + \omega_{EXT}^2} - A_O\frac{\omega_O}{(s+a)^2 + \omega_O^2}\right)$$

Where:

$$X_{ROF}(s) = \frac{RETINA(s)\,EYE(s)\,X_{VOR}(s)\,X_{V_{EST}}(s)\dfrac{k_a}{s}\,X_{\Delta a}(s)\,K}{1+EYE(s)\,RETINA(s)\,G_{OKR}\,K}$$

Because the system is linear, the last equation for ROF corresponds to the response of $ROF(s)$ to the linear combination of two independent input signals, which are damped sinusoidals:

$$L^{-1}\left(A_{EXT}\,\frac{\omega_{EXT}}{(s+a)^2+\omega_{EXT}^2}\right)=A_{EXT}\,e^{-at}\sin\omega_{EXT}t$$

$$L^{-1}\left(A_{O}\,\frac{\omega_{O}}{(s+a)^2+\omega_{O}^2}\right)=A_{O}\,e^{-at}\sin\omega_{O}t$$

Furthermore, because the system is LTI and the input signals are sinusoids (Nise, 2004), the steady-state solution of $ROF(s)$ in time domain (frequency response of $ROF(s)$) will be based on the transfer function $X_{ROF}(s)$ by substituting $s=j\omega$ and taking the magnitude of it $M_{ROF}(\omega)=\left|X_{ROF}(s)\right|_{s=j\omega}$.

Therefore:

$$ROF(s) = X_{ROF}(s)\left(A_{EXT}\frac{\omega_{EXT}}{(s+a)^2+\omega_{EXT}^2} - A_O\frac{\omega_O}{(s+a)^2+\omega_O^2}\right)\left.\right\}$$

$$X_{ROF}(s) = \frac{RETINA(s)\,EYE(s)\,X_{VOR}(s)\,X_{V_{EST}}(s)\dfrac{k_a}{s}X_{\Delta a}(s)K}{1+RETINA(s)G_{OKR}EYE(s)K}\left.\right\} \xrightarrow[system]{LTI}$$

$$\left.\begin{array}{l} ROF(t) = \left|X_{ROF}(s)\right|_{s=j\omega_{EXT}} f_{EXT,1}(t) - \left|X_{ROF}(s)\right|_{s=j\omega_O} f_{EXT,2}(t) \\[2mm] f_{EXT,1}(t) = L^{-1}\left[A_{EXT}\dfrac{\omega_{EXT}}{(s+a)^2+\omega_{EXT}^2}\right] \\[4mm] f_{EXT,2}(t) = L^{-1}\left[A_{EXT}\dfrac{\omega_O}{(s+a)^2+\omega_O^2}\right] \\[4mm] X_{ROF}(s) = \dfrac{RETINA(s)\,EYE(s)\,X_{VOR}(s)\,X_{V_{EST}}(s)\dfrac{k_a}{s}X_{\Delta a}(s)K}{1+RETINA(s)G_{OKR}EYE(s)K} \end{array}\right\} \Rightarrow$$

$$\left.\begin{array}{l} ROF(t) = \left|X_{ROF}(s)\right|_{s=j\omega_{EXT}} f_{EXT,1}(t) - \left|X_{ROF}(s)\right|_{s=j\omega_O} f_{EXT,2}(t) \\[2mm] f_{EXT,1}(t) = A_{EXT}e^{-at}\sin(\omega_{EXT}t) \\[2mm] f_{EXT,2}(t) = A_O e^{-at}\sin(\omega_O t) \\[2mm] X_{ROF}(s) = \dfrac{RETINA(s)\,EYE(s)\,X_{VOR}(s)\,X_{V_{EST}}(s)\dfrac{k_a}{s}X_{\Delta a}(s)K}{1+RETINA(s)G_{OKR}EYE(s)K} \end{array}\right\} \Rightarrow$$

$$\left.\begin{array}{l} ROF(t) = \left|X_{ROF}(s)\right|_{s=j\omega_{EXT}} A_{EXT}e^{-at}\sin(\omega_{EXT}t) - \left|X_{ROF}(s)\right|_{s=j\omega_O} A_O e^{-at}\sin(\omega_O t) \\[4mm] X_{ROF}(s) = \dfrac{KX_{VOR}(s)\,X_{V_{EST}}(s)\dfrac{k_a}{s}X_{\Delta a}(s)}{\dfrac{1}{RETINA(s)\,EYE(s)}+G_{OKR}K} \end{array}\right\}$$

But for the transfer function of the residual optical flow, $X_{ROF}(s)$, stands the following:

$$M_{ROF}(\omega) = \left| X_{ROF}(s) \right|_{s=j\omega} = \frac{K \left| X_{VOR}(s) \right|_{s=j\omega} \left| X_{V_{EST}}(s) \right|_{s=j\omega} \left| \dfrac{k_a}{s} \right|_{s=j\omega} \left| X_{\Delta a}(s) \right|_{s=j\omega}}{\left| \dfrac{1}{RETINA(s) \, EYE(s)} + G_{OKR} K \right|_{s=j\omega}}$$

$$RETINA(s) = \frac{1}{\tau_V s + 1}$$

$$EYE(s) = \frac{\tau_{E1} s + 1}{(\tau_{E2} s + 1)(\tau_{E3} s + 1)(\tau_{E4} s + 1)}$$

$$\left| X_{VOR}(s) \right|_{s=j\omega} = \left| G_{VOR} \left(\frac{\tau_{VOR} s}{\tau_{VOR} s + 1} \right)^2 \right|_{s=j\omega}$$

$$\left| X_{V_{EST}}(s) \right|_{s=j\omega} = \left| \frac{1}{\tau_L s + 1} \right|_{s=j\omega}$$

$$\left| X_{\Delta a}(s) \right|_{s=j\omega} = \left| X_{\Delta g}(s) \left(\frac{1}{S_{OTO}(s)} - 1 \right) \right|_{s=j\omega}$$

$$\left| X_{\Delta g}(s) \right|_{s=j\omega} = \left| -\frac{s S_{OTO}(s)}{s + (k_a - k_g) S_{OTO}(s) - k_a} \right|_{s=j\omega}$$

$$S_{OTO}(s) = \frac{1}{\tau_{OTO} s + 1}$$

$$\left. \right\} \xrightarrow{s=j\omega}$$

$$M_{ROF}(\omega) = \left| X_{ROF}(j\omega) \right| = \frac{K \left| X_{VOR}(j\omega) \right| \left| X_{V_{EST}}(j\omega) \right| \left| \dfrac{k_a}{j\omega} \right| \left| X_{\Delta a}(j\omega) \right|}{\left| \dfrac{(\tau_V j\omega + 1)(\tau_{E2} j\omega + 1)(\tau_{E3} j\omega + 1)(\tau_{E4} j\omega + 1)}{(\tau_{E1} j\omega + 1)} + G_{OKR} K \right|}$$

$$\left| X_{VOR}(j\omega) \right| = G_{VOR} \left| \frac{\tau_{VOR} j\omega}{\tau_{VOR} j\omega + 1} \right|^2$$

$$\left| X_{V_{EST}}(j\omega) \right| = \left| \frac{1}{\tau_L j\omega + 1} \right|$$

$$\left| X_{\Delta a}(j\omega) \right| = \tau_{OTO} \left| \frac{\omega^2}{-(k_g + \tau_{OTO} \omega^2) + j\omega(1 - k_a \tau_{OTO})} \right|$$

$$\left. \right\} \Rightarrow$$

$$M_{ROF}(\omega) = \frac{K\left|X_{VOR}(j\omega)\right|\left|X_{V_{EST}}(j\omega)\right|\left|\dfrac{k_a}{j\omega}\right|\left|X_{\Delta a}(j\omega)\right|\left|\tau_{E1}j\omega+1\right|}{\left|(\tau_V j\omega+1)(\tau_{E2}j\omega+1)(\tau_{E3}j\omega+1)(\tau_{E4}j\omega+1)+(\tau_{E1}j\omega+1)G_{OKR}K\right|}$$

$$\left|X_{VOR}(j\omega)\right| = G_{VOR}\frac{\tau_{VOR}^2\omega^2}{(\tau_{VOR}\omega)^2+1}$$

$$\left|X_{V_{EST}}(j\omega)\right| = \frac{1}{\sqrt{1+(\tau_L\omega)^2}}$$

$$\left|X_{\Delta a}(j\omega)\right| = \frac{\tau_{OTO}\omega^2}{\sqrt{\left(k_g+\tau_{OTO}\omega^2\right)^2+\omega^2\left(1-k_a\tau_{OTO}\right)^2}}$$

$$\left|den(j\omega)\right| \equiv \left|(\tau_V j\omega+1)(\tau_{E2}j\omega+1)(\tau_{E3}j\omega+1)(\tau_{E4}j\omega+1)+(\tau_{E1}j\omega+1)G_{OKR}K\right|$$

$\Rightarrow$

$$M_{ROF}(\omega) = \frac{K\dfrac{k_a}{\omega}\left|X_{VOR}(j\omega)\right|\left|X_{V_{EST}}(j\omega)\right|\left|X_{\Delta a}(j\omega)\right|\left|\sqrt{(\tau_{E1}\omega)^2+1}\right|}{\left|den(j\omega)\right|}$$

$$\left|X_{VOR}(j\omega)\right| = G_{VOR}\frac{\tau_{VOR}^2\omega^2}{(\tau_{VOR}\omega)^2+1}$$

$$\left|X_{V_{EST}}(j\omega)\right| = \frac{1}{\sqrt{1+(\tau_L\omega)^2}}$$

$$\left|X_{\Delta a}(j\omega)\right| = \frac{\tau_{OTO}\omega^2}{\sqrt{\left(k_g+\tau_{OTO}\omega^2\right)^2+\omega^2\left(1-k_a\tau_{OTO}\right)^2}}$$

$$\left|den(j\omega)\right| \equiv \left|(\tau_V j\omega+1)(\tau_{E2}j\omega+1)(\tau_{E3}j\omega+1)(\tau_{E4}j\omega+1)+(\tau_{E1}j\omega+1)G_{OKR}K\right|$$

For the denominator $\left|den(j\omega)\right|$ of X_{ROF} we derive the following:

$$\left|den\left(j\omega\right)\right| = \left|\left(\tau_V j\omega+1\right)\left(\tau_{E2} j\omega+1\right)\left(\tau_{E3} j\omega+1\right)\left(\tau_{E4} j\omega+1\right)+\left(\tau_{E1} j\omega+1\right)G_{OKR}K\right| \Rightarrow$$

$$\left|den\left(j\omega\right)\right| = \left|\left(1-\tau_V \tau_{E2}\omega^2 + j\omega\left(\tau_V + \tau_{E2}\right)\right)\left(1-\tau_{E3}\tau_{E4}\omega^2 + j\omega\left(\tau_{E3} + \tau_{E4}\right)\right)+\left(\tau_{E1} j\omega+1\right)G_{OKR}K\right| \Rightarrow$$

$$\left|den\left(j\omega\right)\right| = \left|\begin{array}{l}\tau_V \tau_{E2}\tau_{E3}\tau_{E4}\omega^4 - \omega^2\left(\tau_{E3}\tau_{E4} + \tau_V \tau_{E2} + \left(\tau_V + \tau_{E2}\right)\left(\tau_{E3} + \tau_{E4}\right)\right)+1+G_{OKR}K + \\ + j\omega\left(\tau_V + \tau_{E2} + \tau_{E3} + \tau_{E4} + \tau_{E1}G_{OKR}K\right) - j\omega^3\left(\tau_V \tau_{E2}\left(\tau_{E3} + \tau_{E4}\right)+\tau_{E3}\tau_{E4}\left(\tau_V + \tau_{E2}\right)\right)\end{array}\right| \Rightarrow$$

$$\left|den\left(j\omega\right)\right| = \left|n_4\omega^4 - \omega^2 n_2 + n_0 + j\left(n_1\omega - n_3\omega^3\right)\right| \Rightarrow$$

$$\left|den\left(j\omega\right)\right| = \sqrt{\left(n_4\omega^4 - \omega^2 n_2 + n_0\right)^2 + \left(n_1\omega - n_3\omega^3\right)^2}$$

Where:

$$n_4 = \tau_V \tau_{E2}\tau_{E3}\tau_{E4}$$

$$n_3 = \tau_V\left(\tau_{E3}\left(\tau_{E4} + \tau_{E3}\right)+\tau_{E2}\tau_{E4}\right)+\tau_{E2}\tau_{E3}\tau_{E4}$$

$$n_2 = \left(\tau_{E2} + \tau_{E3}\right)\left(\tau_V + \tau_{E4}\right)+\tau_V \tau_{E4} + \tau_{E2}\tau_{E3}$$

$$n_1 = \tau_{E4} + G_{OKR}K\tau_{E1} + \tau_{E2} + \tau_{E3} + \tau_V$$

$$n_0 = G_{OKR}K + 1$$

Therefore:

$$\left.\begin{array}{l} M_{ROF}\left(\omega\right) = \dfrac{K\dfrac{k_a}{\omega}\left|X_{VOR}\left(j\omega\right)\right|\left|X_{V_{EST}}\left(j\omega\right)\right|\left|X_{\Delta a}\left(j\omega\right)\right|\sqrt{\left(\tau_{E1}\omega\right)^2 + 1}}{\left|den\left(j\omega\right)\right|} \\[4mm] \left|X_{VOR}\left(j\omega\right)\right| = G_{VOR}\dfrac{\tau_{VOR}^2\omega^2}{\left(\tau_{VOR}\omega\right)^2 + 1} \\[4mm] \left|X_{V_{EST}}\left(j\omega\right)\right| = \dfrac{1}{\sqrt{1+\left(\tau_L\omega\right)^2}} \\[4mm] \left|X_{\Delta a}\left(j\omega\right)\right| = \dfrac{\tau_{OTO}\omega^2}{\sqrt{\left(k_g + \tau_{OTO}\omega^2\right)^2 + \omega^2\left(1-k_a\tau_{OTO}\right)^2}} \\[4mm] \left|den\left(j\omega\right)\right| = \sqrt{\left(n_4\omega^4 - \omega^2 n_2 + n_0\right)^2 + \left(n_1\omega - n_3\omega^3\right)^2} \end{array}\right\} \Rightarrow$$

$$M_{ROF}(\omega) = \frac{G_{VOR}k_a K \tau_{OTO}\tau_{VOR}^2 \omega^3 \dfrac{1}{(\tau_{VOR}\omega)^2+1}\dfrac{1}{\sqrt{1+(\tau_L\omega)^2}}\sqrt{(\tau_{E1}\omega)^2+1}}{\sqrt{(k_g+\tau_{OTO}\omega^2)^2+\omega^2(1-k_a\tau_{OTO})^2}\sqrt{(n_4\omega^4-n_2\omega^2+n_0)^2+(n_1\omega-n_3\omega^3)^2}}$$

So, for ROF we derive the following:

$$ROF_{SS}(t) = M_{ROF}(\omega_{EXT})A_{EXT}e^{-at}\sin(\omega_{EXT}t) - M_{ROF}(\omega_O)A_O e^{-at}\sin(\omega_O t)$$

Where:

- $$M_{ROF}(\omega) = \frac{G_{VOR}k_a K \tau_{OTO}\tau_{VOR}^2 \omega^3 \dfrac{1}{(\tau_{VOR}\omega)^2+1}\dfrac{1}{\sqrt{1+(\tau_L\omega)^2}}\sqrt{(\tau_{E1}\omega)^2+1}}{\sqrt{(k_g+\tau_{OTO}\omega^2)^2+\omega^2(1-k_a\tau_{OTO})^2}\sqrt{(n_4\omega^4-n_2\omega^2+n_0)^2+(n_1\omega-n_3\omega^3)^2}}$$

In summary, the analytical solutions in time domain for the gravity estimation error $\Delta g(t)$ and for the residual optical flow $ROF(t)$, in steady state, are the following:

$$\boxed{\Delta g_{SS}(t) = M_{\Delta g}(\omega_{EXT})A_{EXT}e^{-at}\sin(\omega_{EXT}t) - M_{\Delta g}(\omega_O)A_O e^{-at}\sin(\omega_O t)}$$
(1.23)

$$\boxed{ROF_{SS}(t) = M_{ROF}(\omega_{EXT})A_{EXT}e^{-at}\sin(\omega_{EXT}t) - M_{ROF}(\omega_O)A_O e^{-at}\sin(\omega_O t)}$$
(1.24)

Where:

$$M_{\Delta g}(\omega) = \frac{\omega}{\sqrt{(k_g+\tau_{OTO}\omega^2)^2+\omega^2(1-k_a\tau_{OTO})^2}}$$

- $$M_{ROF}(\omega) = M_{\Delta g}(\omega)\frac{G_{VOR}k_a K \tau_{OTO}\tau_{VOR}^2 \omega^2 \dfrac{1}{(\tau_{VOR}\omega)^2+1}\dfrac{\sqrt{(\tau_{E1}\omega)^2+1}}{\sqrt{1+(\tau_L\omega)^2}}}{\sqrt{(n_4\omega^4-n_2\omega^2+n_0)^2+(n_1\omega-n_3\omega^3)^2}}$$

- $$n_4 = \tau_V\tau_{E2}\tau_{E3}\tau_{E4}$$

- $n_3 = \tau_V \left(\tau_{E3} \left(\tau_{E4} + \tau_{E3} \right) + \tau_{E2} \tau_{E4} \right) + \tau_{E2} \tau_{E3} \tau_{E4}$

- $n_2 = \tau_{E3} \tau_{E4} + \tau_V \tau_{E2} + \left(\tau_V + \tau_{E2} \right) \left(\tau_{E3} + \tau_{E4} \right)$

- $n_1 = \tau_{E4} + G_{OKR} K \tau_{E1} + \tau_{E2} + \tau_{E3} + \tau_V$

- $n_0 = G_{OKR} K + 1$

3. Combined Error Signal Analytical Calculation

The combined error signal is derived from the mean value of the independently normalized errors:

$$\Delta g_{NORM}\left(t\right) = \frac{1}{1 + \left(\dfrac{b_g}{\Delta g_{SS}\left(t\right)} \right)^2} \tag{1.25}$$

Where:

- b_g is the normalization parameter of gravity estimation error

$$ROF_{NORM}\left(t\right) = \frac{1}{1 + \left(\dfrac{b_{VISUAL}}{ROF_{SS}\left(t\right)} \right)^2} \tag{1.26}$$

Where:

- b_{VISUAL} is the normalization parameter of the residual optical flow

$$ERROR\left(t\right) = \frac{\Delta g_{NORM}\left(t\right) + ROF_{NORM}\left(t\right)}{2} \tag{1.27}$$

4. Motion Sickness Incidence Calculation

The error signal is varying linearly with the sine of the external motion, therefore it varies much faster than the cumulate taking place. Thus, at the final calculation of the MSI we will use the mean value of the error (integrated numerically for one period time of the external motion f_{EXT}). This will give the average error during one period.

Finally, the MSI derived from the above combined error, has the following equation:

$$MSI = P(ERROR)_{MEAN}\left[1-\left(\frac{t}{\mu}+1\right)e^{-\frac{t}{\mu}}\right]$$
(1.28)

Where:

- The term $\left[1-\left(\frac{t}{\mu}+1\right)e^{-\frac{t}{\mu}}\right]$ is the equivalent of a second order leaky integrator in t-domain, from (Bos et al., 2001b)

- $ERROR_{MEAN} = \frac{1}{T}\int_{0}^{T}(ERROR)dt \xrightarrow{x=\omega_{EXT}t} ERROR_{MEAN} = \frac{1}{2\pi}\int_{0}^{2\pi}(ERROR)dx$

- $x = \omega_{EXT}t$

- P is a constant used to convert the MSI from [0, 1] to [0, 100]

5. System Stability

To have an asymptotically stable system, all the poles of the transfer function must have a negative real part (lie in the left half of the complex plane). The poles are defined as the roots of the transfer function denominator.

First we will find the poles of $X_{\Delta g}(s)$. Thus, we must modify the transfer function and rewrite it as:

$$
\left.\begin{array}{l}
X_{\Delta g}(s) = -\dfrac{sS_{OTO}(s)}{s + (k_a - k_g)S_{OTO}(s) - k_a} \\[4mm]
S_{OTO}(s) = \dfrac{1}{\tau_{OTO}s + 1}
\end{array}\right\} \Rightarrow X_{\Delta g}(s) = -\dfrac{s}{\tau_{OTO}s^2 + s(1 - k_a\tau_{OTO}) - k_g} \Rightarrow
$$

$$
X_{\Delta g}(s) = -\dfrac{1}{\tau_{OTO}}\dfrac{s}{(s+k)^2 - l^2} \Rightarrow X_{\Delta g}(s) = -\dfrac{1}{\tau_{OTO}}\dfrac{s}{(s+k-l)(s+k+l)}
$$

Where:

$$
k = \dfrac{1 - k_a\tau_{OTO}}{2\tau_{OTO}}
$$

$$
l^2 = \dfrac{(1 - k_a\tau_{OTO})^2 + 4k_g\tau_{OTO}}{4\tau_{OTO}^2}
$$

Therefore, the poles of $X_{\Delta g}(s)$ are:

$$
\left.\begin{array}{l}
p_1 = -k + l \\
p_2 = -k - l
\end{array}\right\} \Rightarrow
\left.\begin{array}{l}
p_1 = -\dfrac{1 - k_a\tau_{OTO}}{2\tau_{OTO}} + \dfrac{(1 - k_a\tau_{OTO})^2 + 4k_g\tau_{OTO}}{4\tau_{OTO}^2} \\[4mm]
p_2 = -\dfrac{1 - k_a\tau_{OTO}}{2\tau_{OTO}} - \dfrac{(1 - k_a\tau_{OTO})^2 + 4k_g\tau_{OTO}}{4\tau_{OTO}^2}
\end{array}\right\} \Rightarrow
$$

$$
\Rightarrow
\left.\begin{array}{l}
p_1 = \dfrac{1}{2\tau_{OTO}}\left(-1 + k_a\tau_{OTO} + \sqrt{(1 - k_a\tau_{OTO})^2 + 4k_g\tau_{OTO}}\right) \\[4mm]
p_2 = \dfrac{1}{2\tau_{OTO}}\left(-1 + k_a\tau_{OTO} - \sqrt{(1 - k_a\tau_{OTO})^2 + 4k_g\tau_{OTO}}\right)
\end{array}\right\}
$$

Multiple values may lead to negative real parts, but we are interested in these values for k_a and k_g that are

simplifying the model. Therefore, we checked four combinations of values with the following results:

	Combinations			
	A	**B**	**C**	**D**
k_a	1	-1	1	-1
k_g	1	-1	-1	1
Pole p_1	1	-1	-0.2576+j1.2037	0.5022
Pole p_2	-1.5152	-1.5152	-0.2576-j1.2037	-3.0173

Combinations A and D lead to unstable systems because at least one pole has non-negative real part. Therefore combinations A and D are excluded.

The same analysis with the transfer function of the residual optical flow leads to the exclusion of combination A and D.

Between combinations B and C we decided to use B because we assume that the same dynamics influencing the input of external motion into the otolith organs, influence the estimation of motion into the neural store. Therefore, because we assumed that $\hat{f}_N(s) = \hat{g}(s) + \hat{a}(s)$, then

$$\hat{f}_{EXT}(s) = \hat{g}_{EST} + \hat{a}_{EST} = \frac{1}{s}\left(\Delta g(s) + \Delta a(s)\right).$$

For the residual optical flow transfer function $X_{ROF}(s)$ we have the following:

$$X_{ROF}(s) = \dfrac{KX_{VOR}(s) X_{V_{EST}}(s) \dfrac{k_a}{s} X_{\Delta a}(s)}{\dfrac{1}{RETINA(s) EYE(s)} + G_{OKR} K}$$

$$RETINA(s) = \dfrac{1}{\tau_V s + 1}$$

$$EYE(s) = \dfrac{\tau_{E1} s + 1}{(\tau_{E2} s + 1)(\tau_{E3} s + 1)(\tau_{E4} s + 1)}$$

$$X_{VOR}(s) = G_{VOR} \left(\dfrac{\tau_{VOR} s}{\tau_{VOR} s + 1} \right)^2$$

$$X_{V_{EST}}(s) = \dfrac{1}{\tau_L s + 1}$$

$$X_{\Delta a}(s) = X_{\Delta g}(s) \left(\dfrac{1}{S_{OTO}(s)} - 1 \right)$$

$$S_{OTO}(s) = \dfrac{1}{\tau_{OTO} s + 1}$$

$\Rightarrow$

$$X_{ROF}(s) = X_{\Delta g}(s) \dfrac{\dfrac{KG_{VOR}\tau_{OTO}k_a}{(\tau_V s + 1)(\tau_{E2} s + 1)(\tau_{E3} s + 1)(\tau_{E4} s + 1)}}{(\tau_{E1} s + 1)} + G_{OKR} K \left(\dfrac{\tau_{VOR} s}{\tau_{VOR} s + 1} \right)^2 \dfrac{1}{\tau_L s + 1} \Rightarrow$$

$$X_{ROF}(s) = X_{\Delta g}(s) \dfrac{KG_{VOR}\tau_{OTO}k_a (\tau_{E1} s + 1)}{den(s)} \left(\dfrac{\tau_{VOR} s}{\tau_{VOR} s + 1} \right)^2 \dfrac{1}{\tau_L s + 1}$$

Where:

- $den(s) = (\tau_V s + 1)(\tau_{E2} s + 1)(\tau_{E3} s + 1)(\tau_{E4} s + 1) + G_{OKR} K (\tau_{E1} s + 1)$

But, for $den(s)$ we have:

$$den(s) = (\tau_V s + 1)(\tau_{E2} s + 1)(\tau_{E3} s + 1)(\tau_{E4} s + 1) + (\tau_{E1} s + 1) G_{OKR} K \Rightarrow$$

$$den(s) = \left(1 + \tau_V \tau_{E2} s^2 + s(\tau_V + \tau_{E2})\right)\left(1 + \tau_{E3} \tau_{E4} s^2 + s(\tau_{E3} + \tau_{E4})\right) + (\tau_{E1} s + 1) G_{OKR} K \Rightarrow$$

$$den(s) = \tau_V \tau_{E2} \tau_{E3} \tau_{E4} s^4 + s^2 \left(\tau_{E3} \tau_{E4} + \tau_V \tau_{E2} + (\tau_V + \tau_{E2})(\tau_{E3} + \tau_{E4})\right) + 1 + G_{OKR} K +$$

$$+ s\left(\tau_V + \tau_{E2} + \tau_{E3} + \tau_{E4} + \tau_{E1} G_{OKR} K\right) + s^3 \left(\tau_V \tau_{E2} (\tau_{E3} + \tau_{E4}) + \tau_{E3} \tau_{E4} (\tau_V + \tau_{E2})\right) \Rightarrow$$

$$den(s) = n_4 s^4 + n_3 s^3 + s^2 n_2 + n_1 s + n_0$$

Where:

- $n_4 = \tau_V \tau_{E2} \tau_{E3} \tau_{E4}$

- $n_3 = \tau_V \left(\tau_{E3} (\tau_{E4} + \tau_{E3}) + \tau_{E2} \tau_{E4}\right) + \tau_{E2} \tau_{E3} \tau_{E4}$

- $n_2 = \tau_{E3} \tau_{E4} + \tau_V \tau_{E2} + (\tau_V + \tau_{E2})(\tau_{E3} + \tau_{E4})$

- $n_1 = \tau_{E4} + G_{OKR} K \tau_{E1} + \tau_{E2} + \tau_{E3} + \tau_V$

- $n_0 = G_{OKR} K + 1$

The poles of $X_{ROF}(s)$ are found to be $p_1 = -3.3363$, $p_2 = -0.2194$, $p_3 = -0.0751 + j0.0146$, and $p_4 = -0.0751 - j0.0146$. Because all the real parts are smaller than zero, we conclude that $X_{ROF}(s)$ gives a stable system.

THIS PAGE INTENTIONALLY LEFT BLANK

IV. MODEL VALIDATION

A. PARAMETER SETTINGS

In the analysis, we dealt with three major categories of parameters:

(1) Category 1: The parameters related to sensory dynamics, which are known values.

(2) Category 2: The parameters for which the values given by accepted research are not fixed. In this case, we established an acceptable interval for each parameter and then investigated the influence of the parameter to the proposed model. The final value of these parameters was derived from the goodness of fit of the proposed model output to the experimental data from McCauley et al. (1976).

(3) Category 3: The parameters, which we included in the model to investigate its performance. The final values of these parameters were fixed to simplify the proposed model.

The following parameter values were used for the analysis:

Parameter	Value
Otolith organs – time constant τ_o (Category 1)	0.66 s
Linear acceleration error estimation loop – Gain k_a (Category 3)	−1.0
Gravity error estimation loop – Gain k_g (Category 3)	−1.0
VOR interface – integrator's time constant τ_L	5.0 s

(Category 2)	
VOR interface - LP filter's time constant τ_{VOR} (Category 2)	1.318 s
Distance between subject and object and focus – $\mathbf{d}$ (Category 3)	1 m
VOR interface – Constant gain $\mathbf{G_{VOR}}$ (Category 3)	1.0
Visual system – Constant gain $\mathbf{G_{OKR}}$ (Category 3)	1.0
Oculomotor plant – time constant τ_{e1} (Category 1)	0.14 s
Oculomotor plant – time constant τ_{e2} (Category 1)	0.28 s
Oculomotor plant – time constant τ_{e3} (Category 1)	0.037 s
Oculomotor plant – time constant τ_{e4} (Category 1)	0.003 s
Visual system – Retinal Slip detection time constant τ_V (Category 1)	0.15 s
Visual system – fixed gain $\mathbf{k_2}$ (Category 2)	0.1
Visual system – distance dependent gain $\mathbf{k_1}$ (Category 2)	0.9
Adaptation – Time constant – $\tau_A = \dfrac{1}{a}$ (Category 2)	5*60*60 s
Error calculation – gravity estimation – $\mathbf{b_g}$ (Category 2)	0.0042 g
Error calculation – ROF – $\mathbf{b_{visual}}$ (Category 2)	0.00008 g
MSI calculation – $\mathbf{P}$ factor (Category 1)	100

Table 4: Model parameters values

B. FREQUENCY ANALYSIS

The following Bode plot depicts the frequency response of the error components in the proposed model (Appendix B. Program 3).
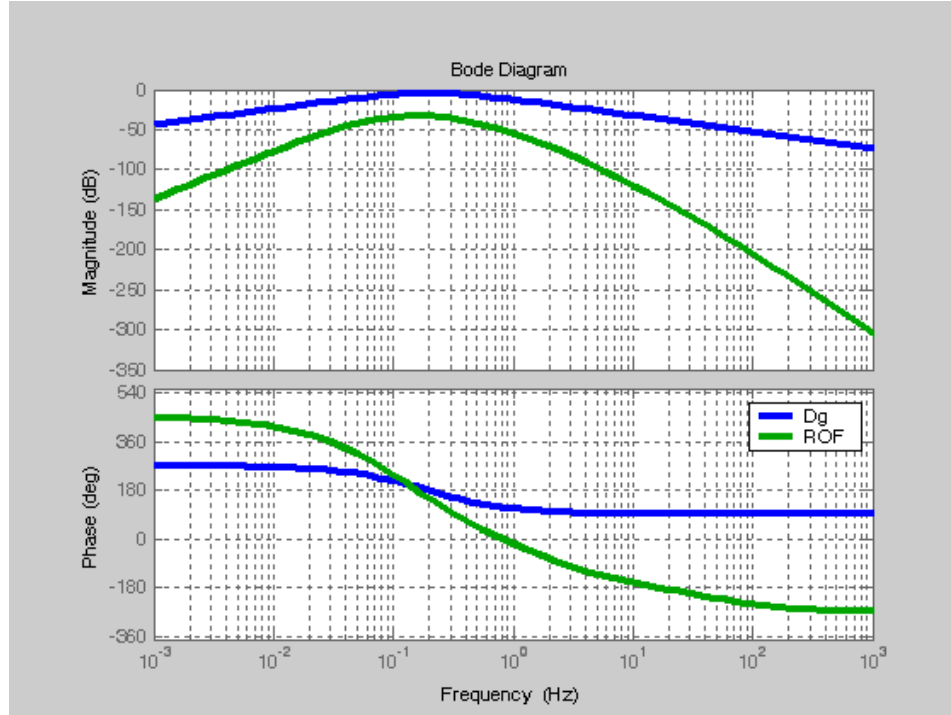
Figure 40: Bode plot of the model frequency response

The gravity estimation error has a maximum at a frequency slightly above 0.196 Hz. The maximum visual error is taking place at frequency 0.167 Hz.

C. AMPLITUDE-FREQUENCY-MSI PLOT ANALYSIS

The following plots (Figure 41 and Figure 42) depict the calculated MSI surface for a two-hour exposure to motion (Appendix B. Program 4).
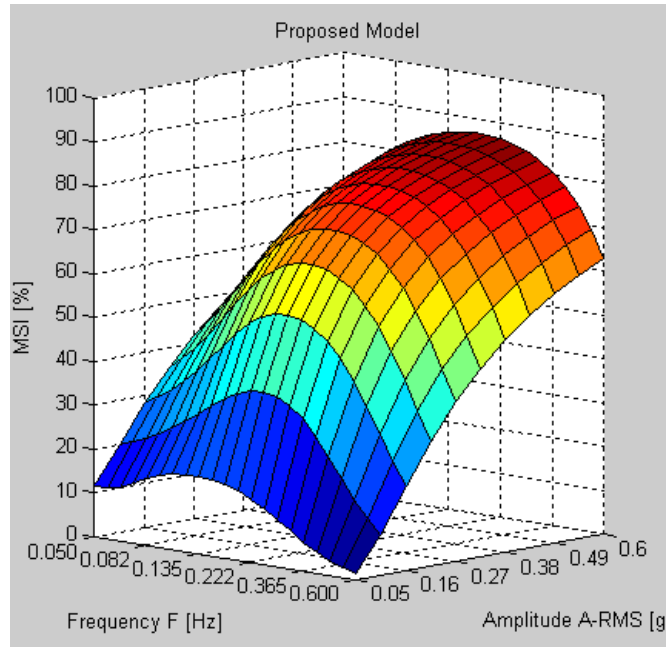
Figure 41: Proposed model's predicted MSI versus frequency and RMS-acceleration amplitude
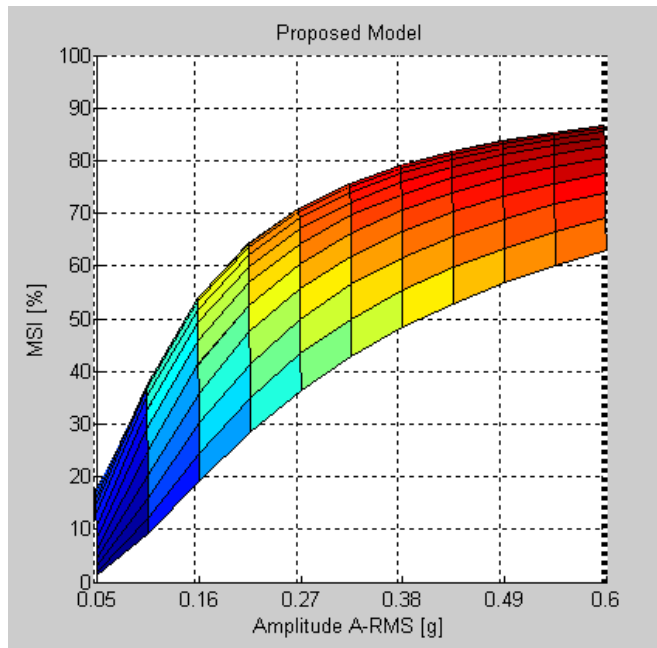
Figure 42: Proposed model's predicted MSI versus frequency and RMS-acceleration amplitude. Horizontal contours refer to frequency.

D. COMPARISON WITH HFR MODEL

In the following table we included the output MSI from three sources, the initial MSI calculated from the raw data in the McCauley et al. (1976) experiment, the MSI from the HFR descriptive model, and the MSI from the proposed model.

F Hz	Data	RMS Vertical Acceleration, in g								
		0.0278	0.055	0.111	0.170	0.222	0.234	0.333	0.444	0.555
0.083	Raw	0	5							
	MC	00.47	04.02							
	Prp	10.78	13.27							
0.167	Raw	0	10	30		60				
	MC	02.42	12.49	36.29		65.01				
	Prp	07.84	14.65	35.98		63.38				
0.180	Raw				60*					
	MC				51.31					
	Prp				57.00					
0.200	Raw						71*			
	MC						62.94			
	Prp						67.79			
0.250	Raw			31		63		69		
	MC			26.83		55.44		71.02		
	Prp			34.23		61.26		73.08		
0.333	Raw		5	15		46		50		
	MC		02.70	13.93		38.30		55.46		
	Prp		07.24	27.00		54.20		67.35		
0.417	Raw							50	40	
	MC							36.28	48.44	
	Prp							59.49	68.08	
0.500	Raw			0		14		25	33	42
	MC			01.45		09.05		19.42	29.60	38.64
	Prp			13.88		36.29		50.79	60.21	66.70
0.600	Raw								8	8
	MC								12.51	18.67
	Prp								50.28	57.27
0.700	Raw									4
	MC									06.74
	Prp									48.20

Table 5: Comparison of calculated MSI in a 2-hour exposure among the HFR model, proposed model and observed MSI in McCauley et al. (1976) experiments (* 90 minute exposure).

In the frequency region between 0.083 Hz and 0.417 Hz, the proposed model produces MSI that is no more than ±10% away from the raw data. In some cases the proposed model is closer to the raw data than the HFR model.

The difference between the proposed model and the raw data grows larger at the frequency edges of the HFR data set.

In the diagrams that follow, we can see the comparison between the HFR MSI model and the MSI predicted by the proposed model (Appendix B. Program 5). The diagrams reflect the difference between the two predicted MSIs.
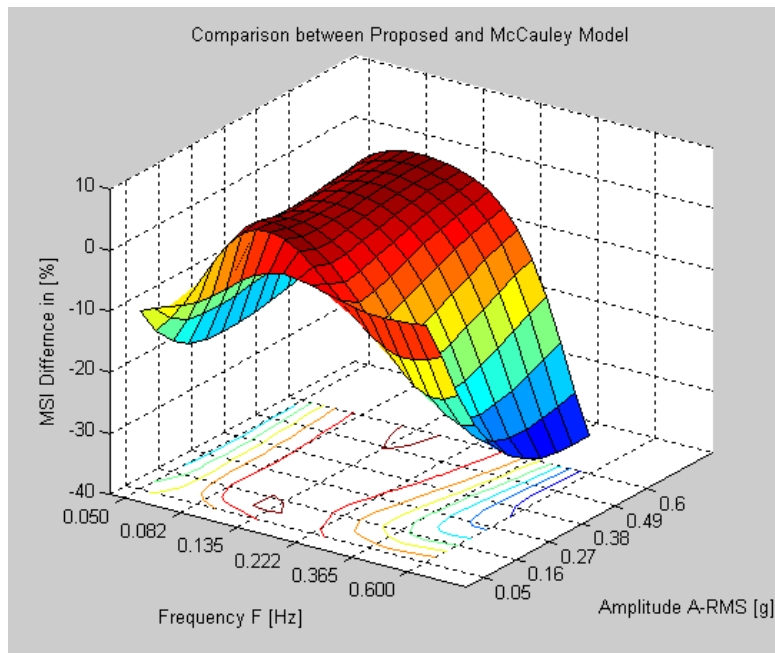
Figure 43: Comparison of predicted MSI (versus frequency and RMS-acceleration amplitude) between the proposed and the HFR MSI model.
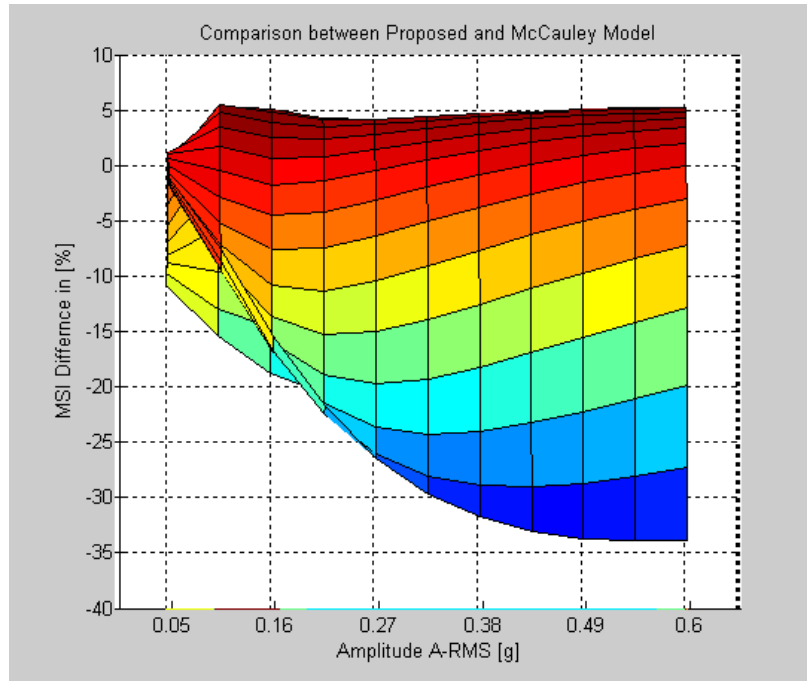
Figure 44: Difference in MSI projection plot.
Horizontal plot contours refer to frequency of induced
motion.
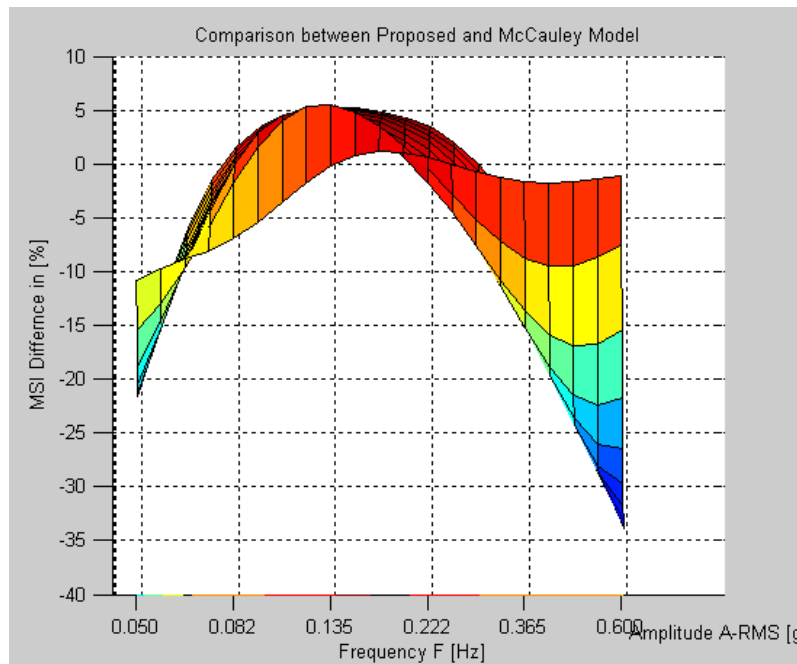
Figure 45: Difference in MSI projection plot.
Horizontal plot contours refer to RMS amplitude of induced
motion.

119

The difference of predicted MSI between the proposed model and the HFR model is less than ±5% in the frequency region between 0.07 Hz and 0.25 Hz.

The difference reaches -33% at 0.6 Hz and -21% at 0.05 Hz. This difference, at the outer frequency regions of the McCauley et al. (1976) experiments, is attributed to the limited number of human sub-systems which are known to provide motion information to the central nervous system (CNS), but are not taken into account into the proposed model. Thus, the corresponding errors from the aforementioned sub-systems, are not included in the prediction of MSI.

We believe that the proposed model may, very easily, be extended to include motion information derived from other sources (e.g. somatosensory input) so as to minimize the difference between the predicted MSI and the MSI found in real life.

E. ADAPTATION PLOTS

Adaptation was implemented in the proposed model with the adaptation mechanism as already described in page 76. The basis for that mechanism was the adaptation time constant, which we set to a value to compare the output MSI with the MSI found by McCauley et al. (1976).

It is obvious that MSI is minimal during the initial ten minutes of motion. After that, a rise time exists, which leads to the observed peak. Practically, MSI stabilizes for a small amount of time at peak values, and then adaptation begins to take effect.

120

The following plots summarize the model behavior in time (F. Program 6). The time constant was chosen to fit the McCauley et al. data.
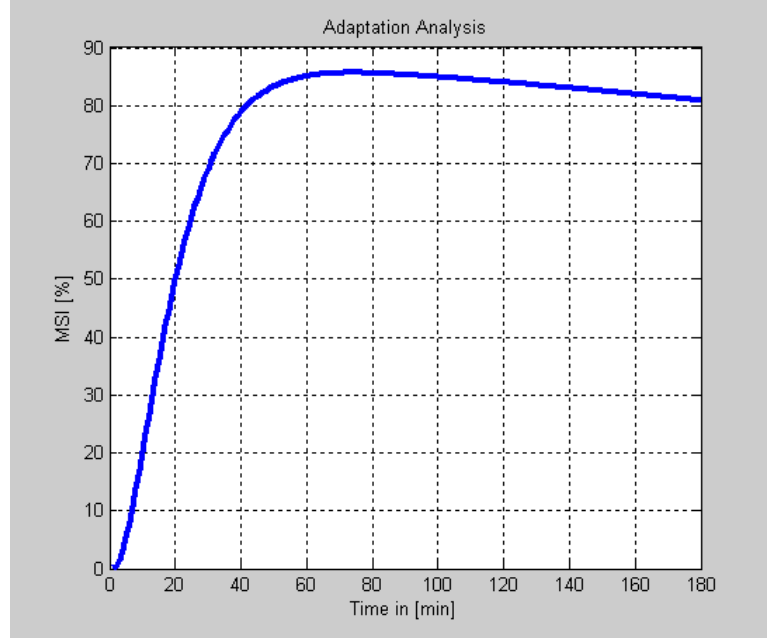
Figure 46: Predicted MSI for a 3-hour period (linear x-axis). $A_{RMS} = 0.5$ g and $f = 0.167$ Hz.
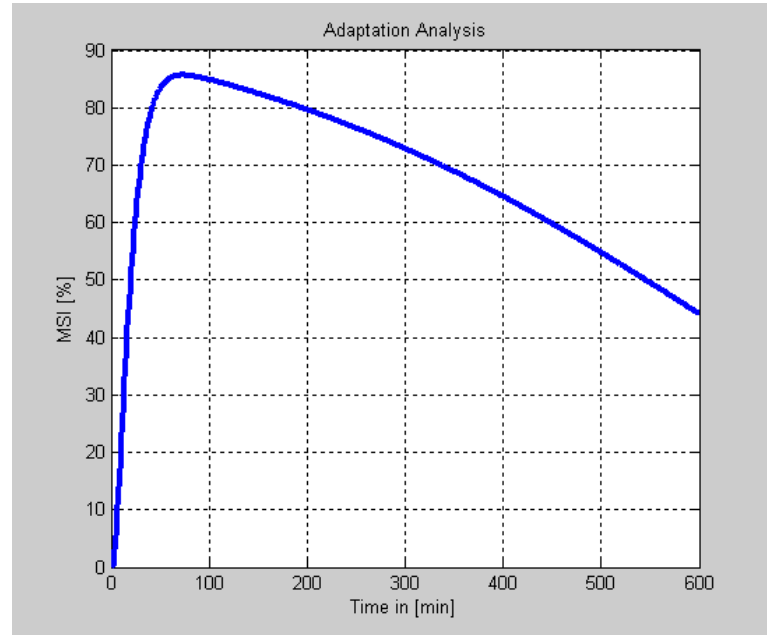
Figure 47: Predicted MSI for a 10-hour period (linear x-axis). $A_{RMS} = 0.5$ g and $f = 0.167$ Hz.
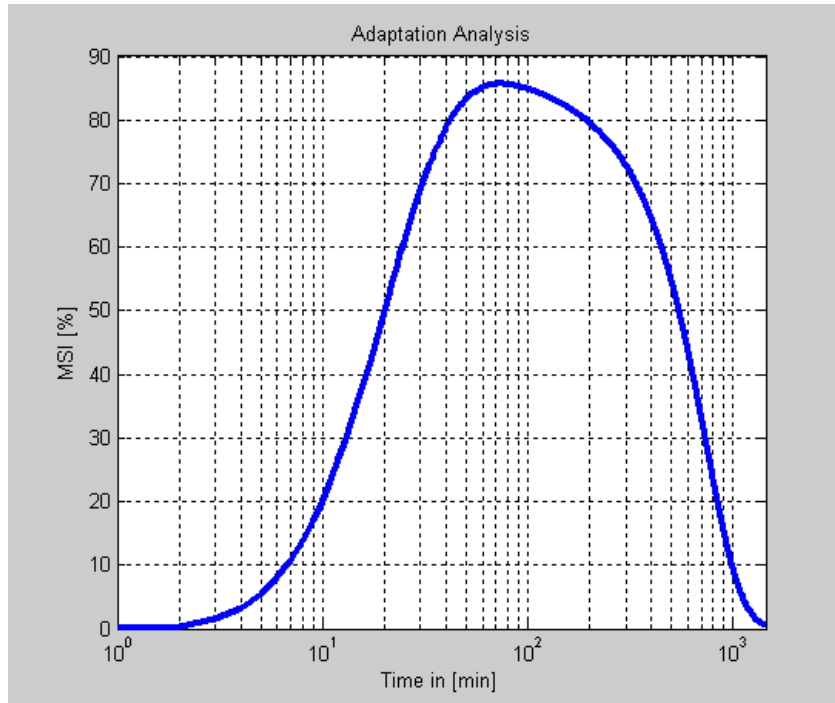
Figure 48: Predicted MSI for an 24-hour period (logarithmic x-axis) . $A_{RMS} = 0.5$ g and $f = 0.167$ Hz.

The following combined diagram depicts the timeline of predicted MSI at a frequency of 0.25 Hz and at three RMS-amplitude values, 0.111 g, 0.222 g and 0.333 g (F. Program 6). The amplitude, frequency, and time values were chosen to resemble to the ones used in the McCauley et al. (1976) report.
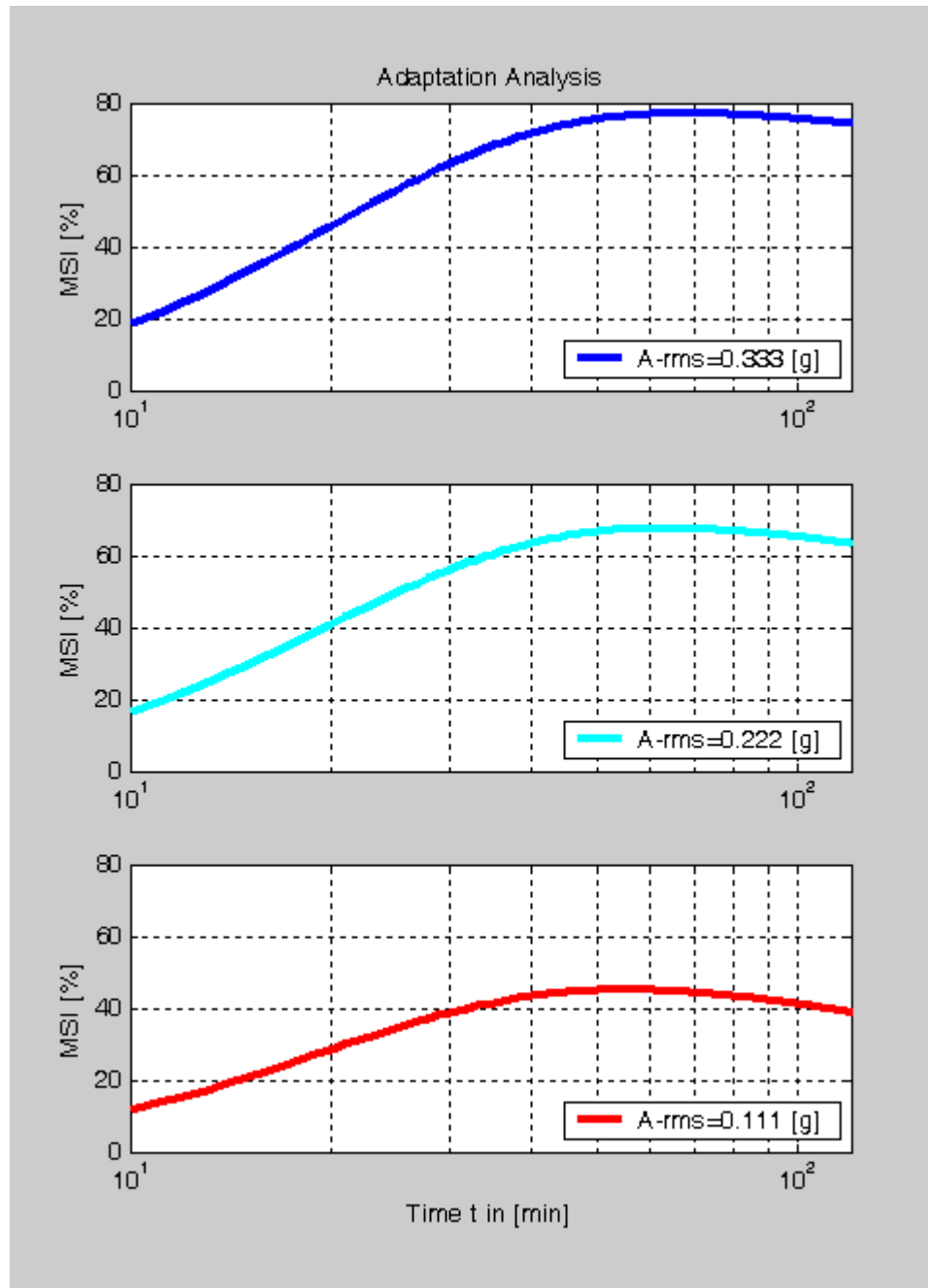
Figure 49: Predicted MSI at 0.25 Hz

THIS PAGE INTENTIONALLY LEFT BLANK

V. CONCLUSIONS AND RECOMMENDATIONS FOR FUTURE WORK

A. CONCLUSIONS

The proposed model combines the error produced in two major sensory systems to estimate the Motion Sickness Incidence:

- The error produced in the estimation of gravity vector in the vestibular system, and

- The error produced by the retinal slip in the visual system (residual optical flow).

The final product compared to the HFR MSI data from McCauley et al. (1976) gives an acceptable approximation for the critical region of frequencies.

The existing differences between the proposed model and the HFR data can be attributed to the constrained nature of this thesis.

The model cannot be used for the prediction of seasickness of a specific individual. After all, connection between a specific parameter and susceptibility to motion sickness is yet to be found (Bles et al., 1984; Lentz, 1984). Nevertheless, its output is close to the experimental statistical data, as already mentioned.

B. RECOMMENDATIONS FOR FUTURE WORK

Many aspects of the proposed model may be redefined and reanalyzed in future research. Furthermore, the existing model may be integrated with other human subsystems, which contribute to the sensory conflict.

- The model must be expanded to include motion with 6 degrees of freedom. The vestibular system submodel, in this case, would include the influence from the semicircular canals' afferent signals.

- The MSI is related non-linearly to the amplitude of the external motion. The proposed model does not explain why this happens. Future research should establish a better understanding of the connection between human physiology and motion characteristics.

- Proprioception is known to play a crucial role in postural control and in motion sickness. Future work may add the influence of proprioception to the overall sensory error estimation.

- The role of human body stabilization and locomotion may play a key role in MSI for subjects who are free to move about, as in a ship's crew (Stoffregen, Hettinger, Haas, Roe, & Smart, 2000; Stoffregen & Smart, 1998).

- An engineering systems approach was taken in modeling this human physiology issue. Nevertheless, other approaches are possible. We believe that the proposed model can be viewed as multi-agent complex adaptive system. Such approach has already been applied in human vigilance, with very promising results (Wellbrink, 2003).

APPENDIX A. GLOSSARY

The following glossary contains the definitions of terms included in the main text but are not defined in it.

The terms fall into two main categories, those commonly used in human factors research, and those related to technical aspects of the model.

The glossary has been derived from (Griffin, 1990a) and National Space Biomedical Research Institute (Institute, 2004).

Absolute value: (a). The absolute value of a real number is a positive number that has the same numerical value as the real number. (b). The absolute value of a complex number is the positive square root of the sum of the squares of the real and imaginary parts. See: *modulus*

Acceleration: A vector quantity that specifies the rate of change of velocity (meters per second squared).

Adaptation: (a). A change, usually a decrease, in sensitivity as a consequence of stimulation. (b). A general advantageous change in response to new conditions. See *habituation.*

Aetiology: A part of medical science concerned with the causes of disease.

Afferent: The conduction of nerve impulses from the sense organs to the central nervous system. See: *efferent*

Amplitude: The maximum value of a sinusoidal quantity. Also called peak amplitude and single amplitude.

127

Arousal: A general term indicating the extent of readiness of the body.

Band-pass filter: A filter that has a single transmission band extending from a lower cut-off frequency (not zero) to an upper cut-off frequency (not infinite).

Caloric stimulation: Stimulation induced by hot or cold water introduced into the outer ear.

Central Nervous System (CNS): Part of the nervous system consisting of the brain and the spinal cord.

Compensatory eye movements: Movements of the eyes which compensate for movements of the head. See: *vestibulo-ocular reflex; pursuit reflex.*

Coriolis force: Additional force which arises when a movement is made on a body which is undergoing rotational motion. The force arises from a cross-coupling of the motions; the resultant motion is called Coriolis acceleration or cross-coupled acceleration.

Cut-off frequency: A frequency above or below the frequency of maximum response of a filter at which the response to a sinusoidal signal is 3 dB below the maximum response.

Disorientation: Inability to orientate with an environment in either space or time.

Doll's eye movement/ reflex: The tendency for the eyes to remain horizontal as the head is tilted backward or forward. See: *vestibulo-ocular reflex.*

Efferent: The conduction of nerve impulses from the central nervous system towards the peripheral nervous system (e.g. to the muscles). See: *afferent.*

Emesis: Vomiting.

Empirical: Based on observation and experiment rather than theory.

Etiology: See: *aetiology.*

Eye movements: See: *compensatory eye movements; pursuit eye movements; saccade; vestibulo-ocular reflex.*

Fatigue: Weariness resulting from bodily or mental exertion.

Feedback: The provision, at the input of a system, of some information on the output of the system.

Filter: A device for separating oscillations on the basis of their frequency: it attenuates oscillations at some frequencies more than those at other frequencies.

Frequency: The reciprocal of the fundamental period. Frequency is expressed in Hz which corresponds to one cycle per second.

Frequency response: The output signal from a system expressed as a function of the frequency of the input signal.

Gain: The amplification/ attenuation provided by a system.

Gravitoinertial environment: A gravitoinertial environment is an environment in which gravity and inertia exist.

Habituation: Reduction in human response to a stimulus as a result of cumulative exposure to the stimulus. (Habituation is often assumed to involve activity of the central nervous system). See: *adaptation.*

High-pass filter: A filter which has a single transmission band extending from a lower cut-off frequency (not zero) up to infinite frequency or, in practice, above the highest frequency of interest.

Hypothesis: A supposition made as a starting point for reasoning or investigation without an assumption as to its truth.

Idiotropic vector: A subjective head-referenced vector always aligned with the head upward axis. The additive effect of the idiotropic vector is to bias the subjective vertical toward the head axis.

Incidence: The number of new cases of a disease in a population over a specified period of time. (Often expressed as a percentage of the population).

Inertia force: The reaction force exerted by a mass when it is being accelerated.

Latency: The period of apparent inactivity between the time a stimulus is presented and the moment that a specified response occurs.

Linear Time-Invariant System (LTI): A linear whose components' characteristics remain unchanged by time.

Low-pass filter: A filter which has a single transmission band extending from zero frequency up to finite frequency.

Modulus: The modulus of a complex number is its *absolute value*.

Motor: In life sciences, a term used to refer to processes or anatomical areas associated with muscular action.

Normalize: To adjust a set of values such that they conform to some requirement. (The requirement may be a defined range, etc.)

Nystagmus: Nystagmus is a rhythmical oscillation of the eyeball, either pendulum-like or jerky. A variety of causes for nystagmus are known. In space-related research, the caloric nystagmus (caused by hot or cold water in the ear), the optokinetic nystagmus (triggered by looking at a rotating dome), and the vestibular nystagmus (when a rotation of the body stops abruptly) are of special interest.

Ocular: Relating to the eye.

Oculo-: The eye, or relating to the eye (combining form).

Oculomotor: Term used to refer to eye movements and their muscular control.

Optokinetic: Relating to eye movements produced by a moving visual stimulus.

Peak value: The maximum value of a quantity during a given interval.

Perception: Awareness of some event; process by which the mind refers its sensations to external objects as cause.

Physiology: The science of the normal functions and phenomena of living things.

Process: A collection of signals.

Proprioception: The perception of information about the position, orientation and movement of the body and its parts. (Involves the *somatosensory system* and the *vestibular system*),

Pursuit eye movement: The rotation of the eye to follow a moving object. See: *compensatory eye movements.*

Reflex: An involuntary reaction in response to a stimulus applied peripherally and transmitted to the nervous centers of the brain or spinal cord.

Root-Mean-Square value (RMS): (a). The RMS value of a set of numbers is the square root of the average of their squared values. (b). The RMS value of a function, $x(t)$, over an interval between t_1 and t_2 is the square root of the average of the squared values of the function over the interval

$$\text{RMS value} = \left(\frac{\int_{t_1}^{t_2} x(t)^2 \, dt}{t_2 - t_1} \right)^{\frac{1}{2}}$$

Sea sickness: A form of motion sickness induced by marine environments.

Sensorimotor: Relating to the neural circuit from a receptor to the central nervous system and back to a muscle.

Sign: Any objective evidence of the presence of a disorder or a disease.

Sopite syndrome: Sleepiness, lassitude or drowsy inattention induced by vibration or low frequency oscillation.

Steven's power law: The law suggests that the relationship between the magnitude, ψ, of psychological sensation produced by a stimulus of magnitude, φ, is given by $\psi = k\varphi^n$.

Strain: In life sciences, the situation where the body is placed under severe load from physical or mental demands. See: *stress, stressor.*

Stress: In life sciences, either the cause of strain or the *strain* which is caused. See: *stressor.*

Stressor: A cause of *strain*, or *stress*.

Subject: A participant in an experiment.

Subjective: In life sciences, something which is dependent on an individual. See: *objective*.

Symptom: In medicine, an abnormality in function, appearance or sensation which is discovered by the patient. (A symptom is a subjective sign of a disease).

Syndrome: In medicine, a combination if signs and *symptoms* which collectively indicate a disease.

Translation: The movement of an object so that all its parts follow the same direction (i.e. movement without rotation).

Translational motion: Movement without (or considered apart from) rotation.

Vection: The illusory perception of self-motion.

Vestibular system: Collective term for the three semicircular canals and the two vestibular sacs (utricle and saccule) within the labyrinth of the inner ear. The vestibular system is involved in the perception of spatial orientation.

Vestibulo-: Combining form denoting vestibule.

Vestibulo-ocular reflex (VOR): Involuntary eye movements arising from excitation of the *vestibular system*.

APPENDIX B. SUPPORTING SOFTWARE CODE

A. PROGRAM 1

The following code computes the motion a subject is adapted to at the beginning of each day

```
clc

clear

tau_A=5*60*60;        % adaptation time constant in [s]

maxDays=3;

Motion_Amplitude_Before_Bed_Average=0;

meanDuration=10*60;   % mean duration, in [s]

maxIter=10000;

sleepDuration=8*60*60;

Ao=0.15;

for (iter=1:1:maxIter)

    Ato=Ao;

    for (day=1:1:maxDays)

        A=exp(-sleepDuration/tau_A)*Ato;

        Ato=A;

        to=0;

        t=8*60*60;

        while (t<=24*60*60)

            motionFlag=rand;  % Motion/ no motion decision

            if (t<=16*60*60 & motionFlag<0.5)

                randMeanDuration=0.5*meanDuration;

            elseif (t>16*60*60 & motionFlag>=0.5)

                randMeanDuration=0.5*meanDuration;
```

```
                else

                    randMeanDuration=meanDuration;

                end

                duration=exprnd(randMeanDuration);      % Duration of
motion/ no motion period, in [sec]

                if (to+duration>24*60*60)

                    duration=24*60*60-to;

                end

                to=t;

                if (motionFlag<0.5)     % No motion

                    A=exp(-duration/tau_A)*Ato;

                else

                    A=exp(-duration/tau_A)*Ato+(1-exp(-
duration/tau_A))*Ao;

                end

                Ato=A;

                t=t+duration;

            end

        end

        AtoIter(iter)=Ato;

    end

    for (iter=1:1:maxIter)

Motion_Amplitude_Before_Bed_Average=Motion_Amplitude_Before_Bed_Average+
AtoIter(iter)/maxIter;

    end

    AtoAverageRMS=Motion_Amplitude_Before_Bed_Average
```

B. PROGRAM 2

The following code computes the average RMS amplitude of motion a subject is adapted to during a day (08:00 – 23:59)

```
clc

clear

tau_A=5*60*60;     % adaptation time constant in [s]

meanDuration=10*60; % mean duration, in [s]

maxIter=10000;

sleepDuration=8*60*60;

totalAverage=0;

Ao=0.0567;

i=0;

for (iter=1:1:maxIter)

    Ato=Ao;

    to=0;

    A=exp(-sleepDuration/tau_A)*Ato;

    average(iter)=0;

    Ato=A;

    t=8*60*60;

    while (t<=24*60*60)

        motionFlag=rand;          % Motion/ no motion decision

        if (t<=16*60*60 & motionFlag<0.5)

            randMeanDuration=0.5*meanDuration;

        elseif (t>16*60*60 & motionFlag>=0.5)

            randMeanDuration=0.5*meanDuration;

        else
```

```matlab
                randMeanDuration=meanDuration;

            end

            duration=exprnd(randMeanDuration);    % Duration of motion/
no motion period, in [sec]

            if (to+duration>24*60*60)

                duration=24*60*60-to;

            end

            to=t;

            if (motionFlag<0.5)      % No motion

                A=exp(-duration/tau_A)*Ato;

                average(iter)=average(iter)-tau_A*Ato*(exp(-
duration/tau_A)-1);

            else

                A=exp(-duration/tau_A)*Ato+(1-exp(-
duration/tau_A))*Ao;

                average(iter)=average(iter)-tau_A*Ato*(exp(-
duration/tau_A)-1)+Ao*duration+tau_A*Ao*(exp(-duration/tau_A)-1);

            end

            Ato=A;

            t=t+duration;

        end

        average(iter)=average(iter)/(16*60*60);

        totalAverage=totalAverage+average(iter)/maxIter;

    end

    totalAverageRMS=totalAverage
```

C. PROGRAM 3

The following code depicts the Bode plot of the proposed model's main errors, Δg and ROF.

```
clc
clear
tau_o=0.66;
ka=-1.0;
kg=-1.0;
tau_L=5.0;          % Integration of a to v
d=1;
tau_VOR=1.318;      % VOR suspension LP filter
Gvor=1.0;
Gokr=1.0;
tau_E1=0.14;        % Eye system
tau_E2=0.28;        % Eye system
tau_E3=0.037;       % Eye system
tau_E4=0.003;       % Eye system
tau_v=0.15;         % Retina slip detection
k2=0.1;             % fixed because VOR gain=1 for d>>
k1=0.9;
K=k2+k1/d;
bg=0.0042;
bv=0.00008;
s=tf('s');
S=1/(tau_o*s+1);    % Otolith transfer function
```

```matlab
leaky_v=1/(tau_L*s+1);

VORsusp=(tau_VOR*s/(tau_VOR*s+1))^2; % VOR suspension HP filter

EYE=(tau_E1*s+1)/((tau_E2*s+1)*(tau_E3*s+1)*(tau_E4*s+1));

RETINA=1/(tau_v*s+1);

Wr=1/s*1/d; % External motion in space referenced frame

Hr=1/s*1/d; % Head motion in space referenced frame

Dg=-s*S/(s+S*(ka-kg)-ka);

Da=-s*(S-1)/(s+S*(ka-kg)-ka);

a=ka*Da/s;

v=a*leaky_v*(1/d);

VOR=Gvor*VORsusp*v;

ROF=RETINA*EYE*K*VOR/(1+EYE*K*Gokr*RETINA);

subplot(1,1,1);

bode(Dg,ROF);

grid on;

legend('Dg','ROF')
```

D. PROGRAM 4

The following code plots Motion Sickness Incidence versus RMS amplitude and frequency of externally induced motion, as predicted from the proposed model.

```matlab
clc

clear

% Model Parameters

Ao=0.0253;   % RMS amplitude Ao of motion in neural store, in [g]

Fo=1.822;    % frequency Fo of motion in neural store, in [Hz]
```

```
T=120;          % T [min] time of the experiment


tau_A=5*60*60;      % [s]

kg=-1.0;

ka=-1.0;

bg=0.0042;          % bg [g]

bv=0.00008;         % bv [g]

mu=10*60;           % time constant of 2nd order leaky integrator

P=100.0;            % P [%]

n=2;

tau_L=5.0;          % Integration of a to v [s]

d=1;                % [m]

tau_VOR=1.318;      % VOR suspension HP filter

Gvor=1.0;

Gokr=1.0;

% Plot Paramaters

MSImin=0.0;

MSImax=100.0;

Anmin=0.05;         % RMS minimum amplitude of new motion An in [g]

Anmax=0.6;          % RMS maximum amplitude of new motion An in [g]

na=10;

Fnmin=0.05;         % minimum frequency of new motion Fn in [Hz]

Fnmax=0.6;          % maximum frequency of new motion Fn in [Hz]

nf=20;

logFnmin=log10(Fnmin);

logFnmax=log10(Fnmax);

tolerance=0.0001;

T=T*60;             % conversion from minutes to seconds
```

```matlab
        logFnmin=log10(Fnmin);

        logFnmax=log10(Fnmax);


        i=0;

        for An=Anmin:(Anmax-Anmin)/na:Anmax,

            i=i+1;

            j=0;

            for Fn=10.^(logFnmin:(logFnmax-logFnmin)/nf:logFnmax),

                j=j+1;

                period=1/Fn;


hmean=1/period*quad(@matsangas3fun,0,period,tolerance,0,An,Ao,Fn,Fo,tau_
L,tau_A,kg,ka,bg,bv,T,n,d,Gvor,Gokr,tau_VOR);

                msi(j,i)=P*hmean*(1-(T/mu+1)*exp(-T/mu));

            end

        end

        surf(msi)

        axis([1 i 1 j MSImin MSImax])

        set(gca,'YDir','rev')

        set(gca,'XTick',[1 3 5 7 9 11])

        set(gca,'XTickLabel',{'0.05';'0.16';'0.27';'0.38';'0.49';'0.6'})

        set(gca,'YTick',[1 5 9 13 17 21])

        set(gca,'YTickLabel',{'0.050';'0.082';'0.135';'0.222';'0.365';'0.6
00'})

        xlabel('Amplitude A-RMS [g]');

        ylabel('Frequency F [Hz]');

        zlabel('MSI [%]');

        title('Proposed Model');
```

E. PROGRAM 5

The following code plots the MSI difference between the proposed model and the HFR model (McCauley et al., 1976), versus RMS amplitude and frequency of externally induced motion.

```
clc

clear

% Model Parameters

Ao=0.0253;

Fo=1.822;

T=120;                % T [min] time of the experiment

tau_A=5*60*60;     % [s]

kg=-1.0;

ka=-1.0;

bg=0.0042;         % bg [g]

bv=0.00008;        % bv [g]

mu=10*60;          % time constant of 2nd order leaky integrator

P=100.0;           % P [%]

n=2;

tau_L=5.0;         % Integration of a to v [s]

d=1;               % [m]

tau_VOR=1.318;     % VOR suspension HP filter

Gvor=1.0;

Gokr=1.0;

% Plot Paramaters

MSImin=0.0;
```

```
MSImax=100.0;

Anmin=0.05;        % RMS minimum amplitude of new motion An, in [g]

Anmax=0.6;         % RMS maximum amplitude of new motion An, in [g]

na=10;

Fnmin=0.05;        % minimum frequency of new motion Fn, in [Hz]

Fnmax=0.6;         % maximum frequency of new motion Fn, in [Hz]

nf=20;

logFnmin=log10(Fnmin);

logFnmax=log10(Fnmax);

tolerance=0.0001;

T=T*60;            % conversion from minutes to seconds

logFnmin=log10(Fnmin);

logFnmax=log10(Fnmax);

i=0;

for An=Anmin:(Anmax-Anmin)/na:Anmax,

    i=i+1;

    j=0;

    for Fn=10.^(logFnmin:(logFnmax-logFnmin)/nf:logFnmax),

        j=j+1;

        % Revised Model

        period=1/Fn;


hmean=1/period*quad(@matsangas3fun,0,period,tolerance,0,An,Ao,Fn,Fo,tau_
L,tau_A,kg,ka,bg,bv,T,n,d,Gvor,Gokr,tau_VOR);

        msi(j,i)=P*hmean*(1-(T/mu+1)*exp(-T/mu));


        % McCauley Model

        flog=log10(Fn);
```

144

```matlab
            amu=0.87+4.36*flog+2.73*flog^2;

            accelog=log10(An);

            za=(accelog-amu)/0.47;

            tlog=log10(T);

            zt=(tlog-1.46)/0.76;

            denom=sqrt(1.0-(-0.75)^2.0);

            ztprime=(zt+0.75*za)/denom;

            msiMcCauley(j,i)=100.0*stdphi(za)*stdphi(ztprime);

        end

    end

    % Comparison of models

    diafora=msiMcCauley-msi;

    subplot(1,1,1);

    surfc(diafora);

    %axis([1 i 1 j MSImin MSImax])

    set(gca,'YDir','rev')

    set(gca,'XTick',[1 3 5 7 9 11])

    set(gca,'XTickLabel',{'0.05';'0.16';'0.27';'0.38';'0.49';'0.6'})

    set(gca,'YTick',[1 5 9 13 17 21])

    set(gca,'YTickLabel',{'0.050';'0.082';'0.135';'0.222';'0.365';'0.6
00'})

    xlabel('Amplitude A-RMS [g]');

    ylabel('Frequency F [Hz]');

    zlabel('MSI Differnce in [%]');

    title('Comparison between Proposed and McCauley Model');
```

F. PROGRAM 6

The following code plots the MSI predicted by the proposed model versus time.

```
clc

clear


% Model Parameters

Ao=0.0253;  % RMS amplitude Ao of motion in neural store, in [g]

Fo=1.822;   % frequency Fo of motion in neural store, in [Hz]

tau_A=5*60*60;      % [s]

kg=-1.0;

ka=-1.0;

bg=0.0042;          % bg [g]

bv=0.00008;         % bv [g]

mu=10*60;           % time constant of 2nd order leaky integrator

P=100.0;            % P [%]

n=2;

tau_L=5.0;          % Integration of a to v [s]

d=1;                % [m]

tau_VOR=1.318;       % VOR suspension HP filter

Gvor=1.0;

Gokr=1.0;


% Plot Paramaters

tolerance=0.0001;
```

146

```matlab
An=0.5;

Fn=0.167;

tmax=24*60*60;     % Maximum time in seconds

step=1*60;         % step time in seconds

i=0;

for t=1:step:tmax,

        i=i+1;

        period=1/Fn;


hmean=1/period*quad(@matsangas3fun,0,period,tolerance,0,An,Ao,Fn,Fo,tau_
L,tau_A,kg,ka,bg,bv,t,n,d,Gvor,Gokr,tau_VOR);

        msi(i)=P*hmean*(1-(t/mu+1)*exp(-t/mu));

    end

end

%plot(msi,'LineWidth',3,'Color',[0 0 1])

semilogx(msi,'LineWidth',3,'Color',[0 0 1])

xlim([0 tmax/60]);

xlabel('Time in [min]');

ylabel('MSI [%]');

title('Adaptation Analysis');

grid on;
```

THIS PAGE INTENTIONALLY LEFT BLANK

LIST OF REFERENCES

Angelaki, D. E. (1998). Three-dimensional organization of otolith-ocular reflexes in rhesus monkeys. III. Responses To translation. *J Neurophysiol, 80*(2), 680-695.

Angelaki, D. E., & Hess, B. J. (1994). Inertial representation of angular motion in the vestibular system of rhesus monkeys. I. Vestibuloocular reflex. *J Neurophysiol, 71*(3), 1222-1249.

Angelaki, D. E., & Hess, B. J. (1995). Inertial representation of angular motion in the vestibular system of rhesus monkeys. II. Otolith-controlled transformation that depends on an intact cerebellar nodulus. *J Neurophysiol, 73*(5), 1729-1751.

Angelaki, D. E., & Hess, B. J. (1996a). Three-dimensional organization of otolith-ocular reflexes in rhesus monkeys. I. Linear acceleration responses during off-vertical axis rotation. *J Neurophysiol, 75*(6), 2405-2424.

Angelaki, D. E., & Hess, B. J. (1996b). Three-dimensional organization of otolith-ocular reflexes in rhesus monkeys. II. Inertial detection of angular velocity. *J Neurophysiol, 75*(6), 2425-2440.

Angelaki, D. E., McHenry, M. Q., & Hess, B. J. (2000). Primate translational vestibuloocular reflexes. I. High-frequency dynamics and three-dimensional properties during lateral motion. *J Neurophysiol, 83*(3), 1637-1647.

Angelaki, D. E., McHenry, M. Q., Newlands, S. D., & Dickman, J. D. (1999). Functional organization of primate translational vestibulo-ocular reflexes and effects of unilateral labyrinthectomy. *Ann N Y Acad Sci, 871*, 136-147.

Angelaki, D. E., Merfeld, D. M., & Hess, B. J. (2000). Low-frequency otolith and semicircular canal interactions after canal inactivation. *Exp Brain Res, 132*(4), 539-549.

Angelaki, D. E., Wei, M., & Merfeld, D. M. (2001). Vestibular discrimination of gravity and translational acceleration. *Ann N Y Acad Sci, 942*, 114-127.

Baarsma, E., & Collewijn, M. (1974). Vetsibulo-ocular and optokinetic reactions to rotations and their interaction in the rabbit. *Journal of Physiology, 238*, 603-625.

Benson, A. J. (1988). Motion Sickness. In J. Ernesting & P. King (Eds.), *Aviation Medicine*: Butterworth.

Benson, A. J. (1999). Motion Sickness. In J. Ernesting, A. N. Nicholson & D. Rainford (Eds.), *Aviation Medicine*. Oxford: Butterworth-Heinemann.

Benson, A. J., & Barnes, G. R. (1978). Vision during angular oscillation: the dynamic interaction of visual and vestibular mechanisms. *Aviat Space Environ Med, 49*(1 Pt. 2), 340-345.

Benson, A. J., Guedry, F. E., & Jones, G. M. (1970). Response of semicircular canal dependent units in vestibular nuclei to rotation of a linear acceleration vector without angular acceleration. *Journal of Physiology, 210*, 475-494.

Birren, J. E. (1949). *Motion sickness: Its psychophysiological aspects.* Washington, D.C.: National Research Counsil.

Bles, W., Bos, J. E., de Graaf, B., Groen, E., & Wertheim, A. H. (1998). Motion sickness: only one provocative conflict? *Brain Res Bull, 47*(5), 481-487.

Bles, W., de Jong, H. A. A., & Oosterveld, W. J. (1984, 3 May 1984). *Prediction of Seasickness Susceptibility.* Paper presented at the Motion Sickness: Mechanisms, Prediction, Prevention, and Treatment, Williamsburg, Virginia, USA.

Bles, W., & Graaf, B. d. (1993). Postural consequences of long duration centrifugation. *Journal of Vestibular Research, 3*, 87-95.

Boff, K. R., & Lincoln, J. E. (1988). *Engineering Data Compendium: Human Perception and Performance*. Wright-Paterson AFB, OH: AAMRL.

Bos, J. E., & Bles, W. (1998). Modelling motion sickness and subjective vertical mismatch detailed for vertical motions. *Brain Res Bull, 47*(5), 537-542.

Bos, J. E., & Bles, W. (2002). Theoretical Considerations on Canal-Otolith Interaction and an Observer Model. *Biological Cybernetics, 86*, 191-207.

Bos, J. E., Bles, W., & Dallinga, R. (2000). *Prediction of Seasickness with more than one Degree of Freedom.* Paper presented at the Human Factors in Ship Design and Operation, UK.

Bos, J. E., Bles, W., & Hosman, R. J. A. W. (2001a, 2001). *Modelling Human Spatial Orientation and Motion Perception.* Paper presented at the AIAA Modeling and Simulation Technologies Conference Proceedings.

150

Bos, J. E., Bles, W., & Hosman, R. J. A. W. (2001b). *Modelling six degrees of freedom motion sickness* (No. TM-01-A007). Soesterberg, the Netherlands: TNO.

Bos, J. E., Bles, W., Hosman, R. J. A. W., & Groen, E. (2002, 15-17 April). *The Cause of Spatial Disorientation.* Paper presented at the RTO HFM Symposium on "Spatial Disorientation in Military Vehicles: Causes, Consequances and Cures", La Coruna, Spain.

Busettini, C., Miles, F. A., Schwarz, U., & Carl, J. (1994). Human Ocular Responses to Translation of the Observer and of the Scene: Dependence on Viewing Distance. *Experimental Brain Research, 100*, 484-494.

Chinn, H. I. (1951). Motion sickness in the military service. *Mil Surg, 108*(1), 20-29.

Citek, K., & Ebenholtz, S. M. (1996). Vertical and horizontal eye displacement during static pitch and roll postures. *J Vestib Res, 6*(3), 213-228.

Clark, B., & Graybiel, A. (1961). Human performance during adaptation to stress in the Pensacola slow rotation room. *Aeromed Acta, 32*, 93-106.

Cohen, B., Suzuki, J., & Raphan, T. (1983). Role of the orolith organs in generation of horizontal nystagmus: effects of selective labyrinthine lesions. *Brain Res, 276*, 159-164.

Collewijn, H., Van der Steen, J., Ferman, L., & Jansen, T. C. (1985). Human ocular counterroll: assessment of static and dynamic properties from electromagnetic scleral coil recordings. *Exp Brain Res, 59*(1), 185-196.

Collins, W. E. (1974). *Adaptation to Vestibular Disorientation. XII. Habituation of Vestibular Responses: An Overview* (No. FAA-AM-74-3): FAA Civil Aeromedical Institute.

Colwell, J. L. (1989). *Human Factors in the Naval Environment: A Review of Motion Sickness and Biodyanmic Problems* (No. Technical Memorandum 89/220): Defense Research Establishment, Canada.

Correia, M. J., & Guedry, F. E., Jr. (1966). Modification of vestibular responses as a function of rate of rotation about an Earth-horizontal axis. *Acta Otolaryngol, 62*(4), 297-308.

Correia, M. J., & Money, K. E. (1970). The effect of blockage of all six semicircular canal ducts on nystagmus produced by dynamic linear acceleration in the cat. *Acta Otolaryngol, 69*, 7-16.

151

Crampton, G. H. (1955). Studies of motion sickness. XVII. Physiological changes accompanying sickness in man. *J Appl Physiol, 7*(5), 501-507.

Crane, B. T., & Demer, J. L. (1999). A linear canal-otolith interaction model to describe the human vestibulo-ocular reflex. *Biol Cybern, 81*, 109-118.

Crane, B. T., Viirre, E. S., & Demer, J. L. (1997). The human horizontal vestibulo-ocular reflex during combined linear and angular acceleration. *Exp Brain Res, 114*, 304-320.

Diamond, S. G., Markham, C. H., & Simpson, N. E. (1979). Binocular counterrolling in humans during dynamic rotation. *Acta Otolaryngologica, 87*, 490-498.

Dobie, T. G. (2000, 13-14 June, 2000). *The Importance of the Human Element in Ship Design.* Paper presented at the Ship Structure Symposium, Washington, DC.

Dobie, T. G. (2003, 8-10 October, 2003). *Critical Significance of Human Factors in Ship Design.* Paper presented at the 2003 RVOC Meeting, Large Lakes Observatory.

Dobie, T. G., McBride, D., Dobie, T., Jr., & May, J. (2001). The effects of age and sex on susceptibility to motion sickness. *Aviat Space Environ Med, 72*(1), 13-20.

Dowd, P. J. (1974). Sleep deprivation effects on the vestibular habituation process. *J Appl Psychol, 56*, 748-752.

Draper, M. (1998). *The Adaptive Effects of Virtual Interfaces: Vestibulo-Ocular Reflex and Simulator Sickness*. Retrieved December 03, 2003, 2003, from http//:www.hitl.washington.edu/publications/r-98-22

Driskell, J. E., Hughes, S. C., Willis, R. C., Cannon-Bowers, J., & Salas, E. (1991). *Stress, stressor, and decision-making* (Technical Report). Orlando, FL: Naval Training Systems Center.

Driskell, J. E., Mullen, B., Johnson, C., Hughes, S. C., & Batchelor, C. (1992). *Development of quantitative specifications for simulating the stress environment* (No. AL-TR-1991-0109). Wright-Patterson AFB, OH: Armstrong Laboratory.

Driskell, J. E., & Salas, E. (1996). *Stress and Human Performance*. Hillsdale, NJ, New England: Lawrence Erlbaum Associates, Inc.

Droulez, J., & Cornilleau-Peres, V. (1993). Application of the coherence scheme to the multisensory fusion problem. In A. Berthoz (Ed.), *Multisensory Control of*

Movement (pp. 485-501). Oxford: Oxford University Press.

Ebenholtz, S. M., & Shebilske, W. (1975). The doll reflex: Ocular counterrolling with head-body tilt in the median plane. *Vision Res, 15*, 713-717.

Fernandez, C., & Goldberg, J. (1976b). Physiology of peripheral neurons innervating the otolith organs of the squirrel monkey. III. Response dynamics. *Journal of Neurophysiology, 39*, 996-1008.

Fuchs, A. F., Scudder, C. A., & Kaneko, C. R. (1988). Discharge patterns and recruitment order of identified motoneurons and internuclear neurons in the monkey abducens nucleus. *Journal of Neurophysiology, 60*, 1874-1895.

Glasauer, S. (1992). Interaction of semicircular canals and otoliths in the processing structure of the sibjective zenith. *Ann N Y Acad Sci, 656*, 847-849.

Glasauer, S. (1993, 1-5 June). *Human spatial orientation during centrifuge experiments: Non-linear interaction of semicircular canals and otoliths.* Paper presented at the 17th Barany Society Meeting, Prague, Czech Republic.

Glasauer, S., & Merfeld, D. M. (1997). Modelling three Dimensional Vestibular Responses during Complex Motion Stimulation. In M. Fetter, T. Haslwanter & H. Misslisch (Eds.), *Three-dimesional kinematics of eye, head and limb movements* (pp. 387-398). Amsterdam: Harwood Academic Publishers.

Graf, W., Simpson, I., & Leonard, C. S. (1988). Spatial organization of visual messages of the rabbit's cerebellar floculus. II. Complex and simple spike responses of Purkinje cells. *Journal of Neurophysiology, 60*, 2091-2121.

Grant, W., & Best, W. (1986). Mechanics of the Otolith Organ - Dynamic Response. *Annals of Biomedical Engineering, 14*, 241-256.

Grant, W., & Best, W. (1987). Otolith-Organ Mechanics: Lumped Parameter Model and Dynamic Responce. *Aviation, Space, and Environmental Medicine, 58*(10), 970-976.

Grant, W., Best, W., & LoNigro, R. (1984). Governing Equations of Motion for the Otolith Organs and their Response to a Step Change in Velocity of the Skull. *Journal of Biomechanical Engineering, 106*(4), 302-308.

Graybiel, A., Deane, R. F., & Colehour, J. K. (1969). Prevention of Overt Motion Sickness by Incremental

Exposure to Otherwise Highly Stressful Coriolis Accelerations. *Aerospace Medicine, 40*(2), 142-148.

Graybiel, A., & Knepton, J. (1976). Sopite syndrome: a sometimes sole manifestation of motion sickness. *Aviat Space Environ Med, 47*(8), 873-882.

Griffin, M. J. (1990a). *Handbook of Human Vibration*. New York: Academic Press.

Griffin, M. J. (1990b). Motion sickness. In *Handbook of Human Vibration*. New York: Academic Press.

Griffin, M. J. (1991). *Physical characteristics of stimuli provoking motion sickness*: AGARD.

Guedry, F. E. (1968). *Conflicting sensory orientation cues as a factor in motion sickness.* Paper presented at the Fourth Symposium on the Role of the Vestibular Organs in Space Exploration.

Guedry, F. E. (1991). *Physical characteristics of stimuli provoking motion sickness*.Unpublished manuscript.

Guignard, J. C., & McCauley, M. E. (1982). Motion sickness incidence induced by complex periodic waveforms. *Aviat Space Environ Med, 53*(6), 554-563.

Guignard, J. C., & McCauley, M. E. (1990). The accelerative stimulus for motion sickness. In G. H. Crampton (Ed.), *Motion and Space Sickness* (pp. 123-152). Boca Raton, FL: CRC Press.

Guitton, D., & Volle, M. (1987). Gaze control in humans: eye-head coordination during orienting movements to targets within and beyond the oculomotor range. *J Neurophysiol, 58*(3), 427-459.

Hallett, P. E. (1986). Eye Movements. In K. R. Boff, L. Kaufman & J. P. Thomas (Eds.), *Handbook of Perception and Human Performance* (Vol. 1, pp. 10-11, 10-112): John Wiley and Sons.

Hannen, R. A., Kabrisky, M., Replogle, C. R., Hartzler, V. L., & Roccaforte, P. A. (1966). Experimental determination of a portion of the human vestibular system response through measurement of eyeball counterroll. *IEEE Trans Biomed Eng, 13*(2), 65-70.

Harris, L. R. (1987). Vestibular and optokineric eye movements evoked in the cat by rotation about a tilt axis. *Exp Brain Res, 66*, 522-532.

Held, R. (1961). Exposure history as a factor in maintaining stability of perception and coordination. *Journal of Nervous and Mental Disease*(132), 26-32.

Hemingway, A. (1945). *Survey of Research on the Problem of Airsickness in Army Air Forces* (No. Research Report No.

1). Randolph Field: Army Air Forces School of Aviation Medicine.

Hess, B. J. (2001). Vestibular Signals in Self-Orientation and Eye Movement Control. *News Physiol. Sci., 16*, 234-238.

Hess, B. J., & Angelaki, D. E. (1997a). Kinematic principles of primate rotational vestibulo-ocular reflex. I. Spatial organization of fast phase velocity axes. *J Neurophysiol, 78*(4), 2193-2202.

Hess, B. J., & Angelaki, D. E. (1997b). Kinematic principles of primate rotational vestibulo-ocular reflex. II. Gravity-dependent modulation of primary eye position. *J Neurophysiol, 78*(4), 2203-2216.

Hess, B. J., & Angelaki, D. E. (2003). Gravity modulates Listing's plane orientation during both pursuit and saccades. *J Neurophysiol, 90*(2), 1340-1345.

Hettinger, L. J., Kennedy, R. S., & McCauley, M. E. (1990). Motion and Human Performance. In G. H. Crampton (Ed.), *Motion and space sickness* (Vol. 1, pp. 411-441). Boca Raton, FL: CRC Press.

Hill, J. (1936). The care of the sea-sick. *The British Medical Journal*(II), 802-807.

Holst, v. E. (1954). Relations between the central nervous system and the peripheral organs. *British Journal of Animal Behaviour, 2*, 89-94.

Howard, I. P. (1986a). The Perception of Posture, Self Motion, and the Visual System. In K. R. Boff, L. Kaufman & J. P. Thomas (Eds.), *Handbook of Perception and Human Performance* (Vol. 1, pp. 62): John Wiley and Sons.

Howard, I. P. (1986b). The vestibular system. In K. R. Boff, L. Kaufman & J. P. Thomas (Eds.), *Handbook of Perception and Human Performance* (Vol. 1, pp. 11.11): John Wiley and Sons.

Howard, I. P. (1993). The stability of the visual world. In F. A. Miles & J. Wallman (Eds.), *Visual Motion and its Role in the Stabilization of Gaze* (pp. 103-118). Amsterdam: Elsevier Science.

Howarth, H. V., & Griffin, M. J. (2003). Effect of roll oscillation frequency on motion sickness. *Aviat Space Environ Med, 74*(4), 326-331.

Hursh, S. R., & Bell, G. B. (2001). *Human Performance Cognitive Model for Air Force Information Operations*: Air Force Research Laboratory.

Inman, V. T., Ralston, H. J., & Todd, F. (1981). *Human Walking*. Baltimore: Williams & Wilkins.

155

Institute, N. S. B. R. (2004). *IDAS Glossary*. Retrieved 04/24/2004, 2004, from www://idas.nsbri.org/IDAS

Jagacinski, R. J., & Flach, J. M. (2003). *Control Theory for Humans. Quantitative Approaches to Modeling Performance* (1st ed.). Mahwah, New Jersey: Lawrence Erlbaum Associates.

Jokerst, M. D., Gatto, M., Fazio, R., Gianaros, P. J., Stern, R. M., & Koch, K. L. (1999). Effects of gender of subjects and experimenter on susceptibility to motion sickness. *Aviat Space Environ Med, 70*(10), 962-965.

Keller, E. (1978). Gain of vestibulo-ocular reflex in the monkey at high rotational frequencies. *Vision Research, 18*, 311-315.

Kellogg, R. S. (1965). *Dynamic counterrolling of the eye in normal subjects and in persons with bilateral labyrinthine defects* (No. SP-77): NASA.

Kennedy, R. S., Dunlap, W. P., & Fowlkes, J. E. (1990). Prediction of motion sickness susceptibility. In G. H. Crampton (Ed.), *Motion and Space Sickness* (Vol. 1, pp. 179-215). Boca Raton, FL: CRC Press.

Kornilova, L. N., Cowings, P., Arlashchenko, N. I., Korneev, D., Sagalovich, S. V., Sarantseva, A. V., et al. (2003). [Individual characteristics of correction of the cosmonauts' vegetative status with a method of adaptive biofeedback]. *Aviakosm Ekolog Med, 37*(1), 67-72.

Kottenhoff, H., & Lindahl, L. (1960). Laboratory studies on the psychology of motion sickness. *Acta Psychologica, 17*, 67-73.

Lauber, J. K., & Kayten, P. J. (1988). Sleepiness, circadian dysrhythmia, and fatigue in transportation system accidents. *Sleep, 11*(6), 503-512.

Laurutis, V. P., & Robinson, D. A. (1986). The vestibulo-ocular reflex during human saccadic eye movements. *J Physiol, 373*, 209-233.

Lawson, B. D., & Mead, A. M. (1998). The Sopite Syndrome Revisited: Drowsiness and Mood Changes during Real or Apparent Motion. *Acta Astronautica, 43*(3-6), 181-192.

Lawther, A., & Griffin, M. J. (1988). A survey of the occurrence of motion sickness amongst passengers at sea. *Aviat Space Environ Med, 59*(5), 399-406.

Lentz, J. M. (1984, 3 May 1984). *Laboratory Tests of Motion Sickness Susceptibility.* Paper presented at the Motion Sickness: Mechanisms, Prediction, Prevention, and Treatment, Williamsburg, Virginia, USA.

Lichtenberg, B. K., Young, L. R., & Arrott, A. P. (1982). Human ocular counterrolling induced by varying linear accelerations. *Exp Brain Res, 48*(1), 127-136.

Light, L. H., & McLellan, G. (1977). Skeletal transients associated with heel strike. *J Physiol, 272*, 9-10.

Mayne, R. (1974). A systems concept of the vestibular organs. In H. H. Kornbucher (Ed.), *Handbook of Sensory Physiology* (pp. 493-580). Berlin Heidelberg New York: Springer.

McCauley, M. E., Royal, J. W., Wylie, D. C., O'Hanlon, J. F., & Mackie, R. R. (1976). *Motion Sickness Incidence: Exploratory Studies of Habituation, Pitch and Roll, and the Refinement of a Mathematical Model* (Technical Report No. 1733-2): Office of Naval Research.

McMahon, T. (1984). Mechanics of Locomotion. *International Journal of Robotics Research, 3*(2), 4-28.

Menz, H. B., Lord, S. R., & Fitzpatrick, R. C. (2003). Acceleration patterns of the head and pelvis when walking on level and irregular surfaces. *Gait Posture, 18*(1), 35-46.

Merfeld, D. M. (1990). *Spatial Orientation in the Squirrel Monkey: An Experimental and Theoretical Investigation.* Unpublished PhD Dissertation, MIT.

Merfeld, D. M. (1995a). Modeling human vestibular responses during eccentric rotation and off vertical axis rotation. *Acta Otolaryngol Suppl, 520 Pt 2*, 354-359.

Merfeld, D. M. (1995b). Modeling the vestibulo-ocular reflex of the squirrel monkey during eccentric rotation and roll tilt. *Exp Brain Res, 106*(1), 123-134.

Merfeld, D. M. (1995a). Modeling the Vestibulo-Ocular Reflex of the Squirrel Monkey during Eccentric Rotation and Roll Tilt. *Experimental Brain Research, 106*, 123-134.

Merfeld, D. M. (1995b). Modelling Human Vestibular Responses during Eccentric Rotation and off Vertical Axis Rotation. *Acta Oto-laryngologica Supplement, 520*, 354-359.

Merfeld, D. M. (2001). Must all action halt during sensorimotor mismatch? *Behavioral and Brain Sciences, 24*(1), 189-190.

Merfeld, D. M., Teiwes, W., Clarke, A. H., Scherer, H., & Young, L. R. (1996). The dynamic contributions of the otolith organs to human ocular torsion. *Exp Brain Res, 110*(2), 315-321.

Merfeld, D. M., & Young, L. R. (1995). The vestibulo-ocular reflex of the squirrel monkey during eccentric rotation and roll tilt. *Exp Brain Res, 106*(1), 111-122.

157

Merfeld, D. M., Young, L. R., Oman, C. M., & Shelhamer, M. (1993). A multidimensional model of the effect of gravity on the spatial orientation of the monkey. *J Vestib Res, 3*(2), 141-161.

Merfeld, D. M., Young, L. R., Paige, G. D., & Tomko, D. L. (1993). Three dimensional eye movements of squirrel monkeys following postrotatory tilt. *J Vestib Res, 3*(2), 123-139.

Merfeld, D. M., & Zupan, L. H. (2002). Neural Processing of Gravitoinertial Cues in Humans. III. Modeling Tilt and Translation Responses. *Journal of Neurophysiology, 87*, 819-833.

Michael, J., & Jones, G. M. (1966). Dependence of visual tracking capability upon stimulus predictability. *Vision Research, 16*, 707-716.

Miura, M., & Shimoyama, I. (1984). Dynamic Walk of a Biped. *International Journal of Robotics, 3*(2), 66-74.

Miyakoshi, S., Cheng, G., & Kuniyoshi, Y. (2001). Transferring Human Biped Walking Function to a Machine - Towards the Realization of a Biped Bike.

Money, K. E. (1970). Motion sickness. *Physiol Rev, 50*(1), 1-39.

Morales, M. F. (1949). Motion sickness: physical considerations regarding its etiology. In *A survey report on human factors in undersea warfare* (pp. 399-414). Washington, DC, US: National Research Council, Committee On Undersea Warfare. Panel on Psychology and Physiology.

Nise, N. S. (2004). *Control Systems Engineering* (4th ed.): John Wiley & Sons, Inc.

O'Hanlon, J. F., & McCauley, M. E. (1974). Motion sickness incidence as a function of the frequency and acceleration of vertical sinusoidal motion. *Aerosp Med, 45*(4), 366-369.

Oman, C. M. (1982). A heuristic mathematical model for the dynamics of sensory conflict and motion sickness. *Acta Otolaryngol Suppl, 392*, 1-44.

Oman, C. M. (1989). *Sensory Conflict in Motion Sickness: An Observer Theory Approach* (No. N90229576). Cambridge, Massachusetts: Massachusetts Inst. of Tech.

Oman, C. M. (1998). Sensory conflict theory and space sickness: our changing perspective. *J Vestib Res, 8*(1), 51-56.

Ormsby, C. C. (1974). *Model of Human Dynamic Orientation.* Massachussets Institute of Technology, Cambridge, MA.

158

Paige, G. D. (1989). The influence of target distance on eye movement responses during vertical linear motion. *Exp Brain Res, 77*(3), 585-593.

Paige, G. D. (1991a). Linear vestibulo-ocular (LVOR) and modulation by vergence. *Acta Oto-laryngologica Supplement, 481*, 282-286.

Paige, G. D. (1991b). Linear vestibulo-ocular reflex (LVOR) and modulation by vergence. *Acta Otolaryngol Suppl, 481*, 282-286.

Paige, G. D., & Sargent, E. W. (1991). Visually-induced adaptive plasticity in the human vestibulo-ocular reflex. *Exp Brain Res, 84*(1), 25-34.

Paige, G. D., Telford, L., Seidman, S. H., & Barnes, G. R. (1998). Human vestibuloocular reflex and its interactions with vision and fixation distance during linear and angular head movement. *J Neurophysiol, 80*(5), 2391-2404.

Paige, G. D., & Tomko, D. L. (1991a). Eye movement responses to linear head motion in the squirrel monkey. I. Basic characteristics. *J Neurophysiol, 65*(5), 1170-1182.

Paige, G. D., & Tomko, D. L. (1991b). Eye movement responses to linear head motion in the squirrel monkey. II. Visual-vestibular interactions and kinematic considerations. *J Neurophysiol, 65*(5), 1183-1196.

Panerai, F., Metta, G., & Sandini, G. (2000a, 26-28 April, 2000). *Learning VOR-like stabilization reflexes in robots.* Paper presented at the ESANN'2000 - European Symposium on Artificial Neural Networks, Bruges, Belgium.

Panerai, F., Metta, G., & Sandini, G. (2000b). Visuo-Inertial Stabilization in Space-variant Binocular Systems. *Robotics and Autonomous Systems, 30*, 195-214.

Parker, D. E., & Money, K. E. (1978). Vestibular/ space motion sickness mechanisms. In *Space Motion Sickness*. NASA Johnson Space Center, Houston, TX: NASA.

Pelisson, D., & Prablanc, C. (1986). Vestibulo-ocular reflex (VOR) induced by passive head rotation and goal-directed saccadic eye movements do not simply add in man. *Brain Res, 380*(2), 397-400.

Pelisson, D., Prablanc, C., & Urquizar, C. (1988). Vestibuloocular reflex inhibition and gaze saccade control characteristics during eye-head orientation in humans. *J Neurophysiol, 59*(3), 997-1013.

Peterka, R. J., Black, F. O., & Schoenhoff, M. B. (1987). Optokinetic and vestibulo-ocular reflex responses to an

unpredictable stimulus. *Aviat Space Environ Med, 58*(9 Pt 2), A180-185.

Pethybridge, R. J. (1982). *Sea sickness incidence in Royal Navy Ships* (No. INM Report 37/82). Gosport, England: Institute of Naval Medicine.

Proctor, R. W., & Proctor, J. D. (1997). Sensation and Perception. In G. Salvendy (Ed.), *Handbook of Human Factors and Ergonomics* (Second ed., pp. 299-656): John Wiley and Sons.

Reason, J. T. (1972). *Factors Contributing to motion sickness susceptibility: adaptability and receptivity.* Paper presented at the Conference Proceedings No. 109, Neuilly-sur-Seine.

Reason, J. T. (1978a). Motion sickness adaptation: a neural mismatch model. *J R Soc Med, 71*(11), 819-829.

Reason, J. T. (1978b). Motion Sickness: Some Theoretical and Practical Considerations. *Applied Ergonomics, 9*(3), 163-167.

Reason, J. T., & Brand, J. J. (1975). *Motion Sickness*. Oxford, England: Academic Press.

Reason, J. T., & Graybiel, A. (1970). Changes in subjective estimates of well-being during the onset and remission of motion sickness symptomatology in the slow rotation room. *Aerosp Med, 41*(2), 166-171.

Reason, J. T., & Graybiel, A. (1973, 1973). *Factors Contributing to Motion Sickness Susceptibility: Adaptability and Receptivity.* Paper presented at the AGARD Confererce Proceedings No. 109 – Predictability of Motion Sickness in the Selection of Pilots, Neuilly sur Seine, France.

Robinson, D. A. (1977). Linear addition of optokinetic and vestibular signals in the vestibular nucleus. *Exp Brain Res, 30*(2-3), 447-450.

Rude, S. A., & Baker, J. F. (1988). Dynamic otolith stimulation improves the low-frequency horizontal vestibulo-ocular reflex. *Exp Brain Res, 73*, 357-363.

Sandini, G., Panerai, F., & Miles, F. A. (2001). The Role of Inertial and Visual Mechanisms in the Stabilization of Gaze in Natural and Artificial Systems. In J. Zanker & J. Zeil (Eds.), *Motion Vision – Computational, Neural, and Ecological Constraints*. New York: Springer Verlag.

Schwab, R. S. (1954). The nonlabyrinthine causes of motion sickness. *Int Rec Med Gen Pract Clin, 167*(12), 631-637.

Schwarz, U., Busettini, C., & Miles, F. A. (1989). Ocular responses to linear motion are inversely proportional to viewing distance. *Science, 245*, 1394-1396.

Schwarz, U., & Miles, F. A. (1991). Ocular responses to translation and their dependence on viweing distance. I. Motion of the observer. *J Neurophysiol, 66*, 851-864.

Smart, L. J., Jr., Stoffregen, T. A., & Bardy, B. G. (2002). Visually induced motion sickness predicted by postural instability. *Hum Factors, 44*(3), 451-465.

Stoffregen, T. A., Hettinger, L. J., Haas, M. W., Roe, M. M., & Smart, L. J. (2000). Postural instability and motion sickness in a fixed-based flight simulator. *Hum Factors, 42*(3), 458-469.

Stoffregen, T. A., & Smart, L. J., Jr. (1998). Postural instability precedes motion sickness. *Brain Res Bull, 47*(5), 437-448.

Telban, R. J., Cardullo, F. M., & Guo, L. (2000). *Investigation of Mathematical models of otolith organs for human centered motion cueing algorithms* (No. AIAA – 2000 - 4291): American Institute of Aeronautics and Astronautics.

Telford, L., Seidman, S. H., & Paige, G. D. (1997). Dynamics of squirrel monkey linear vestibuloocular reflex and interactions with human fixation distance. *J Neurophysiol, 78*, 1775-1790.

Tomko, D. L., & Paige, G. D. (1992). Linear vestibuloocular reflex during motion along axes between nasooccipital and interaural. *Ann N Y Acad Sci, 656*, 233-241.

Tomko, D. L., Wall, C., 3rd, & Robinson, F. R. (1988). Influence of gravity on cat vertical vestibulo-ocular reflex. *Exp Brain Res, 69*, 307-314.

Tomlinson, R. D., & Bahra, P. S. (1986). Combined eye-head gaze shifts in the primate. II. Interactions between saccades and the vestibuloocular reflex. *J Neurophysiol, 56*(6), 1558-1570.

Treisman, M. (1977). Motion sickness: an evolutionary hypothesis. *Science, 197*(4302), 493-495.

Tweed, D. (1997). Three-Dimensional Model of the Human Eye-Hand Saccadic System. *Journal of Neurophysiology, 77*, 654-666.

Tweed, D., Glenn, B., & Vilis, T. (1995). Eye-head coordination during large gaze shifts. *J Neurophysiol, 73*(2), 766-779.

Tyler, D. B., & Bard, P. (1949). Motion Sickness. *Physiol Rev, 29*, 311-369.

Viirre, E., & Demer, J. L. (1996). The human vertical vestibulo-ocular reflex during combined linear and angular acceleration with near-target fixation. *Exp Brain Res, 112*, 313-324.

Viirre, E., Tweed, D., Milner, K., & Vilis, T. (1986). A reexamination of the gain of the vestibuloocular reflex. *J Neurophysiol, 56*, 439-450.

Watt, D. G. (1983). Sensory and motor conflict in motion sickness. *Brain Behav Evol, 23*(1-2), 32-35.

Wellbrink, J. (2003). *Modelling Reduced Human Performance as a Complex Adaptive System.* Naval Postgraduate School, Monterey, CA.

Wertheim, A. H. (1998). Working in a moving environment. *Ergonomics, 41*(12), 1845-1858.

Wilson, V., & Jones, G. M. (1979). *Mammalian Vestibular Physiology*. New York: Plenum Press.

Woellner, R. C., & Graybiel, A. (1959). Counterrolling of the eyes and its dependence on the sensitivity of gravitational or inertial force acting laterally on the body. *J Appl Physiol, 14*, 632-634.

Wylie, D. R., Bischof, W., & Frost, B. J. (1998). Common reference frame for neural coding of translational and rotational optic flow. *Nature, 392*, 278-282.

Wylie, D. R., & Frost, B. J. (1993). Responses of pigeon vestibulocerebellar neurons to optokinetic stimulation. II. The 3-dimensional reference frame of rotation neurons in the floculus. *Journal of Neurophysiology, 70*, 2647-2659.

Yamanaka, T. (1999, October 1999). *Difference of the vibrational characteristics between the human's arm holding and babay buggies' as a reference for design based on riding feeling.* Paper presented at the 4th Asian Design Symposium.

Young, L. R. (1970). *On visual vestibular interaction.* Paper presented at the Fifth Symposium on the Role of the Vestibular Organs in Space Exploration.

Young, L. R., Lichtenberg, B. K., Arrott, A. P., Crites, T. A., Oman, C. M., & Edelman, E. R. (1981). Ocular torsion on earth and in weightlessness. *Ann N Y Acad Sci, 374*, 80-92.

Young, L. R., & Meiry, J. L. (1968). A Revised Dynamic Otolith Model. *Aerospace Medicine, 39*(6), 606-608.

Zupan, L. H., Merfeld, D. M., & Darlot, C. (2002). Using sensory weighting to model the influence of canal, otolith and visual cues on spatial orientation and eye movements. *Biol Cybern, 86*(3), 209-230.

INITIAL DISTRIBUTION LIST

1. Defense Technical Information Center
    Ft. Belvoir, Virginia

2. Dudley Knox Library
    Naval Postgraduate School
    Monterey, California

3. Hellenic General Staff, Department of Personnel-
    Training
    Holargos - Athens
    Hellas

4. Professor Michael E. McCauley
    Naval Postgraduate School
    Monterey, California

5. Professor Nita Lewis-Miller
    Naval Postgraduate School
    Monterey, California

6. Professor Alan Washburn
    Naval Postgraduate School
    Monterey, California

7. Charles M. Oman, Ph.D.
    MIT - Dept of Aeronautics & Astronautics
    Cambridge, MA

8. Robert S. Kennedy, Ph.D.
    President, RSK Assessments
    Orlando, CA

9. Thomas G. Dobie, M.D.
    National Biodynamics Laboratory - C/O UNO College of
    Engineering
    New Orleans, LA

10. CAPT Angus H. Rupert, M.D., Ph.D.
    Naval Aerospace Medical Research Laboratory
    Pensacola, FL

11. J. Robert Bost
     NAVSEA
     Washington Navy Yard, DC

12. James C. Miller, Ph.D.
     AFRL/HEPF
     Brooks City-Base, TX

13. Col. John S. Crowley, MD
     Scientific Program Director
     U.S. Army Aeromedical Research Laboratory
     Fort Rucker, AL

14. Lieutenant Panagiotis Matsangas Hellenic Navy
     Athens, Hellas

15. D.I.K.A.T.S.A.
     Inter-University Center for the Recognition of Foreign
     Academics Titles
     Athens, Hellas